ORNL/Sub-7117/25

WFPS-TME-071

OCTOBER, 1977

FOUR IGNITION TNS TOKAMAK REACTOR SYSTEMS - DESIGN SUMMARY

fusion power systems department

Westinghouse Electric Corporation

P.O. Box 10864, Pgh. Pa. 15236

DISCLAIMER

WFPS-TME-071
OCTOBER, 1977

FOUR IGNITION TNS TOKAMAK REACTOR SYSTEMS - DESIGN SUMMARY

Prepared by: TNS ENGINEERING STAFF

Approved by: _____
T. C. VARLJEN, MANAGER
ENGINEERING

Approved by: _____
C. A. FLANAGAN, MANAGER
MAGNETIC FUSION PROJECTS

Westinghouse Electric Corporation
Fusion Power Systems Department,
P.O. Box 10864, Pgh. Pa. 15236

ORNL/Sub-7117/25
WFPS-TME-071
OCTOBER, 1977

FOUR IGNITION TNS TOKAMAK REACTOR SYSTEMS - DESIGN SUMMARY

C. A. FLANAGAN, EDITOR

CONTRIBUTORS

W. C. BRENNER
R. J. BUDENHOLZER
D. L. CHAPIN
J. W. FRENCH
H. J. GARBER
G. GIBSON
F. M. HECK
H. R. HOWLAND
E. M. IWINSKI
J. S. KARBOWSKI
A. Y. LEE
G. W. RUCK
J. H. SCHULTZ
D. A. SINK
G. S. SMELTZER
R. A. SMITH
M. SNIDERMAN
E. W. SUCOV
F. G. TAUCH
T. C. VARLJEN
T. F. YANG

ACKNOWLEDGEMENT

This work was performed for the Oak Ridge National Laboratory Fusion Energy Division, under U.S. Energy Research and Development Administration Contract W-7405-ENG-26, Subcontract 7117. Reproduction, translation, publication, use and disposal, in whole or in part, by or for the United States Government is permitted.

LEGAL NOTICE

This report was prepared as an account of Government sponsored work. Neither the United States, nor the Administration, nor any person acting on behalf of the Administration:

A. Makes any warranty or representation, expressed or implied, with respect to the accuracy, completeness, or usefulness of the information contained in this report, or that the use of any information, apparatus, method or process disclosed in this report may not infringe privately owned rights; or

B. Assumes any liabilities with respect to the use of, or for damages resulting from the use of any information, apparatus, method, or process disclosed in this report.

FOREWORD

The Division of Magnetic Fusion Energy with the U. S. Department of Energy initiated within the fusion development program for tokamak power reactors a series of systems studies aimed at the definition of subsequent tokamak devices leading to a commercial prototype reactor. Since April 1976, a design team composed of representatives from the ORNL Fusion Energy Division and the Westinghouse Fusion Power Systems Department has been engaged in scoping studies associated with the definition of The Next Step (TNS) in the tokamak program after the TFTR. Provisional goals established for TNS include:

- Achievement of ignition
- Demonstration of burning dynamics
- Evaluation of design requirements and solutions for long pulse operation
- Features which extrapolate to a viable power reactor
- Availability in the mid-to-late 1980's
- Being a technology forcing function in the tokamak magnetic fusion program

It is in this context that the work reported herein was performed.

TABLE OF CONTENTS

TABLE OF CONTENTS (CONTINUED)

LIST OF FIGURES

LIST OF FIGURES (CONTINUED)

LIST OF FIGURES (CONTINUED)

LIST OF TABLES

LIST OF TABLES (CONTINUED)

1.0 SUMMARY

The ORNL/Westinghouse FY'77 program for The Next Step (TNS) tokamak after TFTR examined a large number of potential configurations for D-T burning ignition tokamak systems. It was recognized at the outset of this study that many such candidate systems could be proposed for TNS and that a study to systematically evaluate candidate systems would be valuable. Accordingly, rather than select a particular TNS design for development, a systematic study was performed to quantify and evaluate the trade-offs associated with the many options available. Based upon the results of this study, four TNS tokamak point designs were selected, each representative of a given toroidal field (TF) coil technology. It should be noted that the primary purpose of the present document is to compile information on the four TNS point designs and the key systems comprising those designs. However, to put the development of these four designs into perspective and to provide a brief statement of how the TNS studies proceeded, a section of the report is included which briefly summarizes the methodology used, the manner in which the sizing and costing relationships were developed, and briefly discusses the trade studies which were performed. Each of these areas is more fully discussed in separate documents to which the reader is referred for a more detailed discussion.

The process which led to the selection of the four reference designs included the following elements:

- Formulate a set of study groundrules which would focus on the relative differences in system performance, size and cost associated with the major design alternatives (as well as provide absolute cost estimates).
- Develop system and component point designs and size and cost scaling relationships.
- Develop a digital computer code, called COAST[1], to integrate subsystem models and generate self-consistent tokamak point design descriptions and cost estimates. (COAST is an acronym for COsting And Sizing of Tokamaks.)

- Perform trade and sensitivity studies[2] using COAST.
- Select four reference point designs.

A number of distinctly different options of plasma size and toroidal field (TF) coil technology could satisfy the objectives of TNS. The plasma size is an important parameter because it directly translates into size and cost and is a parameter in evaluating the flexibility of the system to achieve the objectives. The TF coil technology is important because available options exhibit a certain range in the maximum magnetic field and a wide range of system complexities.

Four different types of TF coil technologies were investigated as indicated in the following listing:

Designation	TF Coil Technology
TNS-1	Water-cooled copper
TNS-3	Superconducting NbTi
TNS-4	Superconducting Nb_3Sn
TNS-5	Hybrid consisting of water-cooled copper coil nested within a superconducting NbTi coil

(The designation TNS-2 was used early in the study for a tokamak with a hydrogen plasma using superconducting TF coils. As the program developed, this class of machines was dropped from further consideration.)

The range of device sizes considered for the four TF coil technologies covered a range of the plasma minor radius (or horizontal half-width) from ∿0.75 m to 2.0 m, spanning the range from TFTR size plasmas to those chosen for recent[3,4,5] Experimental Power Reactor (EPR) design studies (Figure 1-1). The device major radius was varied from ∿8-9 m down to some lower limits (∿4-5 m) which were consistent with assumed groundrules and still allowed a viable engineering design. In most cases, the plasma elongation was kept at 1.6, based on physics considerations. The plasma beta value was chosen as the main parameter on which to judge the performance or "confidence of success" of each ignition device, and was allowed to vary in the range from ∿2% to 15%. Two different plasma scalings were used to

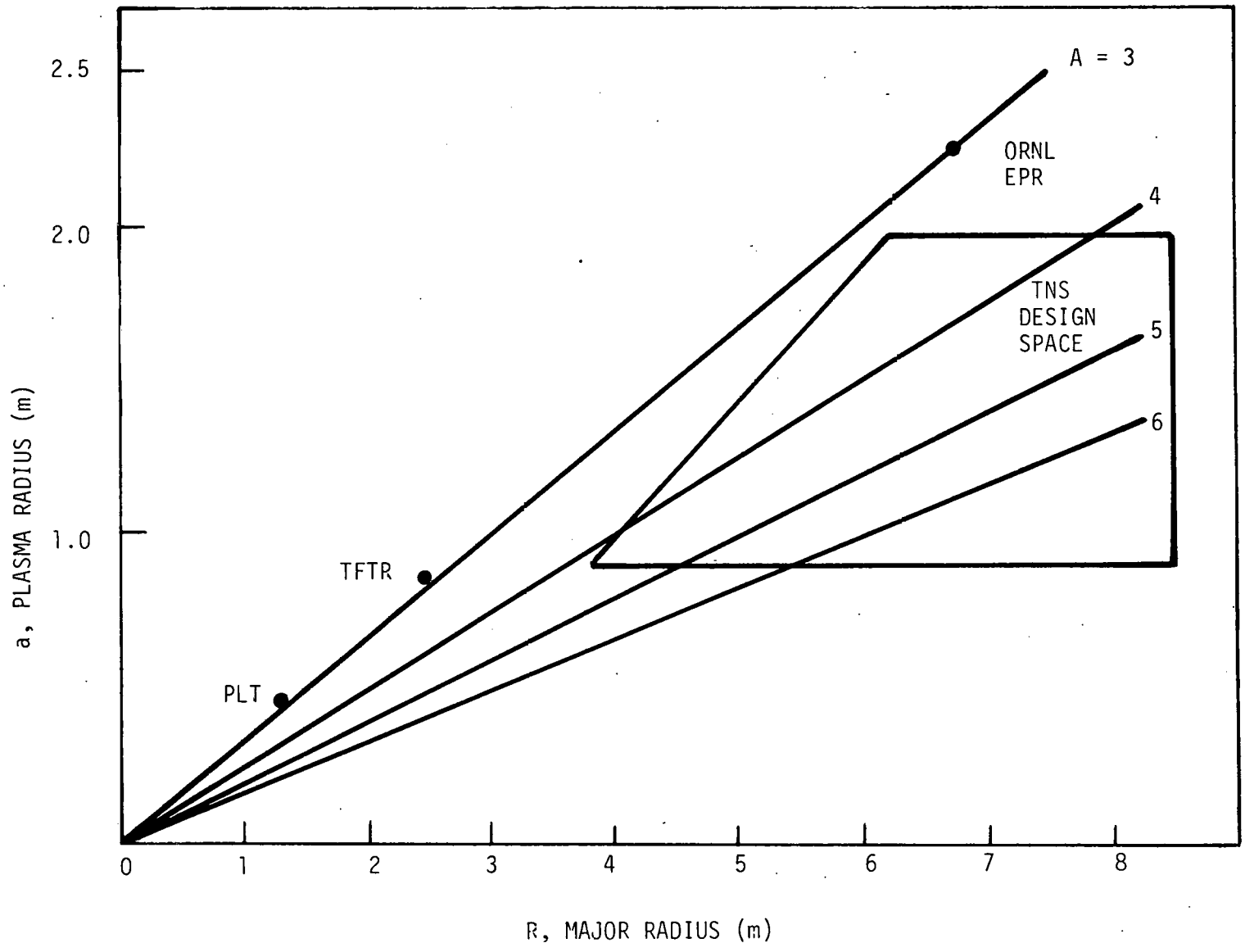

Figure 1-1. TNS Design Space

specify the physics parameters for an ignition device, empirical scaling and trapped-particle-mode scaling.

A critical consideration in the exploration of the parameter space for TNS was the development of groundrules and assumptions to be used in the development of models that are internally consistent and, to the greatest extent possible, do not prejudice the outcome in an unfair manner. A set of design assumptions was established to yield representative model solutions and represent the key size and cost sensitivities that bear on a final decision (see Table 1-1). No attempt was made in this study to provide detailed design solutions or to represent optimum configurations.

To allow the various TNS options to be examined under a common set of engineering groundrules, the COAST code was developed. The code has been written for evaluating, in a quantifiable manner, TNS engineering considerations. The plasma is specified primarily via input data; e.g., results from plasma modeling studies or calculations, and the tokamak device sized by COAST provides all the support systems required for the assumed plasma. Over forty subsystems or principal components are represented in the code calculation, thus providing both flexibility and refinement in examining any given design.

The basic logic of COAST is shown in Figure 1-2. The calculations are separated into a section to determine the size feature of a given design based on engineering models and a section to determine the costs. The device features and component sizes are specific to the tokamak and plasma dimensions under consideration. The cost representations were developed based on unit cost relationships and are independent of a given tokamak design. The input is divided into three distinct types of data as indicated in Figure 1-2. In general, the physics input is device independent; whereas the engineering constraints are associated with a specific device design. The cost data are mainly in the form of cost coefficients for a component unit size; e.g., cost per kg of fabricated stainless steel for a TF coil bucking cylinder.

All of the major systems comprising a complete TNS tokamak device and associated facility are described in COAST. Table 1-2 presents a summary of these systems.

TABLE 1-1

KEY GROUNDRULES AND ASSUMPTIONS

OPERATION	
Design Basis Facility Lifetime	10 years
Total Number of Pulsing Cycles	10^6
Pulse Repetition Period	300 seconds
Pulse Scenario:	
Pulse OH	0-1 s
Neutral Beam Injection	1-7 s
Ignition Excursion	7-15 s
Burn	15-31 s
Quench	31-33 s
D-T Operation Envelope (Design Basis):	
Annual Dose at Site Boundary	≤5 mrem
On-Site Restricted Area Annual Dose	≤1 rem
On-Site Restricted Area Quarterly Dose	≤600 mrem
On-Site Unrestricted Area Annual Dose	≤100 mrem
Copper Electrical Insulation Dose Limit	10^{10} rads
Upper Limits on Number of D-T Pulses:	
Lifetime Limit	Equivalent to 4000 full energy pulses
Annual Limit	Equivalent to 1000 full energy pulses
VACUUM VESSEL	
Vessel Material	AISI 316 SS
Construction	I-Beam stiffened shells (w/o bellows)
Vessel Cross-Section	Elliptical
Segmentation	Not factored into models
Wall Thickness	Variable
Toroidal Limiter	One or two tungsten segments (radiation cooled)
Diagnostic Penetrations	Fixed number
Peak Bulk Wall Temperature	400°C
Vessel Coolant	Water
TOROIDAL FIELD COILS	
Number of Coils	Variable
Conductor Type	
TNS-1	Copper (H_2O-cooled)
TNS-3	NbTi (LHe-cooled)
TNS-4	Nb_3Sn (LHe-cooled)
TNS-5	Copper/NbTi (H_2O-LHe-cooled)
Coil Shape	Constant tension "D"
Peak Field at Conductor	Copper - Variable, but values considered up to 14T
	NbTi - Variable, but values considered up to 10T
	Nb_3Sn - Variable, but values considered up to 14T
Cooling Mode	Single phase forced flow
Fault Protection	Electrical provisions only
POLOIDAL FIELD SYSTEM	
Conductor Material	Oxygen Free High Conductivity (OFHC) Copper
Location	OH windings outside TF; VF windings inside TF
OH Flux Swing	Variable
Conductor Current Limit	20 kA
Conductor Current Density Limit	1.5 kA/cm^2
Conductor Coolant	Forced flow water

TABLE 1-1 (Continued)

IMPURITY CONTROL TECHNIQUE	Wall treatment (low sputtering liner, low Z wall, etc.) Note: It is recognized that a magnetic divertor may be necessary. This was examined in a parallel study.
VACUUM PUMPING	
Final Pumping Stage	Cryosorption pumps
Base Pressure (Pre-Pulse)	1×10^{-8} torr
Outgassing Surface Area	Ten times smooth area of vessel
TRITIUM SYSTEMS	
On-Site/In-Process T_2 Inventory	Variable
Tritium Storage	Uranium chip beds
Fuel Recovery-Recycling Plant	Variable Capacity (common approach)
Tritium Cleanup Systems	Variable Capacity (common approach)
Fueling	Prefill: Gaseous D-T Refueling: Solid T and D-T pellets
NEUTRAL BEAM INJECTION LINES	
Beam Power Energy	150 keV; variable power
Single Arm Specifications	
Sources	3-100 A positive ion
Dimensions	7.5 m long x 4 m wide x 6 m high
Number	Varies with plasma conditions
Vessel Aperture per Line	Duct 44 cm wide x 120 cm high
Duct Shielding	As required by coil type
HEAT DISSIPATION SYSTEMS	
Final Facility Heat Sink	Mechanical draft evaporative cooling towers to atmosphere
Vacuum Vessel Coolant	Water - variable capacity
Shield Coolant	Borated water - variable capacity
Buffer Loop Coolant	Water - variable capacity
Cryogenic Refrigeration Systems	Variable capacity
Facility Air Conditioning	Fixed base load, reactor cell air conditioning variable
Thermal Loads	Variable - depending on option
OPERATIONAL DIAGNOSTICS	
Number, Type, Penetrations	Constant in all studies
ELECTRICAL SYSTEMS	
Facility Feed	Fixed utility constraints
S/C TF Supplies	Line-driven rectifier supplies (except for hybrid)
Cu TF Supplies	AC-MG storage-rectifier conversion
Neutral Beam Supplies	AC-MG storage-rectifier conversion
Poloidal Field Power Supplies	AC-MG storage-rectifier conversion
Electrical Loads	Variable - depending on option
Instrumentation and Control	Fixed for all options
ARCHITECTURAL AND FACILITY	
Site	150 m radius site boundary "free-standing"
Reactor Cell	Reinforced ordinary concrete Fixed: walls (~2.9 m); ceiling (~2.3 m) Vertical height fixed Floor space, basement: variable
Electrical Power System Buildings	Variable
Balance of Plant Buildings	Fixed

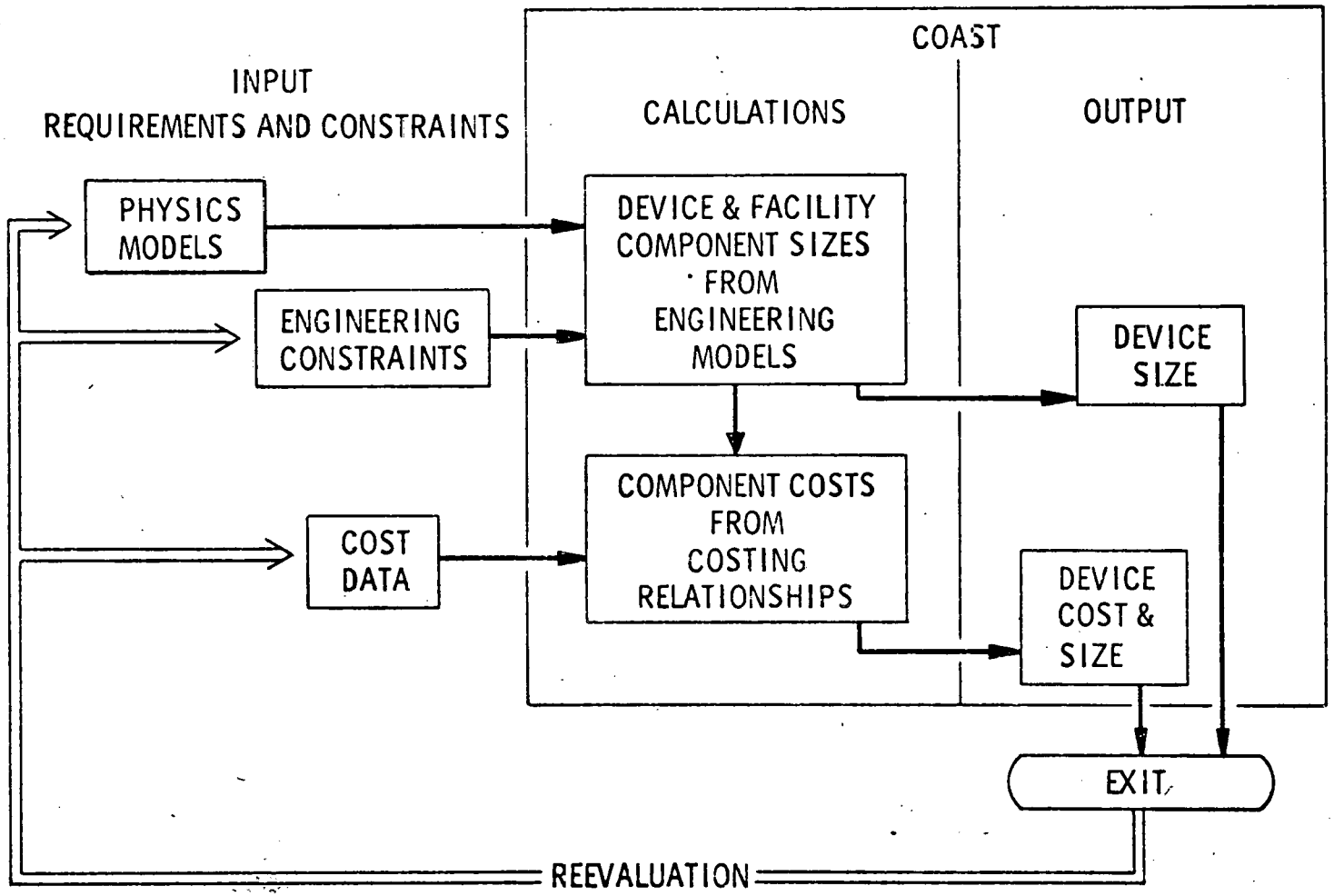

Figure 1-2. A Logic Diagram Showing the General Features of the COAST Code

TABLE 1-2

SYSTEMS REPRESENTED IN COAST

Tokamak Systems	Basic device including the plasma, plasma exhaust system, vessel, shield, structure, divertor, toroidal and poloidal field coils.
Electrical Power and Control	All power conversion, energy storage, instrumentation and control for all TF, PF coils, NB arms, plasma diagnostics and emergency systems.
Tokamak Support Systems	Vacuum pumping; gas handling including tritium storage, fuel fabrication, fuel processing, cryogenic distillation, tritium cleanup; heat transport, ventilation and air conditioning; radioactive waste handling; and remote servicing.
Neutral Beam Injection System	Neutral beam arms and power conversion equipment.
Plant Facilities	Reactor cell, buildings for power equipment.

For most of these studies, the plasma pulse time operating scenario has been held fixed under the assumptions of a one second initiation and startup period, a six second neutral beam injection period to reach ignition, an eight second period during which a thermal excursion occurs to reach steady state conditions, followed by a 16 second steady state burn period and then a two second quench. Hence, the total pulse length is $\simeq$ 33 seconds. The time between pulses is fixed at five minutes (300 s), and there are assumed to be the equivalent of 1,000 full power D-T pulses per year.

Using COAST, a series of parametric trade studies was performed to evaluate the performance and relative costs of D-T burning, ignition, TNS tokamaks over the size range indicated in Figure 1-1.

In Figure 1-3, the relative cost of devices with Cu TF coils is plotted vs. major radius R_o for different values of the plasma half-width a. These curves were obtained based on empirical plasma scaling for 20 TF coils and an elongation of 1.6. The plasma β is kept constant at 5% for these cases by varying the peak field at the TF coil, B_{max}, for each device size. Lines of constant values of B_{max} of 9T and 10T are shown for reference. Note that there is a minimum in the cost for each plasma radius at a certain major radius R_o. For larger values of R_o, the overall size of the device dominates the cost, even though the field at the TF coil is decreasing in order to keep β at 5%. For smaller values of R_o, the cost also increases due to two effects - increased cost of the TF coils at the higher B_{max} values and increased power conversion costs to supply the necessary flux swing through the smaller machine bore. The curves terminate at the "bore size limit" due to the fact that there is a minimum allowable R_o which is set by engineering considerations.

Similar data were generated for other values of β and for the other TF coil technologies. The results of these calculations indicate that for each coil technology there is some minimum cost device at a particular a, R_o, and B_{max} which achieves ignition at a given β. A composite plot of these minimum cost devices vs. the operating β value is shown in Figure 1-4 for the four TF coil technology options. Values of a, R_o, and B_{max} at the end points of β = 2.5% and β = 10% for each coil type are shown for reference. There is a rather sharp increase in cost as the β is decreased, due to the larger device sizes and peak

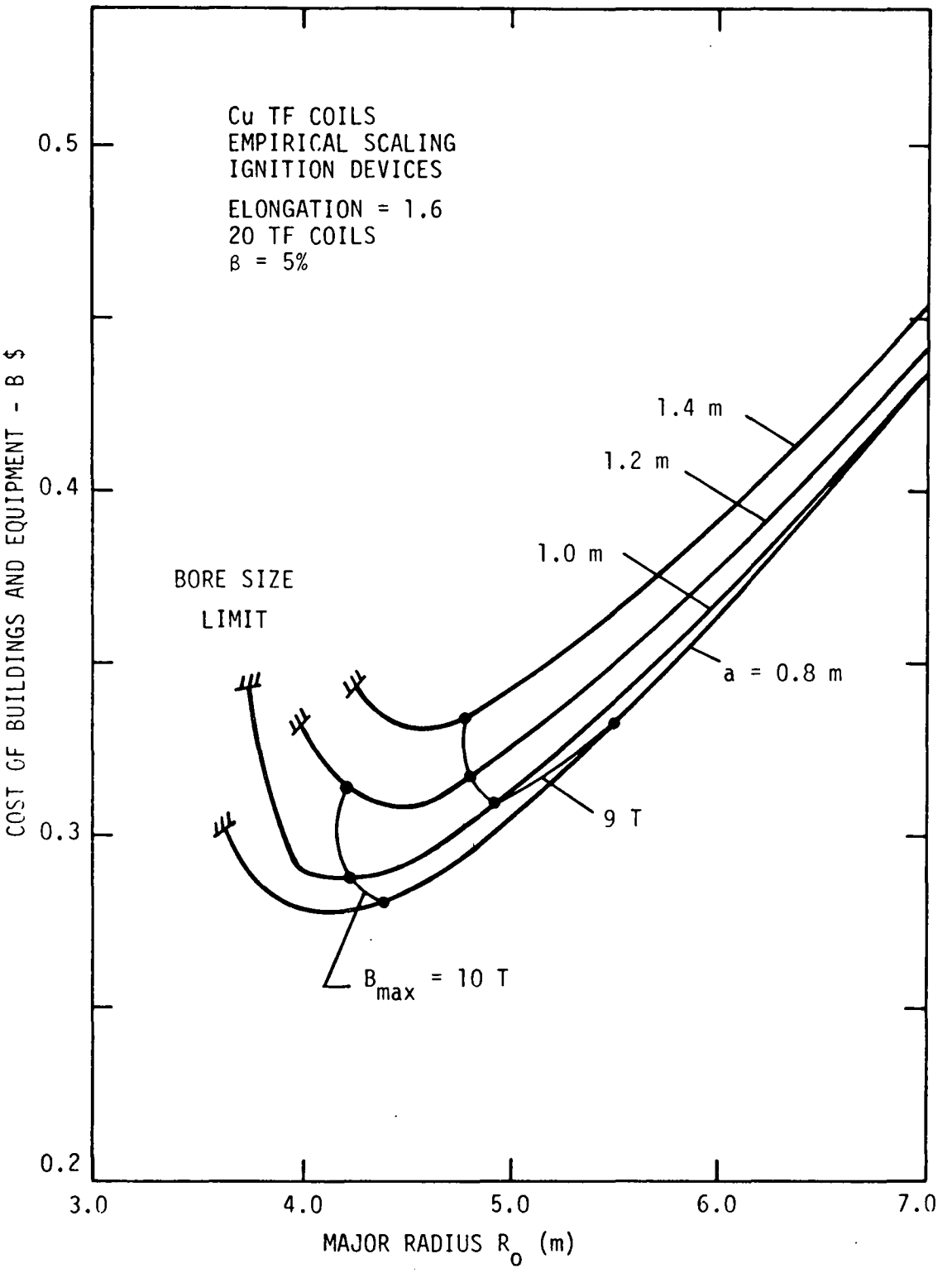

Figure 1-3. Cost of Cu TF Devices at β = 5%

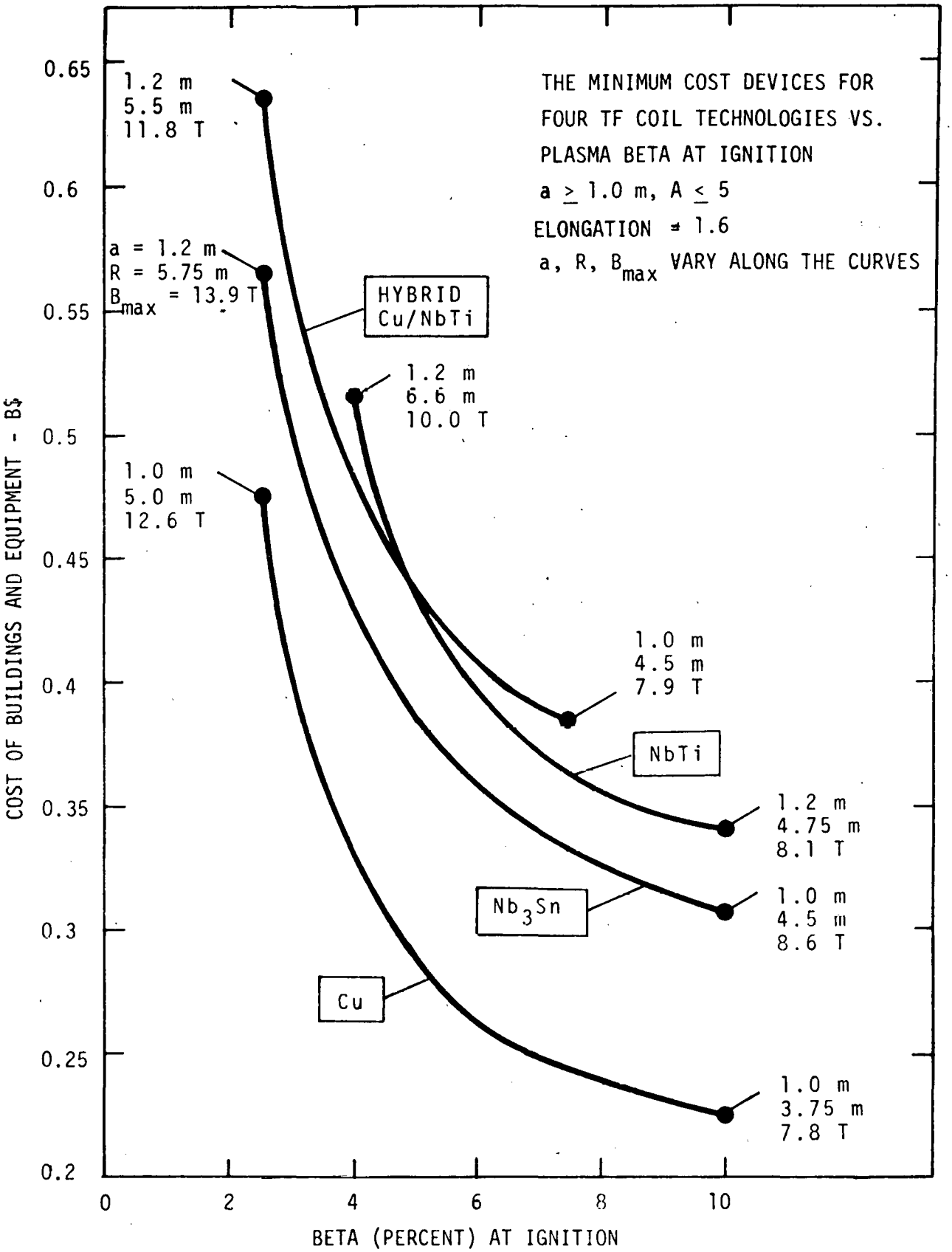

Figure 1-4. Minimum Cost Devices vs. Percent Beta

fields. Likewise, the cost decreases for higher β because a, R_o, and B_{max} can be decreased. Also, it can be seed that for any β, the CuTF coil devices can be built for the least cost. The Nb_3Sn coil devices are about 30% more expensive than the Cu, while the NbTi and Cu/NbTi hybrid options are about 50% more costly for most β values. A similar observation is that for the same cost, a Cu TF coil device can operate at a lower β value than either NbTi or Cu/NbTi devices for the same cost. Details of the trade study evaluation are contained in Reference 2.

Based upon the trade study results and criteria for selecting typical point designs, four reference point designs were identified. These designs have not been optimized from either cost or performance considerations, but each design is self-consistent and fully delineated in terms of the necessary systems and subsystems. Section 4.0 presents the key features of the four designs in a comparative way. Table 1-3 presents an overall summary of the key features of each design.

As indicated in Table 1-3, the minor radius for these designs is either 1.0 or 1.2 m with a major radius ranging from 4.0 m for TNS-1 (Cu) to 5.7 m for TNS-3 (NbTi). The peak toroidal field at the winding for TNS-1 (Cu) is 10.4 T. For the superconducting designs, the peak field for TNS-3 (NbTi) is 9.9 T (which is judged to represent a significant technological risk); for the TNS-4 (Nb_3Sn) design, the peak field at the winding is 10.9 T. Using these peak fields, the magnetic field on axis for each design is 5-6 T. Note that the maximum plasma current for these designs exceeds 3.5 MA in each case. With respect to the toroidal field coils, these designs result in coil sizes of approximately 4-5 m x 6-7 m.

Also indicated in Table 1-3 is the estimated total cost in 1977 dollars for each of these designs. These costs are building and equipment costs only and do not include engineering, design, inspection and administration (EDIA), contingency or escalation. Note that the least expensive design is TNS-1 (Cu) at $\sim$289M\$. Of the two all superconducting designs, TNS-4 (Nb_3Sn) is estimated to cost 388M\$, about 34% more expensive than TNS-1, but representing a more significant advance in technology

TABLE 1-3

KEY FEATURES OF FOUR REFERENCE POINT DESIGNS

	TNS-1	TNS-3	TNS-4	TNS-5
TF Coil Conductor	Cu	NbTi	Nb_3Sn	Cu/NbTi
Plasma Minor Radius, a (m)	1.0	1.2	1.2	1.0
Plasma Major Radius, R (m)	4.0	5.7	5.0	4.5
Plasma Elongation, δ (-)	1.6	1.6	1.6	1.6
Aspect Ratio, A (-)	4.0	4.7	4.2	4.5
Field at TF Coil, B_m (T)	10.4	9.9	10.9	9.7
Field on Axis, B_t (T)	5.8	5.3	5.3	5.8
Toroidal Beta, β_t (%)	5.0	5.0	5.0	5.0
Plasma Current, I_p (mA)	4.1	3.8	4.3	3.6
Mean Electron Density, $\bar{n}_e$ (m^{-3})	1.6×10^{20}	1.3×10^{20}	1.3×10^{20}	1.6×10^{20}
Mean Ion Temperature, $\bar{T}_i$ (keV)	13.0	13.0	13.0	13.0
Energy Confinement Time, τ_E (s)	1.5	1.8	1.8	1.5
$\bar{n}_e \tau_E$ (m^{-3} s)	2.4×10^{20}	2.4×10^{20}	2.4×10^{20}	2.4×10^{20}
Total Volt-Seconds	41.0	55.2	51.6	43.5
Plasma Volume, V_A (m^3)	126.3	259.2	227.6	142.1
Neutron Wall Load (MW/m^2)	1.50	1.28	1.28	1.50
Total Fusion Power (MW)	558	795	698	628
Fusion Power Density (MW/m^3)	3.7	2.6	2.6	3.7
Neutral Beam Power (MW)	40.0	57.0	50.0	45.0
Steady State Burn Time (s)	16.0	16.0	16.0	16.0
Time Between Pulses (s)	300.0	300.0	300.0	300.0
TF Coil Vertical Bore (m)	6.1	7.4	7.6	9.5
TF Coil Horizontal Bore (m)	3.8	5.1	4.9	5.7
Plasma Energy/Energy Consumed	0.32	0.85	1.57	0.51
Number of TF Coils	20	20	20	20
*Cost, Building & Equipment (M$)	288.7	434.4	388.3	436.0
Relative Cost	1.0	1.50	1.34	1.51
Annual Utility Cost (M$)	4.1	3.0	2.0	3.4

*These costs are building and equipment costs only and do not include engineering, design, inspection and administration (EDIA), contingency or escalation.

beyond TFTR than TNS-1. The other superconducting design, TNS-3 (NbTi), is estimated to cost 434M$, or 10% more than TNS-4 (Nb_3Sn). A detailed discussion of the costs and reasons for the differences is contained in Section 4.5 of the report.

Section 5.0 of this report presents a brief description of the features of many of the systems comprising each design. Included are descriptions of the vacuum vessel approaches considered, impurity control, the nuclear shielding considerations, the magnet systems (toroidal and poloidal), the electrical systems, the heat transport systems, the tritium systems, the plasma heating system, the remote servicing system, the vacuum pumping system, and the plant facility considerations.

Based on these TNS studies which have been conducted and reported in this and companion documents, the trends and conclusions from the trade-off studies suggest that decisions about what the role of the TNS device should be must be made on a qualitative basis. The quantitative results which have been generated suggest that if the TNS objective is limited to the demonstration of ignition as quickly as possible with the least cost, then a TNS design using copper TF coils appears most attractive.

However, should the TNS objective be to include a demonstration of engineering advancement and reactor technology as well as to achieve ignition, then TNS should be designed as a superconducting machine. Such a decision would result in a higher cost and would require more technology development than if the copper option were selected. Of the superconducting options examined, this study suggests that the Nb_3Sn option provides for greater field capability at an overall lower cost. However, the cost differential is modest ($\sim$10%) between the superconducting options, compared to the cost differential ($\sim$30-40%) between a copper TF machine and a superconducting TF machine.

2.0 INTRODUCTION

An ORNL/Westinghouse design team has been engaged in the study of alternative strategies for a near-term (after TFTR) ignition test reactor, provisionally designated The Next Step (TNS), which could provide answers to the most pressing physics and technical feasibility questions associated with ignition. Principal TNS objectives assumed included: 1) demonstration of ignition and burning dynamics; and 2) reactor technology forcing. The selection of an overall design approach for TNS required an early quantitative assessment of the most important design issues; namely, choice of ignition plasma design conditions (principally size and confining field of axis), and choice of toroidal field coil technology (resistive or superconducting windings). The design space investigated in this study ranged from ignited plasmas (elongated) with minor radii varying between 0.8 m (TFTR-like) and ~2.0 m (EPR-like). Four TF coil types were examined; these included copper, NbTi, Nb_3Sn, and a hybrid design employing nested coils of copper and NbTi.

The process which led to the selection of the four reference designs included the following elements:

- Formulation of a set of study groundrules to permit the study to focus on the relative differences in system performance, size, and cost associated with the major design alternatives (as well as provide absolute cost estimates).
- Development of system and component point designs and size and cost scaling relationships.
- Development of a digital computer code, called COAST (COsting and Sizing of Tokamaks), to integrate subsystem models and generate self-consistent tokamak point design descriptions and cost estimates.
- Performance of trade and sensitivity studies using COAST.
- Determination of selection criteria and selection of four reference point designs.

A final step[6] involved a further comparison of the four reference concepts using decision modeling techniques as a mechanism for selecting a preferred design approach for the TNS mission.

Section 3.0 describes the TNS study process. Section 4.0 presents a summary of the parameters for the four reference point designs. Finally, Section 5.0 presents a brief description of the design features of many of the systems comprising the TNS design.

3.0 TNS STUDY LOGIC AND PROCESS

The studies for TNS in FY'77 were performed to support the overall objectives identified for TNS. The objectives identified for TNS and associated studies were the following:

- Achieve ignition and demonstrate burning dynamics
- Provide for potential design solutions for long pulse operation
- Extrapolate to a viable reactor
- Be available in the mid-1980s
- Be a technology forcing function

In the work performed in FY'77, a study logic was developed and implemented. This logic and associated study process is described in the following sections to indicate the path followed to select and develop the specific point designs presented later in this report.

3.1 FORMULATION OF STUDY GROUNDRULES

The initial task of the TNS studies was to provide the basis for the selection of toroidal field coil technology and system size. A critical consideration in the exploration of the parameter space for TNS was the development of groundrules and assumptions to be used in the development of models that are internally consistent and, to the greatest extent possible, do not prejudice the evaluation process in an unfair manner.

A set of design assumptions was established to yield representative model solutions and represent the key size and cost sensitivities that bear on a final decision (see Table 3-1). No attempt was made in this study to provide detailed design solutions or to represent optimum configurations, in view of the time and effort constraints which were identified for the work.

TABLE 3-1

KEY GROUNDRULES AND ASSUMPTIONS

OPERATION	
Design Basis Facility Lifetime	10 years
Total Number of Pulsing Cycles	10^6
Pulse Repetition Period	300 seconds
Pulse Scenario:	
Pulse OH	0-1 s
Neutral Beam Injection	1-7 s
Ignition Excursion	7-15 s
Burn	15-31 s
Quench	31-33 s
D-T Operation Envelope (Design Basis):	
Annual Dose at Site Boundary	≤5 mrem
On-Site Restricted Area Annual Dose	≤1 rem
On-Site Restricted Area Quarterly Dose	≤600 mrem
On-Site Unrestricted Area Annual Dose	≤100 mrem
Copper Electrical Insulation Dose Limit	10^{10} rads
Upper Limits on Number of D-T Pulses:	
Lifetime Limit	Equivalent to 4000 full energy pulses
Annual Limit	Equivalent to 1000 full energy pulses
VACUUM VESSEL	
Vessel Material	AISI 316 SS
Construction	I-Beam stiffened shells (w/o bellows)
Vessel Cross-Section	Elliptical
Segmentation	Not factored into models
Wall Thickness	Variable
Toroidal Limiter	One or two tungsten segments (radiation cooled)
Diagnostic Penetrations	Fixed number
Peak Bulk Wall Temperature	400°C
Vessel Coolant	Water
TOROIDAL FIELD COILS	
Number of Coils	Variable
Conductor Type	
TNS-1	Copper (H_2O-cooled)
TNS-3	NbTi (LHe-cooled)
TNS-4	Nb_3Sn (LHe-cooled)
TNS-5	Copper/NbTi (H_2O-LHe-cooled)
Coil Shape	Constant tension "D"
Peak Field at Conductor	Copper - Variable, but values considered up to 14T
	NbTi - Variable, but values considered up to 10T
	Nb_3Sn - Variable, but values considered up to 14T
Cooling Mode	Single phase forced flow
Fault Protection	Electrical provisions only
POLOIDAL FIELD SYSTEM	
Conductor Material	Oxygen Free High Conductivity (OFHC) Copper
Location	OH windings outside TF; VF windings inside TF
OH Flux Swing	Variable
Conductor Current Limit	20 kA
Conductor Current Density Limit	1.5 kA/cm^2
Conductor Coolant	Forced flow water

TABLE 3-1 (Continued)

IMPURITY CONTROL TECHNIQUE	Wall treatment (low sputtering liner, low Z wall, etc.) Note: It is recognized that a magnetic divertor may be necessary. This was examined in a parallel study.
VACUUM PUMPING	
Final Pumping Stage	Cryosorption pumps
Base Pressure (Pre-Pulse)	1×10^{-8} torr
Outgassing Surface Area	Ten times smooth area of vessel
TRITIUM SYSTEMS	
On-Site/In-Process T_2 Inventory	Variable
Tritium Storage	Uranium chip beds
Fuel Recovery-Recycling Plant	Variable Capacity (common approach)
Tritium Cleanup Systems	Variable Capacity (common approach)
Fueling	Prefill: Gaseous D-T Refueling: Solid T and D-T pellets
NEUTRAL BEAM INJECTION LINES	
Beam Power Energy	150 keV; variable power
Single Arm Specifications	
Sources	3-100 A positive ion
Dimensions	7.5 m long x 4 m wide x 6 m high
Number	Varies with plasma conditions
Vessel Aperture per Line	Duct 44 cm wide x 120 cm high
Duct Shielding	As required by coil type
HEAT DISSIPATION SYSTEMS	
Final Facility Heat Sink	Mechanical draft evaporative cooling towers to atmosphere
Vacuum Vessel Coolant	Water - variable capacity
Shield Coolant	Borated water - variable capacity
Buffer Loop Coolant	Water - variable capacity
Cryogenic Refrigeration Systems	Variable capacity
Facility Air Conditioning	Fixed base load, reactor cell air conditioning variable
Thermal Loads	Variable - depending on option
OPERATIONAL DIAGNOSTICS	
Number, Type, Penetrations	Constant in all studies
ELECTRICAL SYSTEMS	
Facility Feed	Fixed utility constraints
S/C TF Supplies	Line-driven rectifier supplies (except for hybrid)
Cu TF Supplies	AC-MG storage-rectifier conversion
Neutral Beam Supplies	AC-MG storage-rectifier conversion
Poloidal Field Power Supplies	AC-MG storage-rectifier conversion
Electrical Loads	Variable - depending on option
Instrumentation and Control	Fixed for all options
ARCHITECTURAL AND FACILITY	
Site	150 m radius site boundary "free-standing"
Reactor Cell	Reinforced ordinary concrete Fixed: walls (~2.9 m); ceiling (~2.3 m) Vertical height fixed Floor space, basement: variable
Electrical Power System Buildings	Variable
Balance of Plant Buildings	Fixed

To reduce the number of variables to a manageable level, engineering (and physics) judgement was used to fix certain parameters for these studies. This does not preclude treating these items as variables in later cost/size sensitivity studies. As the study progressed, for example, many items that were fixed at the beginning were revised and permitted to be a variable in subsequent evaluations. All of the groundrules remain subject to change as new information becomes available or modeling improvements are made.

3.2 DEVELOPMENT OF SYSTEM AND COMPONENT DESIGNS AND SIZE/COST SCALING RELATIONSHIPS

In creating the system modeling to be used in performing the TNS trade studies, it was necessary to ensure that a firm engineering basis for technical decisions was established. This was done by developing engineering representations for each of the major tokamak systems and subsystems necessary in any given TNS and then developing algorithm representations of these engineered systems and subsystems so as to permit scaling each system in size in a manner consistent with the changes in plasma size and coil technology.

This part of the process required separate engineering design studies to be performed in many of the tokamak systems and subsystems to examine the most promising alternatives and from these make a selection and then adopt that alternative for incorporation into the computerized calculational model employed in performing the trade studies.

Similarly, it was necessary to develop costing information on system and facility components and based upon this costing information develop scaling algorithms for use in performing the trade study investigations. The details of this process are more thoroughly discussed in the progress reports issued during this study (References 7, 8, 9, 10). A description of many of the key systems is given in Section 5.0.

3.3 DEVELOPMENT OF COAST, A COMPUTER CODE FOR THE COSTING AND SIZING OF TNS TOKAMAKS

The engineering characteristics of the tokamak device to follow TFTR could take on a number of different forms with plasmas ranging from TFTR size (and smaller)

to EPR (Experimental Power Reactor) size. The variations in cost and degree of performance margin for a successful demonstration of ignition are as equally varied. To allow the various options to be examined under a common set of engineering groundrules, the COAST (COast And Sizing of Tokamaks) code was developed. This code was extended and upgraded several times, and the current version is version three.

The code has been written for evaluating, in a quantifiable manner, TNS engineering considerations. The plasma is specified primarily via input data; e.g., results from plasma modeling studies or calculations, and the tokamak device sized by COAST provides all the support systems required for the assumed plasma. Over forty subsystems or components are represented in the code calculations, thus providing both flexibility and refinement in examining any given design.

3.3.1 CODE LOGIC

The basic logic of COAST is shown in Figure 3-1. The calculations are separated into sections which provide for the component and system sizing based on engineering models and the costing of components and systems based on cost relationships. The device features and component sizes are specific to the tokamak and plasma dimensions under consideration. The cost representations have been developed based on unit cost relationships and are independent of a given tokamak design. As an example, the OH coil assembly is sized consistent with the available machine bore, but costs for the coils are obtained on the basis of fabricated conductor mass required. In this example, the volt-seconds and bore requirements are specific to a particular design, while the costing depends only on quantity of materials and fabrication.

The code input is divided into three distinct types of data as indicated in Figure 3-1. In general, the physics input is device independent; whereas the engineering constraints are associated with a specific device design. The cost data are in the form of cost coefficients for a component unit size; e.g., cost per kg of fabricated stainless steel for a TF coil bucking cylinder.

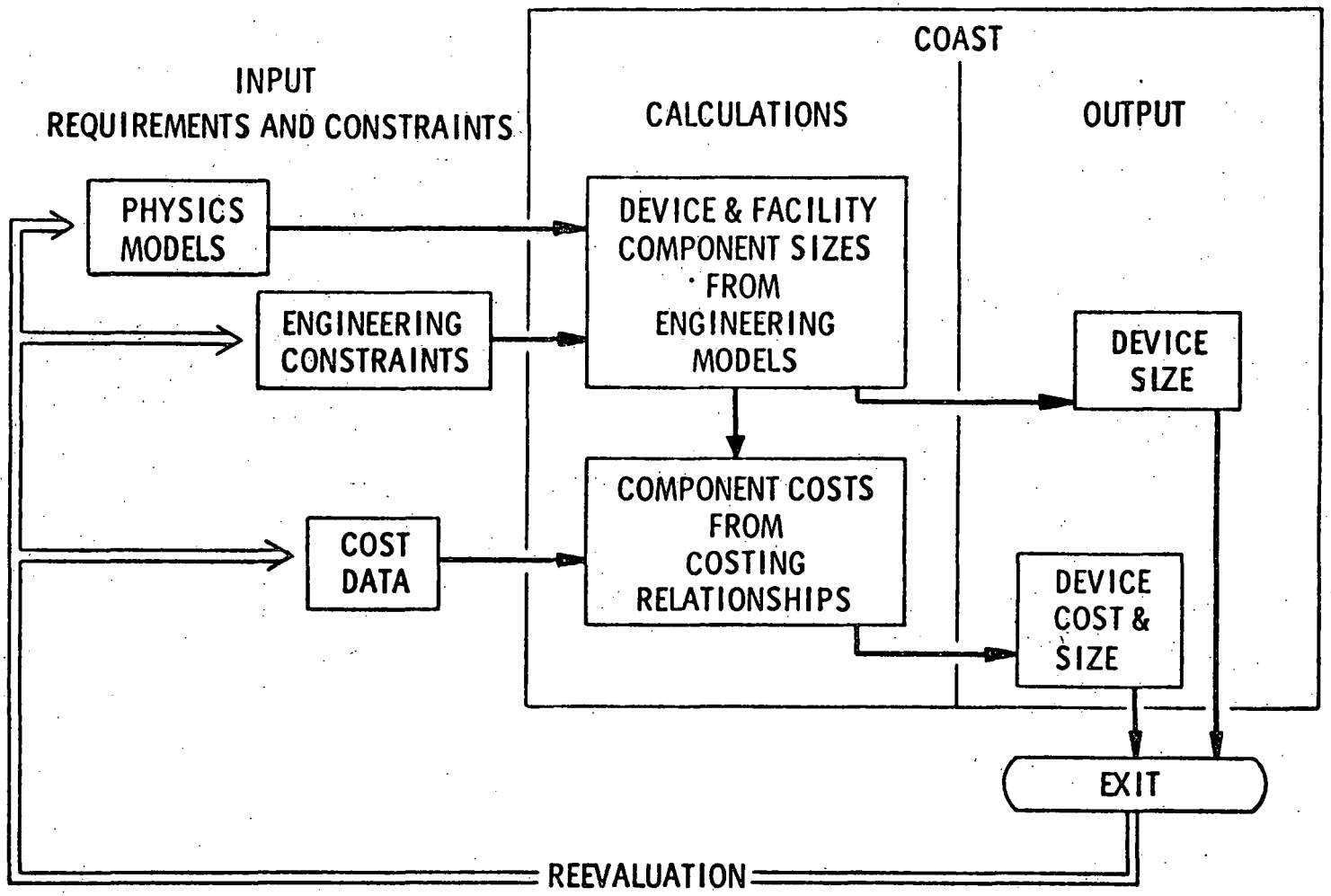

Figure 3-1. A Logic Diagram Showing the General Features of the COAST Code and Its Incorporation in the TNS Trade Study

The code was written consistent with groundrules established for TNS. Within limits set by those groundrules, the code was generalized to the greatest extent possible. As much as possible, constraints and groundrules have been incorporated as input data and these can be readily changed to be compatible with the design assumptions, but there are a number of constraints which could only be incorporated directly in the code logic. Examples include the following:

- The sizing of four TF coil technologies are incorporated in the code logic. Included are copper, niobium-titanium (NbTi), niobium-tin (Nb_3Sn), and a hybrid design using both a copper and a superconducting (NbTi) coil system.
- The TF coils are modeled as having a D-shape (circular TF coils were later added to model TFTR) and a trapezoidal cross-section over the entire coil circumference.
- The Cu TF coil power conversion system requires a motor-generator-flywheel set.
- For the PF coils, only copper conductors are permitted.
- OH coils are within the machine bore.
- The shaping field coil currents follow the plasma current at a fixed ratio.
- The plasma is assumed to be elliptical and heated by neutral beams to the required temperature.
- The vessel and shield cooling system employs water coolant.
- There is no thermal-to-electrical power conversion.
- There is no tritium breeding.
- The code sizes a complete facility including a cylindrical dome-topped reactor cell which is a shielded structure.
- The tritium systems include recycling of spent fuels with the incorporation of cryogenic distillation processing and equipment for pellet fabrication.
- Complete remote servicing, a standby emergency system, and a radioactive waste handling service are also represented.
- Poloidal field coils located within the TF coil bore.

To maintain flexibility in COAST to allow further development and expansion, each subsystem calculation not only generates relevant data to size the subsystem, but at the same time generates any data which has been identified to impact the sizing and costing of any other subsystem.

3.3.2 CODE REPRESENTATION OF TWO KEY TOKAMAK SYSTEMS

TOROIDAL FIELD (TF) COILS

The selection of coil technologies and associated parameters is provided by a number of input control integers. Prior to any calculations on the sizing of the TF coils, a number of device and plasma parameters are known either as input or calculated values. For example, these include the space required in the TF coil bore for the vacuum vessel, shielding, etc.; the TF ripple limits at the coil conductor and at the plasma edge; and the neutral beam (NB) access space. The design parameters required for the TF coil calculations are basic to most coil designs and include: maximum allowable field at conductor, structure area to conductor area ratio, packing factor for conductor elements, conductor current density, heat loads to the coil cooling system, refrigerant pumping powers, specifications for power conversion equipment, etc. All coils are assumed to have a trapezoidal-shaped cross section over the entire coil circumference and centering forces are handled either via wedging, or a bucking cylinder, or a combination of the two. In each coil calculation, various device requirements must be met to assure system self-consistency. Requirements such as TF ripple limits, NB access, vertical and horizontal space required, machine bore space required, and magnetic field limits are checked for such self-consistency.

The resistive copper coil employs a stainless steel structure and uses either water-cooling or liquid-nitrogen cooling for a pulsed-mode of operation. The energy storage system for the copper option has been modeled with considerable refinement. For the two superconducting systems under present study, i.e., NbTi and Nb_3Sn, if a bolted construction with stainless steel is assumed, the structure-to-conductor ratio is calculated; otherwise, this ratio is required as input. The superconducting options have dewars around the coils (a common dewar for the inner legs) and the heat dissipation system is modeled taking into account a number of heat sources (ac losses, joint losses, etc.). The power

supply requirements for the superconducting coils, which are operated in the steady state, are modest and involve only the charging and discharging of the coils before and after periods of downtime. The fourth coil type is a hybrid having an inner coil of copper operated in a pulsed mode and an outer coil of superconducting NbTi. The code logic for developing the sizing of the hybrid system is considerably more complex than for the other coil types and is a combination of the logic developed for the copper option and the superconducting NbTi option. To handle the mutual interaction between the pulsed copper coils and the superconducting coils, the power conversion system for the superconducting coils is comparable to that for the copper coils. Fiqure 3-2 indicates a plan and elevation view of a device with superconducting TF coils as represented in COAST.

POLOIDAL FIELD (PF) COILS

The poloidal field coils consist of an ohmic heating (OH) coil set which initiates the plasma current and an equilibrium field (EF) coil set. All of the PF coil assemblies are copper systems. The OH coils are located in the machine bore and have an air core. The equilibrium field (EF) coils can be located either within the TF bore or outside the TF coils. The various self-inductances and mutual inductances between various coil groups and between each group and the plasma can be input data or can be calculated from the coil geometry. If the EF coils are external to the TF coils, the various inductances must be supplied to COAST. The coil voltages and currents are calculated as a function of pulse time for purposes of rating the various power supplies. The code logic does not involve any system for establishing plasma stability or equilibrium criteria; it is assumed that such considerations are handled elsewhere either before or after a COAST calculation. For these calculations, the EF coil currents are modeled as a ratio of the plasma current for three groupings of coils - one group between the TF inner leg and plasma, a second between the TF outer leg and plasma, and a third group above as well as below the plasma. The coil voltages and the OH current are functions of the plasma volt-seconds (both inductive and resistive), the plasma current, and the coil current biasing on the OH, as well as the various self and mutual inductances. A model allows the resistive volt-seconds dissipated in the plasma to be estimated. The coil resistances are also calculated (or read in as an alternative), and the total energy per pulse required to operate the EF coils is estimated.

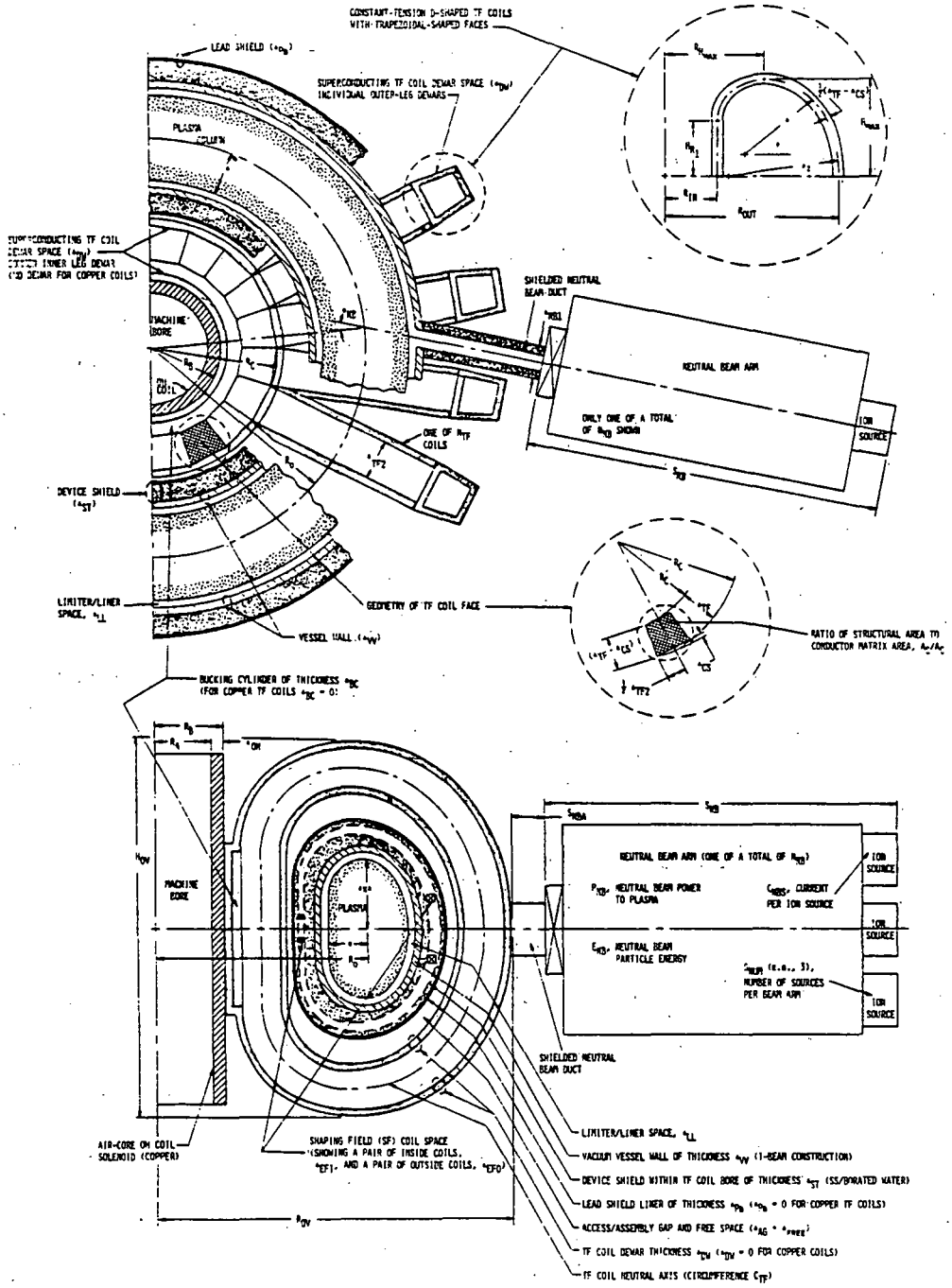

Figure 3-2. Two View Schematic of S/C TF Coil Device

3.3.3 TOKAMAK SUPPORT SYSTEMS CONSIDERATIONS

The tokamak support systems modeled in COAST are those involving remote servicing, gas handling, vacuum pumping, heat removal, ventilation and air conditioning, and radioactive waste handling. Each of the models is based on a reference system which resulted from an engineering study to develop a reasonably detailed pre-conceptual design. These systems support the plasma and tokamak device and are modeled as functions of the plasma volume, reactor cell volume, or the various power and energy levels. Only the remote servicing was modeled independent of the device size or option. The gas handling systems include tritium storage, fuel fabrication, fuel processing, cryogenic distillation, and tritium cleanup (of vacuum vessel and reactor cell). Dependence on the volume of the reactor cell is modeled in the gas handling, the ventilation, and the radioactive waste handling systems. The heat transport systems have been modeled with sufficient refinement to size the individual subsystems for the water cooling of the vacuum vessel, the copper magnetic field coils, the radiation shielding, and the general plant cooling. In addition, the superconducting liquid helium system and the liquid nitrogen systems (for the superconducting coils) are modeled with reasonable detail. The vacuum pumping system is modeled as a function of the pumping speed required to reach base pressure and of the amount of vessel surface area on which each pumping station will operate to provide that pressure. Figure 3-3 is an illustration of how the reactor cell is modeled in COAST.

3.3.4 DEVICE AND PLASMA OPERATING SCENARIO

A number of parameters are required as input in order to specify the operating mode for the device and plasma. For the plasma, these include values for the various time periods, i.e., gas ionization and plasma initiation, plasma startup, neutral beam injection, thermal excursion to steady state, ignition or burn steady state, and plasma termination. Input is required for the time interval between plasma initiation, Cu TF coil charging time, Cu TF coil flat-top time, superconducting TF coil charging time, operating hours per day, operating days per week, device down time, etc. The plasma resistivity during the pulsing period, safety factor during initiation, and required externally-applied breakdown voltage must be specified by the user. The plasma time-dependent characteristics such as the current and temperature profiles are assumed to vary linearly or are constant with time over each time interval. The plasma radius is a constant over the initiation

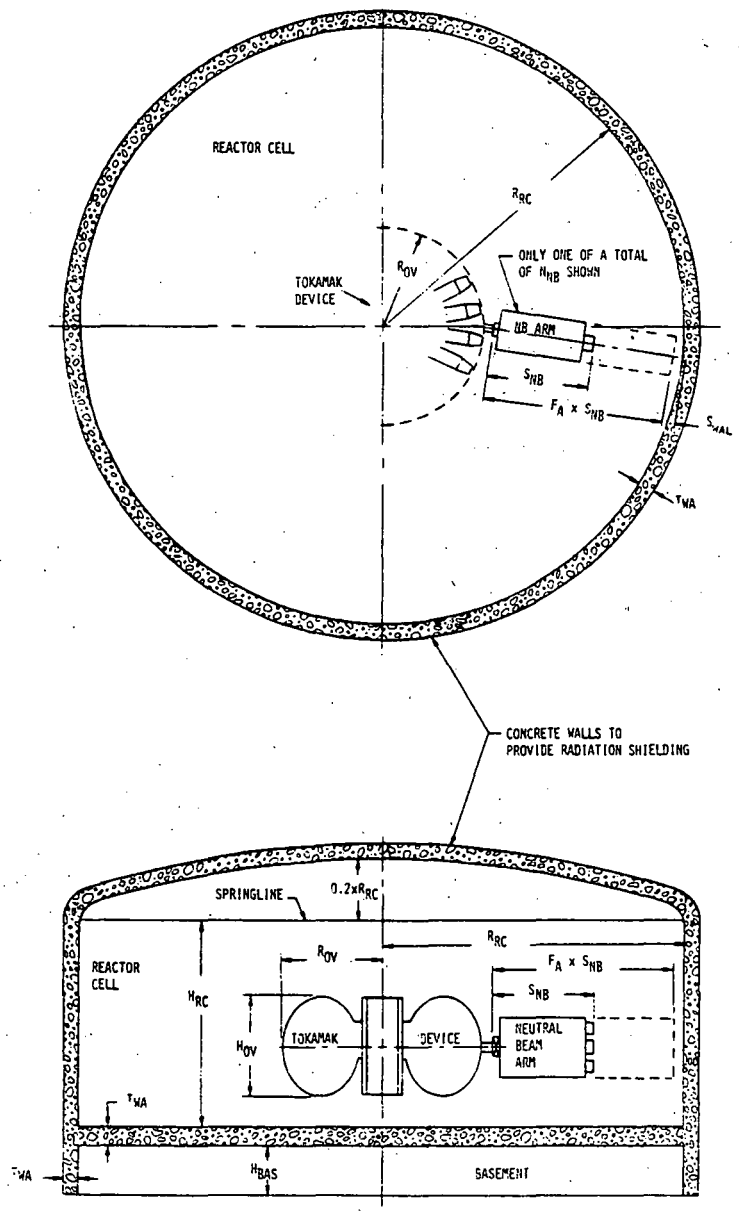

Figure 3-3. Two Views of the Reactor Cell Enclosing TNS are Shown. Dimensions are Indicated to Show the Cell Size Dependence on the Device and NB Arm Sizes

period (specified by input data) and then increases linearly with time until the end of the plasma startup at which time the plasma is at full radius. The plasma inductance at each time is calculated consistent with the plasma radius at that time. With these calculations, the volt-seconds required of the PF coil systems are estimated so that the power conversion systems can be rated and costed.

3.3.5 COSTING REPRESENTATION

For the purpose of costing TNS, the main subsystems and components making up the device and facility have been divided into five categories. The first is the tokamak systems which involve the basic device including the magnetic field coils and all the systems within the TF and machine bores such as the vessel, poloidal divertor, machine structure, and device shielding. The next category is the electrical power and control systems which include all the energy storage, power conversion, instrumentation, and controls for all the coils and the NB arms, plasma diagnostics, and emergency systems. The tokamak support systems represent the third category. The fourth set of systems involves the structures and service equipment for the facility. Included in this are the reactor cell (a shielded structure); buildings for power equipment, neutral beams, controls, etc.; cranes and crane erections, shops, etc. The last category is the neutral beam injection system including the NB arms and the power conversion equipment.

The cost relationship for each of the individual subsystems or components is represented in a manner to allow maximum flexibility. Specifically, each component cost is calculated as the product of a cost per unit of size (or rating) multiplied by the size (or rating) calculated in the sizing portion of the COAST code. The cost coefficients are supplied as input data and for the TNS study were obtained by performing a bottoms-up estimate of each system or subsystem. There are some variations which involve linear combinations of this pattern or which involve raising the sizing magnitude to a power. For an example of the normal pattern, the cost of the vacuum vessel assembly is obtained as the product of a unit cost per kg of fabricated stainless steel multiplied by the mass of the vessel. As an example of a variation, the PF coil water cooling system is obtained as the sum of three terms involving a unit cost for each term multiplied by a peak power level, an average power level, or a total energy per pulse. Each

of these three ratings are exponentiated in the cost equation. The many unit costs (~100) incorporated in COAST are separate from the details of sizing the tokamak and can be evaluated independently from studies of fabrication, machining, and assembly engineering considerations as in the TNS study.

3.4 TRADE STUDIES USING COAST

A series of parametric trade studies was performed to consistently evaluate the relative costs and performance parameters of D-T burning tokamaks over a range of plasma sizes and toroidal field (TF) coil technologies. As indicated earlier, four different types of TF coil technologies were investigated: water-cooled copper coils, superconducting NbTi and Nb_3Sn coils, and a "hybrid" coil arrangement consisting of a normal conducting Cu coil nested within a superconducting NbTi coil. This section presents a condensed description of the trade studies which were performed which provided the quantitative basis from which the four reference design systems described later in Section 4.0 were selected. A more detailed description of these trade and sensitivity studies is contained in a companion report[2].

3.4.1 GENERAL CONSIDERATIONS

There are a number of distinctly different options of plasma size and toroidal field (TF) coil technology which could satisfy the objectives of The Next Step (TNS) tokamak. The plasma size is an important parameter because it directly translates into machine and plant size and cost. In addition, the plasma size is a key parameter in evaluating the flexibility of the system to achieve the objectives. The TF coil technology is important because available options exhibit a certain range in the maximum magnetic field and a wide range of system complexities. Accordingly, this parametric trade study was performed and the results of this analysis are available for use in selecting the features of a particular ignition device.

The device sizes considered in these trade studies for the four TF coil technologies covered a range in the plasma radius (or half-width) from ~0.75 m to 2.0 m, thereby spanning the range from TFTR size plasmas to those chosen for recent Experimental Power Reactor (EPR) design studies. The device major radius was

varied from 8-9 m down to some lower limits (4-5 m) which were consistent with the groundrules and engineering design considerations. This design space is illustrated in Figure 3-4. In most cases, the plasma elongation was kept at 1.6. The plasma beta value was selected as a key parameter on which to judge the performance or "confidence of success" of each ignition device, and was allowed to vary in the range from 2% to 15%. Two different plasma confinement scaling relationships (empirical and trapped-particle-mode) were used to specify the physics parameters for an ignition device.

3.4.2 METHOD OF ANALYSIS

An indicated, the major tool used in performing these trade studies was COAST. As described in Section 3.3, an extensive set of numerical calculations are performed in the code to assess the dominant features of TNS ignition tokamaks with different TF coil conductor materials. Required input data include parameters characterizing engineering constraints such as conductor current densities, magnetic field ripple limits, nuclear heating and dose limits, and power supply parameters, in addition to the plasma parameters obtained independently from the scaling laws. Sizing and costing models are incorporated for various components of the tokamak system. Sizing and costing calculations are also performed for several auxiliary components such as tritium and fueling systems, power conversion systems, heat removal systems, and the reactor cell and other facilities. The COAST code provides a generalized description of TNS and allows one to study the impact of the design features of individual components on the overall system.

Required input to the COAST code includes the physics parameters such as density, temperature, and field on axis required for predicted ignition in a given size device. In these trade studies, two plasma scaling laws have been used to predict this information. The first model is based on empirical plasma scaling,[11] which has been observed in present day resistively heated, high collisionality tokamak experiments. The second scaling is based on a trapped-particle-mode (TPM) plasma transport model,[12] which involves numerically solving the spatially averaged plasma energy balance equations using theoretical models for the different regimes of particle transport. The main trends and conclusions from the study are found to be fairly

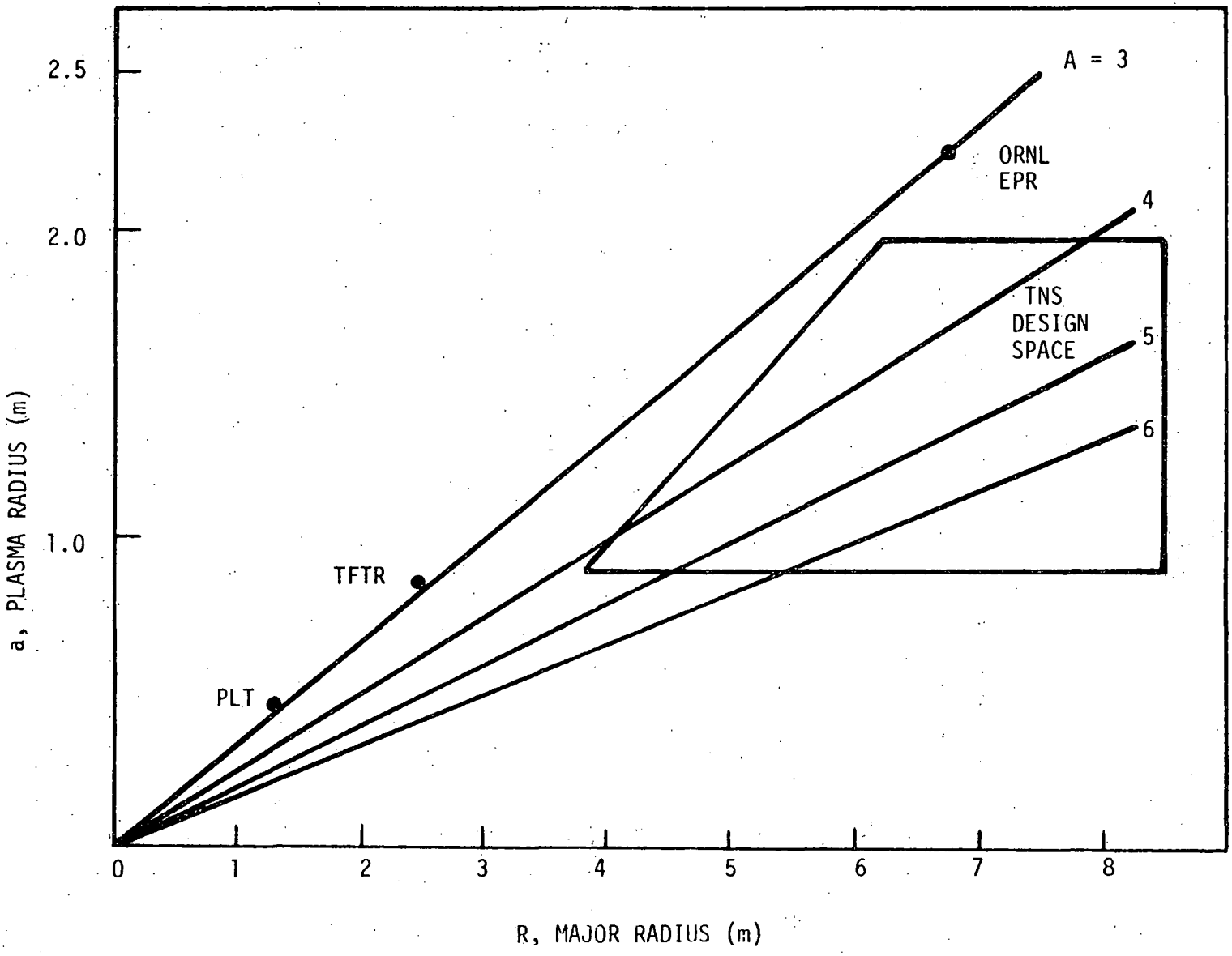

Figure 3-4. TNS Design Study

insensitive (within ∿10%) to the scaling law used to specify the physics parameters of an ignition device over the range of design space investigated. The plasma temperature has been assumed to be 13 keV, representing a volume averaged value for steady state operation under ignition conditions.

For most of these studies, the plasma pulse time operating scenario has been held fixed under the assumptions of a one second initiation and startup period, a six second neutral beam injection period to reach ignition, an eight second period which a thermal excursion occurs to reach steady state conditions, followed by a 16 second steady state burn period and then a two second quench. Hence, the total pulse length is $\simeq$ 33 seconds. The time between pulses is fixed at five minutes (300 s), and there are assumed to be the equivalent of 1,000 full power D-T pulses per year.

The costs determined for the TNS devices are those for the buildings and equipment in 1977 dollars. They include all of the hardware for the tokamak system and the support systems, the electrical power conversion and control systems, the neutral beam systems, and the reactor site and buildings. Not included are the costs for installation and costs for engineering, design, inspection, and administration (EDIA), Also, not included is a factor for contingency. The values used in this study are thus direct costs only.

3.4.3 SUMMARY OF TRADE STUDY ANALYSIS RESULTS

In this section the results of an analysis using the COAST code are presented and discussed for the four TF coil technologies considered for the TNS design studies. In order to consistently evaluate and compare the relative costs and sizes of different TNS options, it is necessary to also consider some measure of the confidence of success of each device. An important device parameter is the plasma beta, β, defined as the ratio of the volume averaged plasma pressure to the toroidal magnetic field pressure. The plasma β is a critical parameter for at least two reasons; because the plasma MHD stability is dependent on β and also because β is a measure of how efficiently the magnetic field strength is utilized. Since the primary mission of TNS will be to demonstrate ignition conditions and burn dynamics under the long pulse durations, the minimum β for which it is designed to operate will be an extremely important quantity in judging probability for success. Current estimates based on linear ideal MHD stability calculations indicate that values of β

in the range of 5-10% should be acceptable. Although TNS will be designed with the capability of operation at some minimum β, operation at higher β's could be tested either by increasing the density or decreasing the field strength at the TF coil. These tests of high β operation in TNS will be extremely important in establishing what the upper limit on is for stable plasmas, which is very important from a reactor viewpoint. However, TNS should not be designed only to operate at these high β's; i.e., TNS should have the capability to test high β but should not rely on it for successful demonstration of ignition until high β operation is experimentally demonstrated.

In Figure 3-5, the relative cost of devices with Cu TF coils is plotted as a function of major radius, R_o, for different values of the plasma half-width a. These curves were obtained using empirical scaling, 20 TF coils, and an elongation of 1.6. The plasma β is kept constant at 5% for these cases by varying the peak field at the TF coil, B_{max}, for each device size. Lines of constant values of B_{max} of 9T and 10T are shown for reference. From the figure, it can be seen that there is a minimum in the cost for each plasma radius at a certain major radius R_o. For larger values of R_o, the overall size of the device dominates the cost, even though the field at the TF coil is decreasing in order to keep β at 5%. For smaller values of R_o, the cost also increases due to two effects - increased cost of the TF coils at the higher B_{max} values and increased power conversion costs to supply the necessary flux swing through the smaller machine bore. The curves terminate at the "bore size limit" due to the fact that there is a minimum allowable R_o which is set by engineering considerations.

In Figures 3-6 and 3-7, similar plots of the cost versus R_o are shown for the superconducting TF coil technologies for a plasma β of 5%. In Figure 3-6 for the NbTi coil devices, one can see the consequences of the lower peak field limits of the NbTi conductor, namely that the relative cost is higher due to the larger machine sizes necessary to achieve β = 5%. The curves terminate at a peak field limit of 10T, with an associated technological risk for the NbTi coils. Note that 5% β devices with 8T at the NbTi coils require very large and costly sizes. In Figure 3-7 for the Nb_3Sn deivces, it can be seen that peak fields in the range of 11 - 12T are needed for β = 5% in smaller size and cost devices. The reason that the superconducting options require a higher peak field

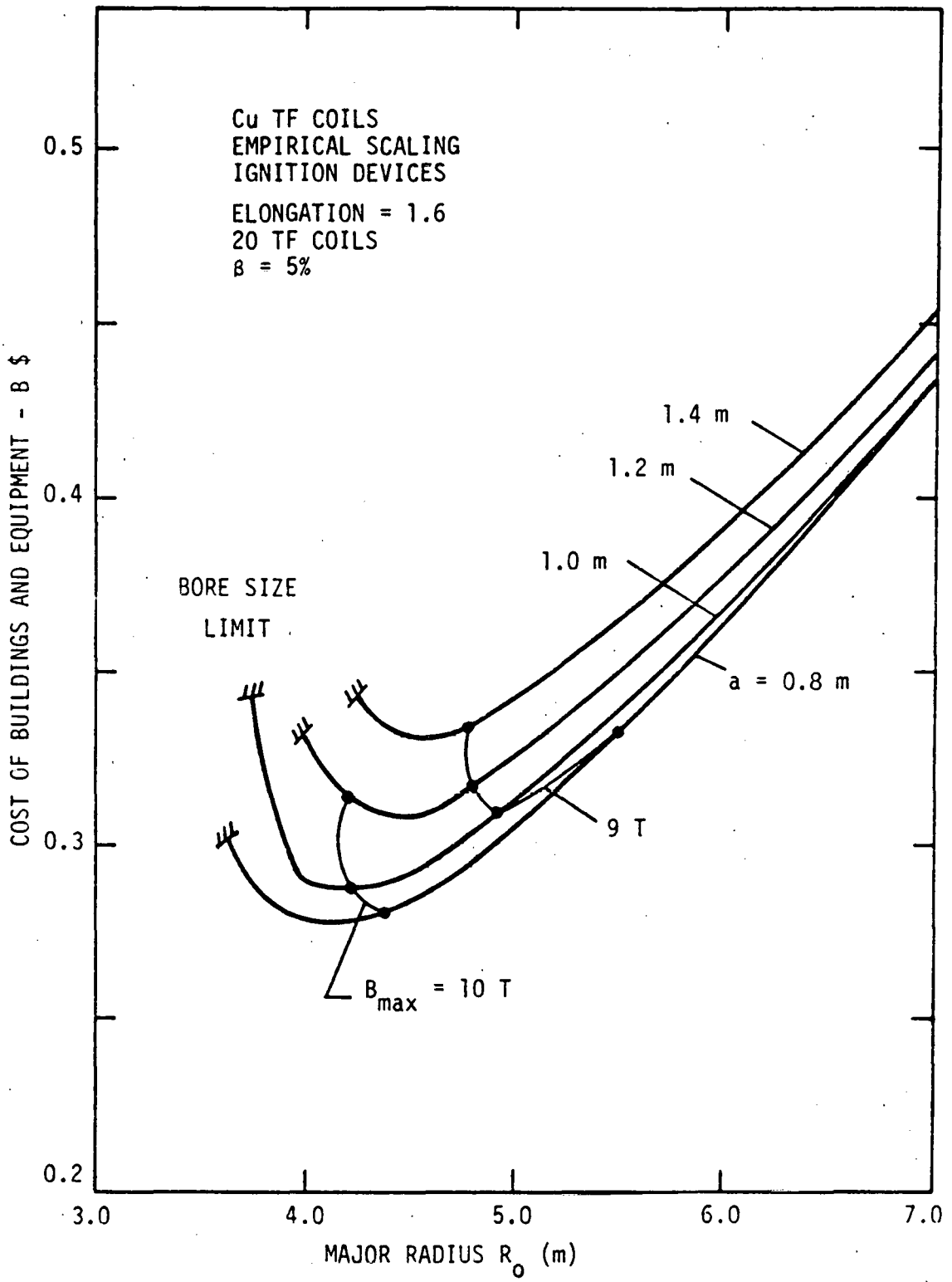

Figure 3-5. Cost of CU TF Devices at β = 5%

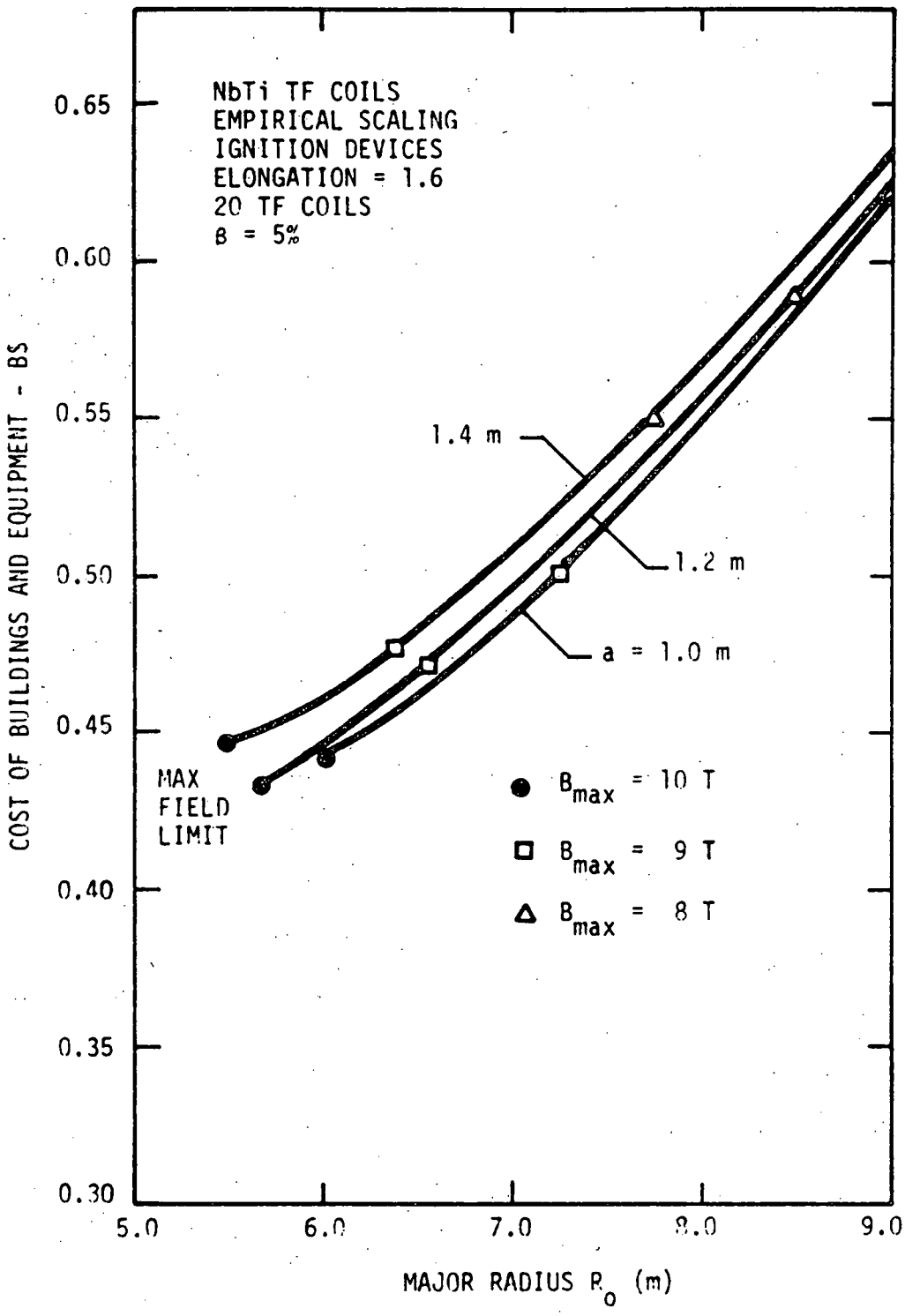

Figure 3-6. Cost of NbTi TF Devices at β = 5%

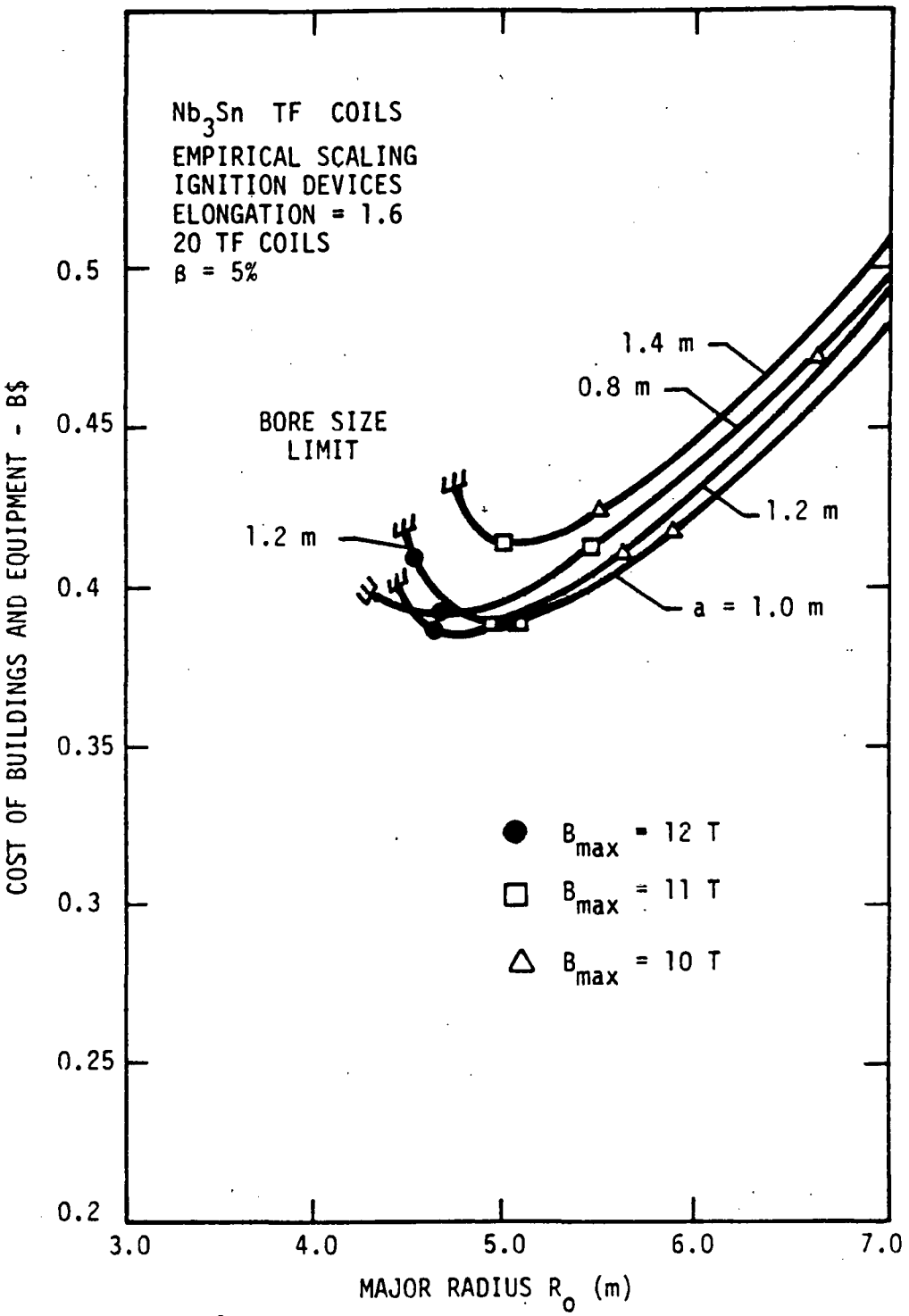

Figure 3-7. Cost of Nb_3Sn TF Devices at β = 5%

than the Cu option in order to achieve the same field on axis (i.e., same β) is the additional shielding space required to reduce the nuclear heating in the superconducting coils. This shielding space plus a dewar thickness results in a larger distance between the plasma center and the edge of the TF coil, and hence a higher peak field requirement for the NbTi and Nb_3Sn coils. Similar curves for the hybrid NbTi/Cu coil option shows peak fields at the Cu coil in the range of 9 - 10T are necessary to achieve β = 5% in smaller sized devices.

By examining these three figures, one can make several observations. For example, for each coil technology, there is a minimum cost device at a particular a, R_o, and B_{max} which achieves ignition at a β of 5%. Similarly, curves for other β values exhibit this same trend. For the Cu and Cu/NbTi options, this minimum occurs at the smallest minor radius which was examined, 0.8 m. However, for the superconducting NbTi and Nb_3Sn options, the least costly device does not occur for the 0.8 m plasmas. This is because the smaller plasmas must operate at higher densities in order to reach ignition, and thus require higher fields to still achieve a β of 5%. For superconducting devices, the TF coils constitute a higher fraction of the total cost, and hence smaller devices can be more expensive than slightly larger ones which operate at the same β. Of these minimum cost devices, the Cu TF option is the least expensive due to its ability to deliver a higher field on axis in a more compact device. These figures also are able to answer the question of what is the cheapest way to deliver a certain field on axis - by increasing the device size at lower TF coil peak fields or increasing the peak field for smaller device sizes? The results tend to show there is a compromise between the two, but in general, it appears to be less expensive to go to higher fields in more compact device sizes.

Information similar to that presented in Figures 3-5, 3-6, and 3-7 was generated for the hybrid (Cu/NbTi) TF coil devices. In addition, similar evaluations were performed for other values of β, for a varying number of TF coils, for a range of assumed elongations and for trapped-particle-mode confinement.

As noted above, for each technology and plasma beta at ignition, there is a minimum cost device at a specific a, R_o, and B_{max}. A composite plot of these minimum

cost devices vs. the operating β value is shown in Figure 3-8 for the four TF coil technology options. Values of a, R_o, and B_{max} at the end points of β = 2.5% and β = 10% for each coil type are shown for reference. Note that there is a rather sharp increase in cost as the β is decreased, due to the required larger device sizes and peak fields. Likewise, the cost decreases for higher β because a, R_o, and B_{max} can be decreased. Also, it can be seen that for any β the Cu TF coil devices can be built for the least cost. The Nb_3Sn coil devices are about 30% more expensive that the Cu, while the NbTi and Cu/NbTi hybrid options are about 50% more costly for most β values. A similar observation is that for the same cost, a Cu TF coil device can operate at a lower β than the other technologies. Likewise, Nb_3Sn devices can operate at lower β values than either NbTi or Cu/NbTi devices for the same cost.

This brief summary of the approach used in the TNS trade studies has been incorporated here to demonstrate the broad range of potential sizes which exist from which to select the parameters for a specific device size for a specific toroidal field technology. The remainder of this document focuses on the characteristics of four specific TNS reference point designs, one of each of four toroidal field technologies under consideration. The considerations forming the basis for this selection are discussed in the following section.

3.5 BASIS FOR SELECTION OF FOUR REFERENCE POINT DESIGNS

The process of choosing four "typical" point designs, each representing a candidate TF magnet technology, was complicated by the desire to use these designs for a consistent comparison of the implications of TF technology selection. Simply choosing the minimum cost devices on a global basis was not practical since these devices would tend to have uncomfortably high values of toroidal beta or uncomfortably small plasma dimensions. The criteria developed were the following:

- Ignition as calculated using empirical scaling. No margin in $n\tau$ or magnetic field would be provided for in the selection, though, of course, margins in these areas would be considered in a final design.
- Plasma minor radius $\geq$1 m. While the assumed scaling laws predicted smaller ignition devices at relatively high magnetic fields, a

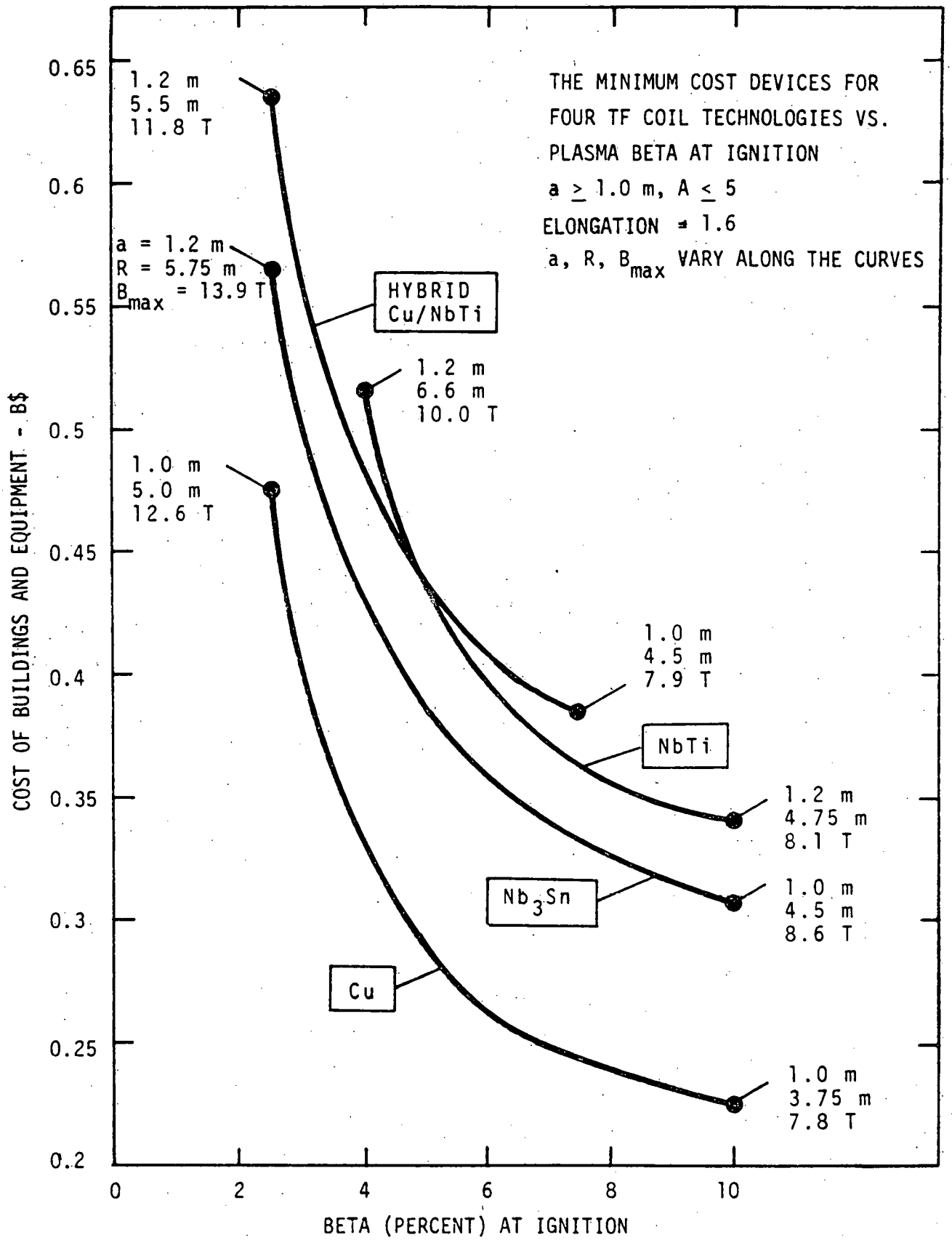

Figure 3-8. Minimum Cost Devices vs. Percent Beta

radius larger than 1 m was generally required to provide a plasma current, Ip, >3 MA. Based on alpha-particle confinement considerations, a plasma current $\geq$3 MA was considered essential.

- Aspect ratio <5 - based upon gross stability considerations.
- Minimum cost at an average toroidal beta fixed at 5%.

The plasma β is a critical parameter as indicated earlier. The achievement of high values of beta will permit the development of relatively compact and potentially less expensive machines, however, current estimates based on linear, ideal MHD stability calculations indicate that the largest achievable β's will be in the range of 5 - 10%. On this basis it was felt reasonable to use a fixed β of 5% as a common measure of plasma performance, along with the other stated criteria. Each of the devices selected would then be capable of testing high β operation, but successful demonstration of ignition would be predicated on achieving β = 5%.

Using the preceding criteria, including a fixed β = 5%, and using the COAST generated trade study results as typically illustrated by Figures 3-5 through 3-8, four reference point designs were selected.

4.0 PARAMETERS FOR FOUR REFERENCE POINT DESIGNS FOR TNS

The design features for four reference point designs for TNS are presented in this section. These features include the key plasma parameters, the overall machine parameters, the magnetic field coil specifications, the thermal and auxiliary heat loads, the electrical load parameters, the fuel parameters, the neutral beam arm parameters, and the torus vacuum vessel and pumping system. These parameters are presented in the form of comparative tables for easy reference. In addition to the key size and performance parameters, the associated capital equipment and operating costs are presented for the four designs, again in comparative tables. Also, the operating scenarios are given. Finally, layouts of each of the four designs are presented.

The four reference point designs have not been optimized on a total system basis (from either the cost or performance point of view). However, each design is self-consistent and fully delineated in terms of the arrangement, size and/or rating of major components in both the tokamak and in the required overall facility.

4.1 PLASMA RELATED PARAMETERS

Table 4-1 summarizes the key plasma related parameters for the reference designs. Key parameters which are fixed for all four designs include plasma elongation (1.6), toroidal beta (5%), mean ion temperature (13 keV), ignition parameter ($\bar{n}_e \tau_E = 2.4 \times 10^{20}$ m^{-3} s), maximum TF ripple at the plasma (peak to avg = 1.0%), number of TF coils (20), the neutral beam energy (150 keV) and operating scenarios. Figure 4-1 illustrates the standard operating scenarios assumed in the studies. A plasma burn time of 16 s and a pulse operation interval of 300 s was fixed for the present comparison; however, these quantities were varied in the trade study to establish cost sensitivity.

Note that the maximum plasma current for these designs exceeds 3.5 MA in each case. The average neutron wall loading is $\sim$1.25 - 1.50 MW m^{-2}. The total fusion power (based on 21 MeV per reaction) developed by the reference designs ranges from 558 to 795 MW, which is judged reasonable from the point of view of heat

TABLE 4-1

KEY PLASMA RELATED PARAMETERS

(Empirical Scaling)

	TNS-1	TNS-3	TNS-4	TNS-5
TF Coil Conductor	Copper	NbTi	Nb_3Sn	Copper/NbTi
Major Radius (m)	4.0	5.7	5.0	4.5
Minor Radius (m)	1.0	1.2	1.2	1.0
Elongation	1.6	1.6	1.6	1.6
Shape Factor	1.3	1.3	1.3	1.3
Aspect Ratio	4.0	4.75	4.17	4.5
Energy Confinement Time (s)	1.36	1.63	1.63	1.36
Volume (m^3)	126.3	259.2	227.6	142.1
Safety Factor	3.0	3.0	3.0	3.0
Toroidal Field on Axis (T)	5.78	5.28	5.28	5.78
Average Ignition, β	0.05	0.05	0.05	0.05
Max. Plasma Current (MA)	4.07	3.76	4.28	3.62
Plasma Inductance (10^{-6} H)	7.58	11.99	9.74	9.17
Max. TF Ripple (Pea--Avg. %)	1.0	1.0	1.0	1.0
Ion Density (10^{20} m^{-3})	1.6	1.33	1.33	1.6
Ion Temperature (keV)	13.0	13.0	13.0	13.0
Neutral Beam Power (MW)	40	57	50	45
Neutral Beam Energy (keV)	150	150	150	150
Average Neutron Wall Loading (MW m^{-2})	1.50	1.28	1.28	1.50
Total Fusion Power Generated, 21.0 MeV/Event (MW)	558	795	698	627
Fusion Power Density (MW M^{-3})	3.70	2.57	2.57	3.70
EF Volt Seconds	21.8	34.3	31.2	23.9
OH Volt Seconds	19.1	20.9	20.4	19.6
Total Fusion Energy Per Pulse (GJ)	13.4	19.1	16.8	15.1

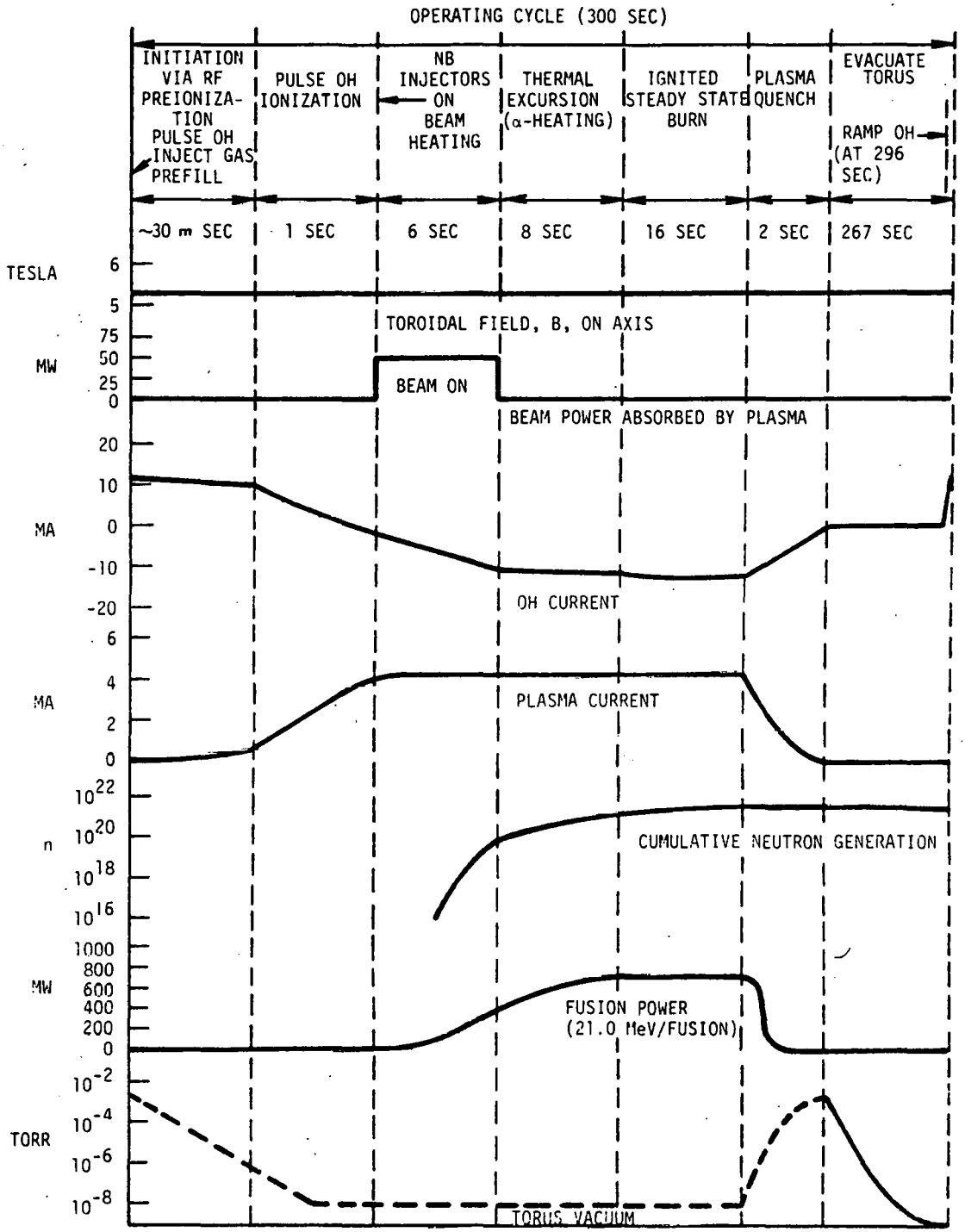

Figure 4-1. TNS Operating Scenarios

transport and rejection without production of electrical power. The neutral beam power requirements (at 150 keV) vary from 40 - 57 MW as indicated.

4.2 OVERALL MACHINE PARAMETERS

Table 4-2 summarizes the key overall machine parameters. The only key parameter which was fixed for all four designs is a thickness (0.25 m) for a liner/limiter. The remaining key parameters vary with each design.

Note that these designs result in a TF coil size of approximately 4-5 m x 6-7 m. The overall machine dimensions are about 10 m maximum vertical height by 18 m maximum horizontal length. The required reactor cell dimensions are approximately 25 m in radius by about 20 m in internal height.

Schematic layouts of the four designs are given in Figures 4-2 through 4-5 respectively for the reference design with copper TF coils, NbTi TF coils, Nb_3Sn TF coils and the hybrid design with nested copper/NbTi TF coils. Each drawing presents an elevation view of each device with the key features identified and key dimensions provided. From these schematic representations, the relative size and location of the TF and PF coil systems can be compared.

4.3 MAGNETIC FIELD COIL PARAMETERS

Table 4-3 presents the key parameters for the magnetic field coil sets. Included are key parameters for both the toroidal field (TF) coils and the poloidal field (PF) coils including the various EF and OH coil systems. A key parameter which was fixed for all four designs was the number of TF coils (20); however, this parameter was varied in the trade studies over the range from 12 to 24.

The peak field at the winding for the TNS-4 Nb_3Sn design is 10.9 T, providing some engineering margin. In contrast, the TNS-3 design which employs NbTi requires a peak field of 9.9 T, which is presently judged to represent a significant technological and operational risk with little potential design margin. It is possible obviously to maintain the same machine size but reduce the design peak field to a lower, more comfortable value. However, calculations indicate that a reduction to 8 T in NbTi would require operation at a toroidal β of at least 7.5% and would result in a decreased toroidal field on axis (4.3 T versus 5.3 T).

TABLE 4-2

OVERALL MACHINE PARAMETERS

	TNS-1 (Copper)	TNS-3 (NbTi)	TNS-4 (Nb_3Sn)	TNS-5 (Cu/NbTi)
Liner/Limiter Thickness (m)	0.25	0.25	0.25	0.25
Vacuum Vessel Thickness (m)	0.165	0.175	0.175	0.165
Shielding Thickness (m)	0.169	0.48	0.469	0.689
Assembly Clearances (m)	0.25	0.25	0.25	0.45
Clear Horizontal TF Bore (m)	3.8	4.78	4.56	4.19/5.31
Clear Vertical TF Bore (m)	6.13	7.05	7.23	5.74/9.13
TF Coil Bobbin Thickness (m)	1.02	0.78	0.814	0.354/0.633
Bucking Cylinder Thickness (m)	0.0	0.304	0.224	0.171
OH Coil Thickness (m)	0.177	0.099	0.134	0.339
Clear Bore of Torus (m)	1.00	1.87	1.21	0.63
Maximum Machine Horizontal Length (m)	14.10	18.9	17.2	17.1
Maximum Machine Vertical Height (m)	8.2	9.4	9.7	11.2
Reactor Cell Internal Radius (m)	23.1	25.5	24.6	24.5
Reactor Cell Internal Height (m)	18.2	19.5	19.7	21.2

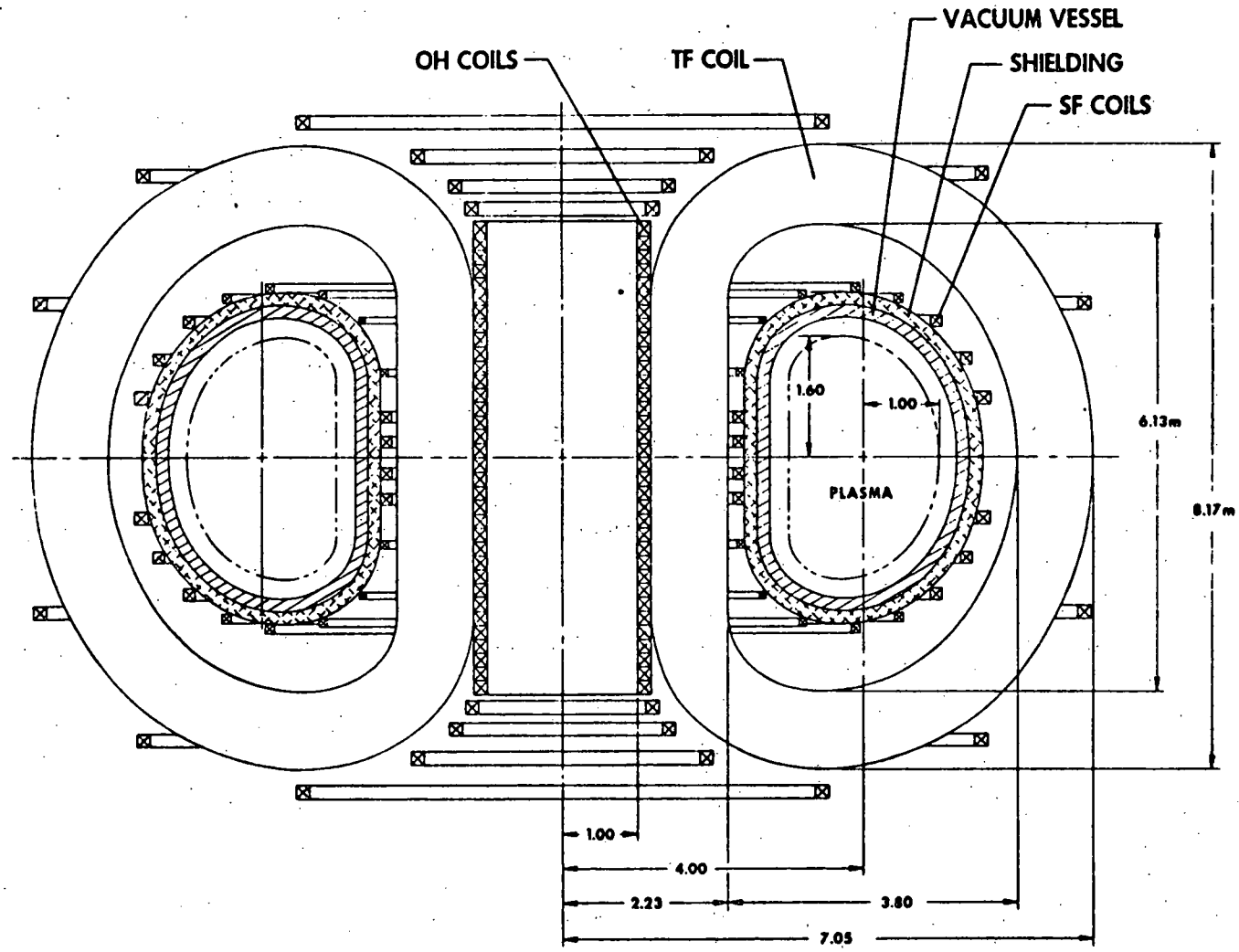

Figure 4-2. Reference TNS with Copper TF Coils

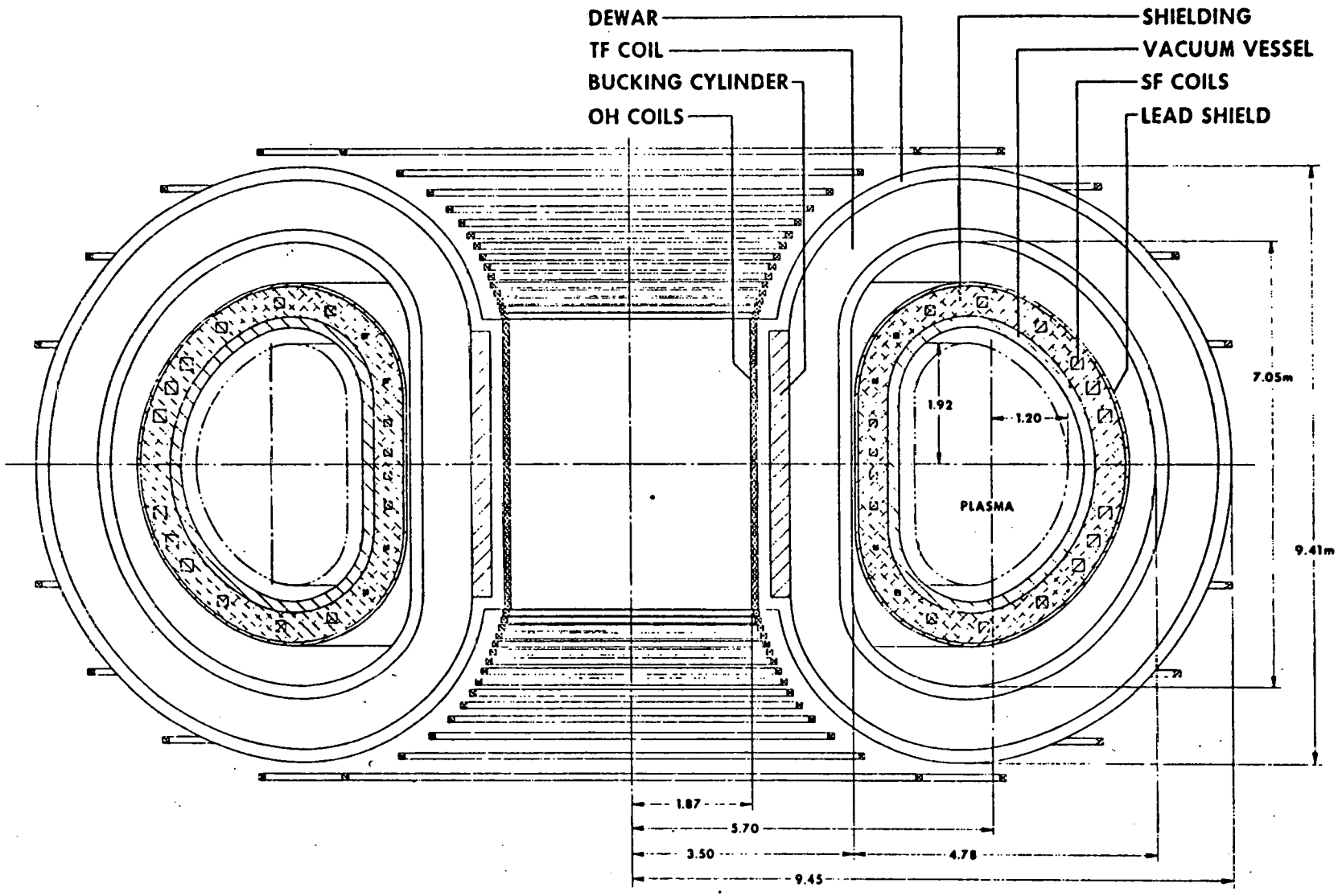

Figure 4-3. Reference TNS with NbTi TF Coils

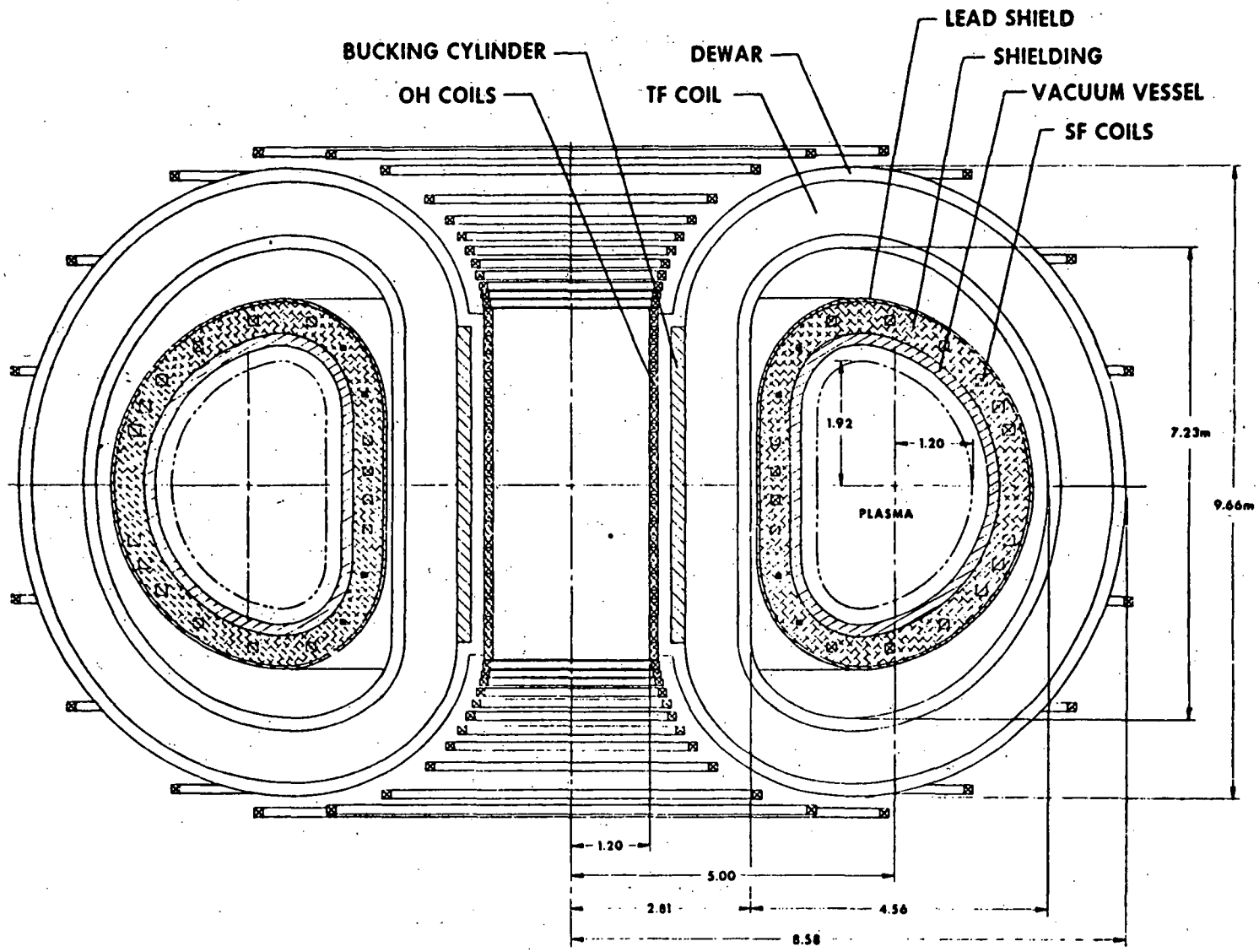

Figure 4-4. Reference TNS with Nb_3Sn TF Coils

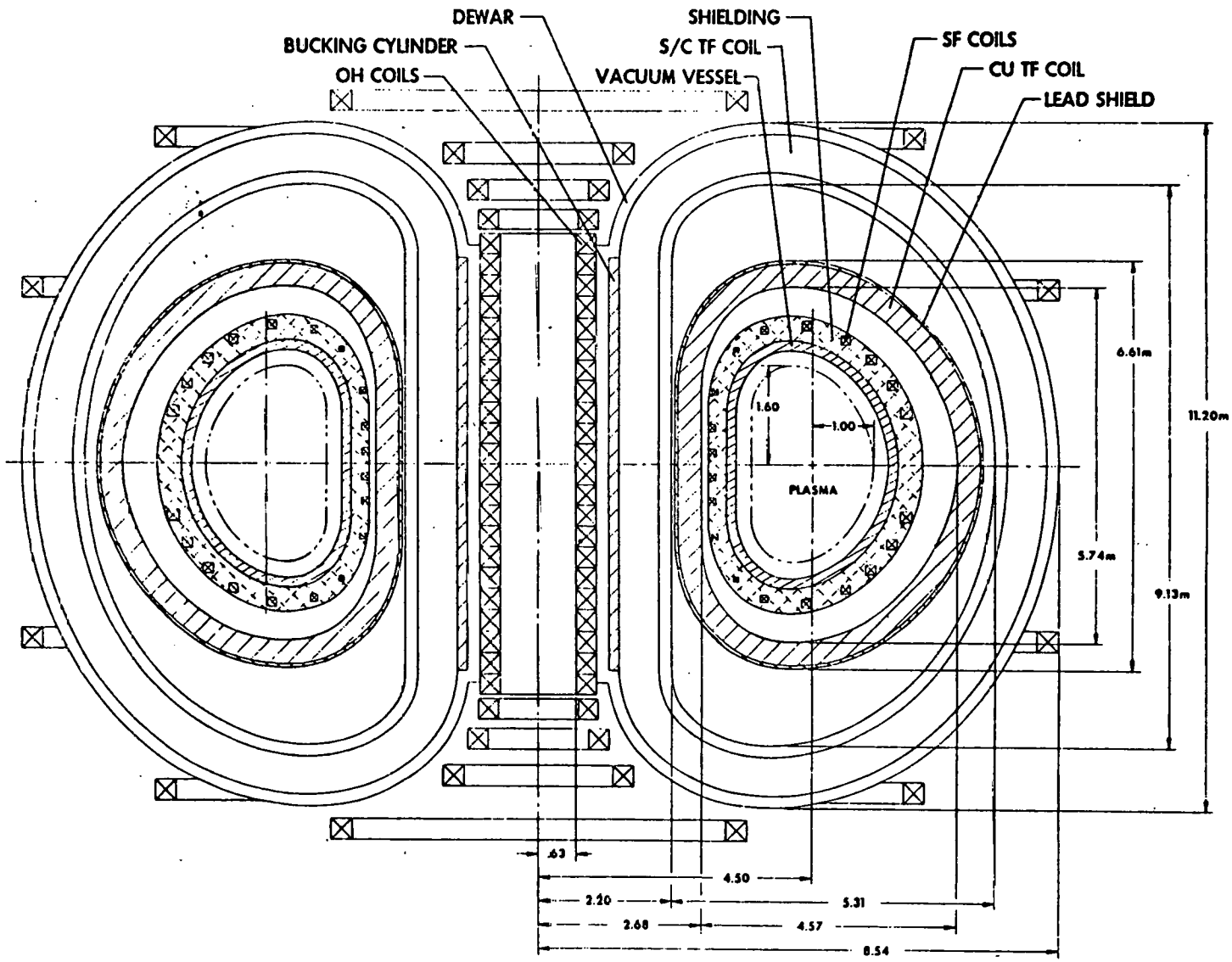

Figure 4-5. Reference TNS with Copper/NbTi TF Coils

TABLE 4-3

MAGNETIC FIELD COIL PARAMETERS

	TNS-1	TNS-3	TNS-4	TNS-5
B_{OH} (T)	2.18	0.86	1.81	3.33
$B_{OH, Max}$ (T)	2.55	0.90	2.0	4.82
Number of EF Coils	20	20	20	20
Total Number of Constant Tension D-Shaped TF Coils	20	20	20	20/20
Peak TF Field at Winding (T)	10.4	9.9	10.9	9.7/8.0
Structure/Conductor Area Ratio for TF Coils	0.07	1.33	2.14	0.13/1.22
Number of Turns/Bobbin TF Coils	-	5	8	5
Radius of High Field Side of TF Coils (m)	2.23	3.30	2.61	2.68/2.0
Total Ampere-Turns in TF Coil Set (MA·T)	116	150	132	56/74
Average Current Density (MA m^{-2})				
Copper OH and EF	15	15	15	15
TF	15	25	37.5	15/25
TF Coil Assembly Dimensions				
Inner Radius to Neutral Axis (m)	1.70	2.86	2.17	2.49/1.66
Outer Radius to Neutral Axis (m)	6.54	8.86	7.97	7.06/8.02
Max. Half-Height to Neutral Axis (m)	3.57	4.11	4.22	3.05/5.08
Free Vertical Bore (m)	6.13	7.05	7.23	5.74/9.13
Free Horizontal Bore (m)	3.80	4.78	4.56	4.19/5.31
Circumference (m)	19.73	23.25	23.42	17.38/27.41
Area (m^2)	10.83	14.00	11.07	5.48/6.58
Number of Turns in Poloidal Coils				
EF-1	49	45	51	43
EF-D	8	8	8	8
EF-0	68	62	71	60
OH	118	78	91	115
Max. TF Coil Width (m)	0.70	1.03	0.82	0.35/0.63
TF Coil System Stored Energy (GJ)	8.07	14.2	12.8	11.1
TF Coil System Mass				
Conductor (Tonne)	1360	698	506	582/387
Structure (Tonne)	86	1568	1325	67.4/868
Dewars (Tonne)	0	375	332	303

4.4 THERMAL AND AUXILIARY ELECTRICAL LOADS

Table 4-4 gives the key thermal (peak and average) and auxiliary electrical loads for the four designs. Loads are presented for the following systems: vacuum vessel, shield, neutral beam, magnetic field coils (TF, EF and OH), refrigeration (He and N_2), experimental area ventilation and the general plant circulating water.

4.5 ELECTRICAL LOAD PARAMETERS

Table 4-5 presents a listing of the electrical and load parameters for the magnetic field coil sets for the four point designs. Included are peak volt/turn values for the coils comprising the PF system (OH, EF-I, EF-O, and EF-D) and the TF coils. Note that the peak values for the PF system are all of the order of several hundred volts/turn. The peak values for M-amp turns are given and range from values of 0-3 for the EF systems, 5-40 for the OH systems, and 100-150 for the TF systems. The peak electrical power requirements are <100 MW for EF-D systems, 400-800 MW for the EF-I, EF-O systems, and 2000-4000 MW for the OH systems (except for the hybrid which requires ∿9000 MW). The peak stored energy in the TF coil systems typically range from 8000-14000 MJ. The energy consumed per pulse is <100 MJ for the EF-D systems, 200-1000 MJ for the EF-I, EF-O systems, 300-1400 MW for the OH systems and for the copper TF coils for TNS-1, the value is ∿36000 MJ. Section 5.6 presents further discussion on the electrical system considerations.

4.6 FUEL PARAMETERS

The fuel requirements for the four point designs are given in Table 4-6. The tritium inventory required on-site is 1-2 MCi and the monthly tritium replenishment is 50-75 kCi with the largest requirements for TNS-3 and the least requirement for TNS-1. The tritium requirements for the gaseous pre-fill range from about 1500 Ci/pulse for TNS-1 to about 2600 Ci/pulse for TNS-3. The tritium pellet refueling requirements are of the order of 1000 Ci/pulse. The requirements for reprocessing and the composition of the material that is reprocessed are as indicated. Section 5.8 presents further discussion on the fuel system characteristics.

TABLE 4-4

THERMAL AND AUXILIARY ELECTRICAL LOADS

	TNS-1			TNS-5		
	THERMAL LOAD		Peak Elec.	THERMAL LOAD		Peak Elec.
	Peak (MW)	Avg (MW)	Load (kW)	Peak (MW)	Avg (MW)	Load (kW)
Vacuum Vessel	195	16	807	220	18	908
Shield	362	29	1499	408	33	1686
Neutral Beam	224	4	830	252	5	933
TF Coil	322	119	3546	116	40	1535
EF Coil	13	4	~0	14	4	
OH Coil	10	3	~0	18	6	
HE Refrigeration		0	0		~0	34262
N_2 Refrigeration		0	0		~0	2525
Exp. Area Ventilation		7	3633		9	4621
Gen. Plant Circ. Water		195	2137		164	1810
Total			12452			48279

	TNS-3			TNS-4		
	Peak (MW)	Avg (MW)	Peak Elec. Load (kW)	Peak (MW)	Avg (MW)	Peak Elec. Load (kW)
Vacuum Vessel	278	22	1150	244	19	1009
Shield	517	41	2135	454	36	1875
Neutral Beam	319	6	1182	280	6	1038
TF Coil	0	0	277	0	0	309
EF Coil	18	6		17	5	
OH Coil	4	1		10	3	
HE Refrigeration		~0	51295		~0	12625
N_2 Refrigeration		~0	2525		~0	2525
Exp. Area Ventilation		9	4695		9	4397
Gen. Plant Circ. Water		152	1688		104	1193
Total			64948			24972

TABLE 4-5

ELECTRICAL LOAD PARAMETERS

	TNS-1 (Copper)	TNS-3 (NbTi)	TNS-4 (Nb_3Sn)	TNS-5 (Cu/NbTi)
Volts/Turn (Peak), v				
OH	211	322	276	217
EF-I	227	329	289	255
EF-O	233	333	294	260
EF-D	220	325	284	249
TF	5.74	0	0	0
M · Amp · Turns (Peak), MA · T				
OH	16.0	6.27	14.3	40.3
EF-I	1.83	1.69	1.93	1.63
EF-O	2.53	2.34	2.66	2.25
EF-D	0.293	0.27	0.31	0.26
TF	115.7	150.5	132.1	56.2/73.9
Power (Peak), MW				
OH	3383	2020	3948	8764
EF-I	416	557	557	415
EF-O	592	778	783	586
EF-D	64	88	87	65
TF	664	0	0	284
Stored Energy in Field Coil System (Peak), MJ				
TF	8069	14194	12762	1413/5751
Energy Consumed Per Pulse, MJ				
OH	766	360	872	1366
EF-I	252	370	348	269
EF-O	827	1003	1043	795
EF-D	49	70	68	51
TF	35590	0	0	12113

TABLE 4-6

PRINCIPAL FUEL PARAMETERS FOR THE FOUR TNS POINT DESIGNS

	TNS-1	TNS-3	TNS-4	TNS-5
TF Coil Conductor	Cu	NbTi	Nb_3Sn	Cu/NbTi
Plasma Minor Radius, m	1.0	1.2	1.2	1.0
Plasma Major Radius, m	4.0	5.7	5.0	4.5
Plasma Elongation	1.6	1.6	1.6	1.6
Plasma Volume, m^3	126	259	227	142
Torus Internal Smooth Surface, m^2	247	411	361	278
On-site Standby T Inventory, Mci	0.62	1.03	0.90	0.70
Peak On-site T Inventory, Mci	1.36	1.85	1.70	1.45
Monthly Required T Replenishment, kCi	52.9	74.9	66.1	59.1
U Change in T Generator-Storage Units, kg	3.28	5.44	4.77	3.69
T Generator Internal Volume, cm^3	5470	9070	7950	6150
T Gaseous Prefill, Ci/Pulse	1520	2590	2270	1700
T Pellet Refueling, Ci/Pulse	869	1361	1194	977
Fusion Fraction	0.195	0.168	0.168	0.195
Reprocessing Quantity, gatm/campaign	7.925	13.294	11.668	8.909
Composition of Material Reprocessed, a/o*				
H	4.81	4.77	4.77	4.81
D	41.9	42.8	42.8	41.9
T	41.8	42.7	42.7	41.9
He-4	10.2	8.6	8.6	10.2
He-3	1.31	1.05	1.10	1.24

*Treated on a smeared basis.

4.7 NEUTRAL BEAM ARM PARAMETERS

The system of neutral beam arms for a given TNS point design consists of a number of standard arms composed of three positive-ion sources which have a nominal current of 100 A each. The features of a standard beam arm are given in Table 4-7. Section 5.9 provides further discussion of the neutral beam system considerations.

4.8 REFERENCE DESIGN COST COMPARISON

4.8.1 CAPITAL EQUIPMENT COSTS

A comparison of the cost estimates of the four TNS designs is shown for the five major reactor systems in Table 4-8. Also, a breakdown of the major cost contributors by percentage of the total cost are shown for the four designs in Figures 4-6 through 4-9. The building and equipment costs shown in Table 4-8 do not include engineering, design, inspection, and administration (EDIA), contingency or escalation.

Of the four designs, note that TNS-1 with water-cooled copper TF coils is the least costly (and also smallest) system ($\sim$290 M$) and represents a more modest step-up from TFTR in terms of magnet technology. Of the two totally superconducting systems, TNS-4 with Nb_3Sn at $\sim$388 M$ is 34% more costly than the copper TNS-1; however, if selected for TNS, would represent a strong technology forcing function and would constitute an important step toward demonstration of reactor technology. The TNS-3 NbTi design at 434 M$ is about 10% more costly than the TNS-4 Nb_3Sn design and about 50% more costly than the TNS-1 copper design. The reasons for the cost difference between the Nb_3Sn and NbTi TF coil devices are shown in Table 4-9 for a typical machine with $a = 1.2\,m$, $R_o = 5.0\,m$ and $B_{max} = 9.0T$. Note that the TF coil conductor cost is larger for the Nb_3Sn, as expected; however, the TF coil structure cost is larger for the NbTi because its radial build is larger due to its lower current density limitation. The unit costs used for the superconductor cable, based on recent vendor quotes, were \$100/kg for Nb_3Sn and \$50/kg for NbTi. The main cost item difference is in the liquid He refrigeration costs, which are about twice as high for the NbTi due to its lower thermal operating margin. There is also a slight difference in the OH power supply cost due to the smaller machine bore space of the NbTi device.

TABLE 4-7

NEUTRAL BEAM ARM PARAMETERS

Injection Energy	150 keV
NB Pulse Length	6 s
Charge State of Source Ions	+1
Fraction of Source Current Due to D^+ Ions	0.9
Injection Angle at Midplane*	16°
Current per Source	100 A
Sources per NB Arm	3
NB Power to Plasma per NB Arm (150 keV)	10.4 MW
Transmission Coefficient through Arm	0.87
Neutralization Efficiency**	29%
Source Gas Efficiency	50%
Clear Opening of NB Duct	0.44 m x 1.20 m
Total Accel. Power per NB Arm	45 MW
Total Electrical Power per NB Arm	∿55 MW
Gas Throughput per Arm	∿53 torr l s^{-1}
HV Pumping Speed per Arm***	∿5 x 10^6 l s^{-1}
Overall Length of NB Arm	7.5 m
Overall Cross-sectional Dimensions	3.3 m x 5.0 m

*Horizontal Injection

**90% of Asymptotic Value

***Based on 50 m^2 of Cryopanel

TABLE 4-8

COST ESTIMATE COMPARISON FOR FOUR TNS POINT DESIGNS

System	Copper TF	NbTi TF	Nb_3Sn TF	Copper/NbTi TF
Tokamak System	79.3 M$	202.1 M$	199.1 M$	163.0 M$
Electrical Power Systems	94.6	29.8	35.9	99.4
Tokamak Support Systems	48.8	118.2	76.1	100.1
Structures and Site Services	31.5	35.2	34.1	34.7
Neutral Beam Systems	34.5	49.1	43.1	38.8
TOTAL	288.7 M$	434.4 M$	388.3 M$	436.0 M$

TABLE 4-9

COMPARISON OF THE COSTS OF DEVICES WITH SUPERCONDUCTING NbTi AND Nb_3Sn TF COILS FOR THE SAME SIZE DEVICES AND SAME PEAK FIELD AT THE COIL

Item	NbTi	Nb_3Sn	NbTi-Nb_3Sn
Total Cost (M$)	370	348	22
TF Coil Cost	85	92	-7
Conductor*	24	37	-13
Structure and Dewar	61	55	6
Refrigeration Cost	50	23	27
OH Cost	10	8	2
TF Coil Build (M)	0.73	0.61	0.12
Device Bore (M)	1.30	1.40	-0.10

*Based on $100/kg for Nb_3Sn and $50/kg for NbTi.

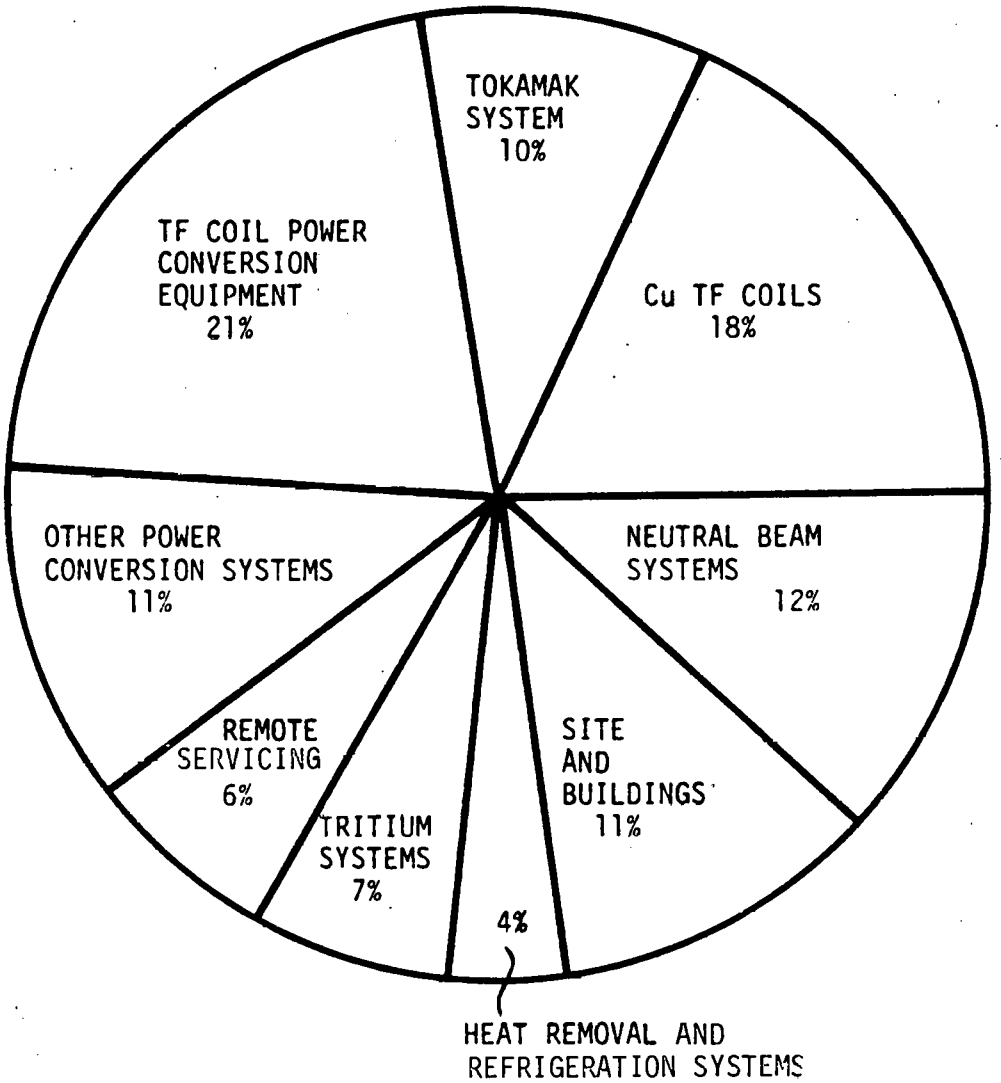

TOTAL COST, BUILDINGS & EQUIPMENT = $289M

a = 1.0 m, R_o = 4.0 m, Elongation = 1.6, B_{max} = 10.4 T

Figure 4-6. Cost Distribution by System for TNS-1, A Cu TF Coil Device

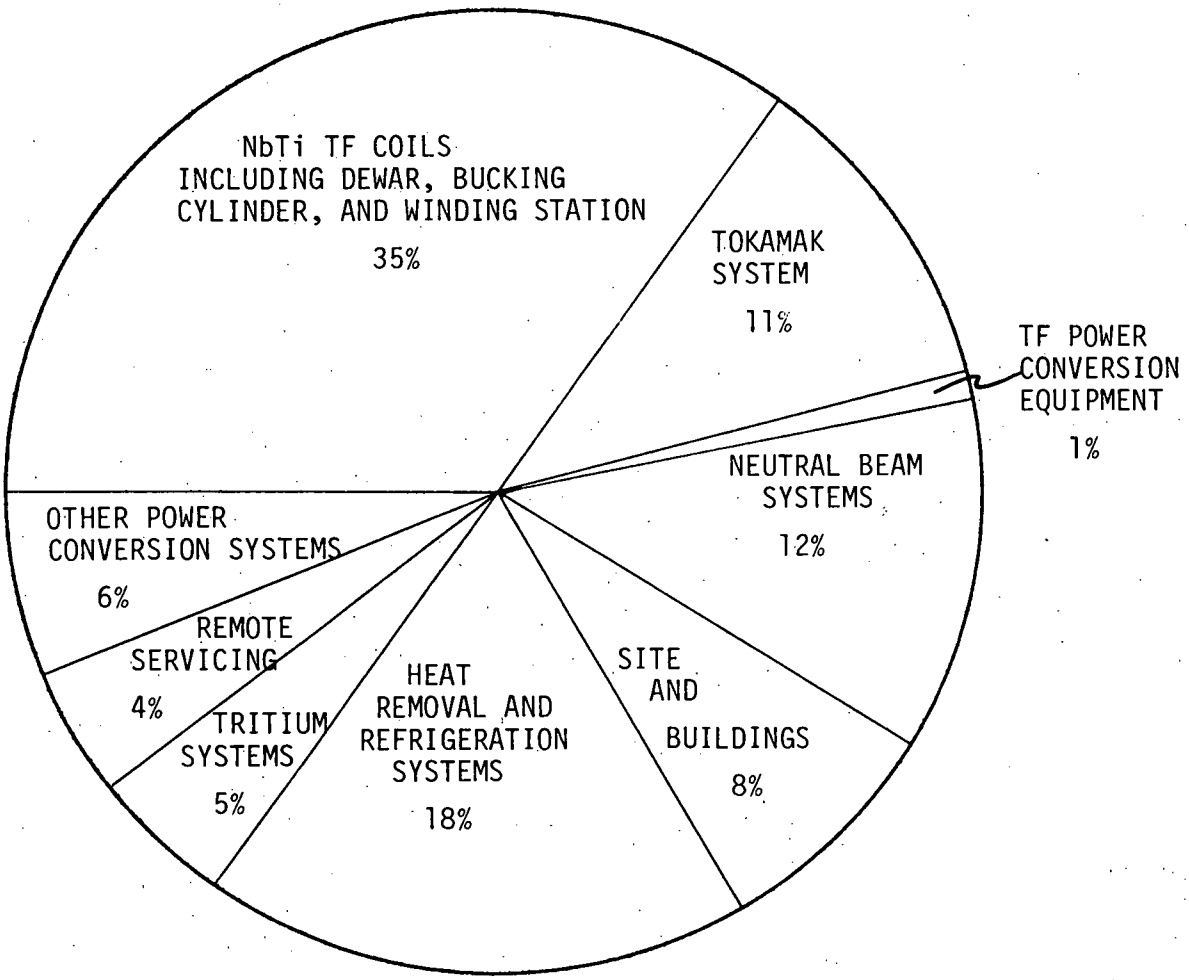

TOTAL COST, BUILDINGS & EQUIPMENT = $434M

a = 1.2 m, R_o = 5.7 m, Elongation = 1.6, B_{max} = 9.9 T

Figure 4-7. Cost Distribution by System for TNS-3, An NbTi TF Coil Device

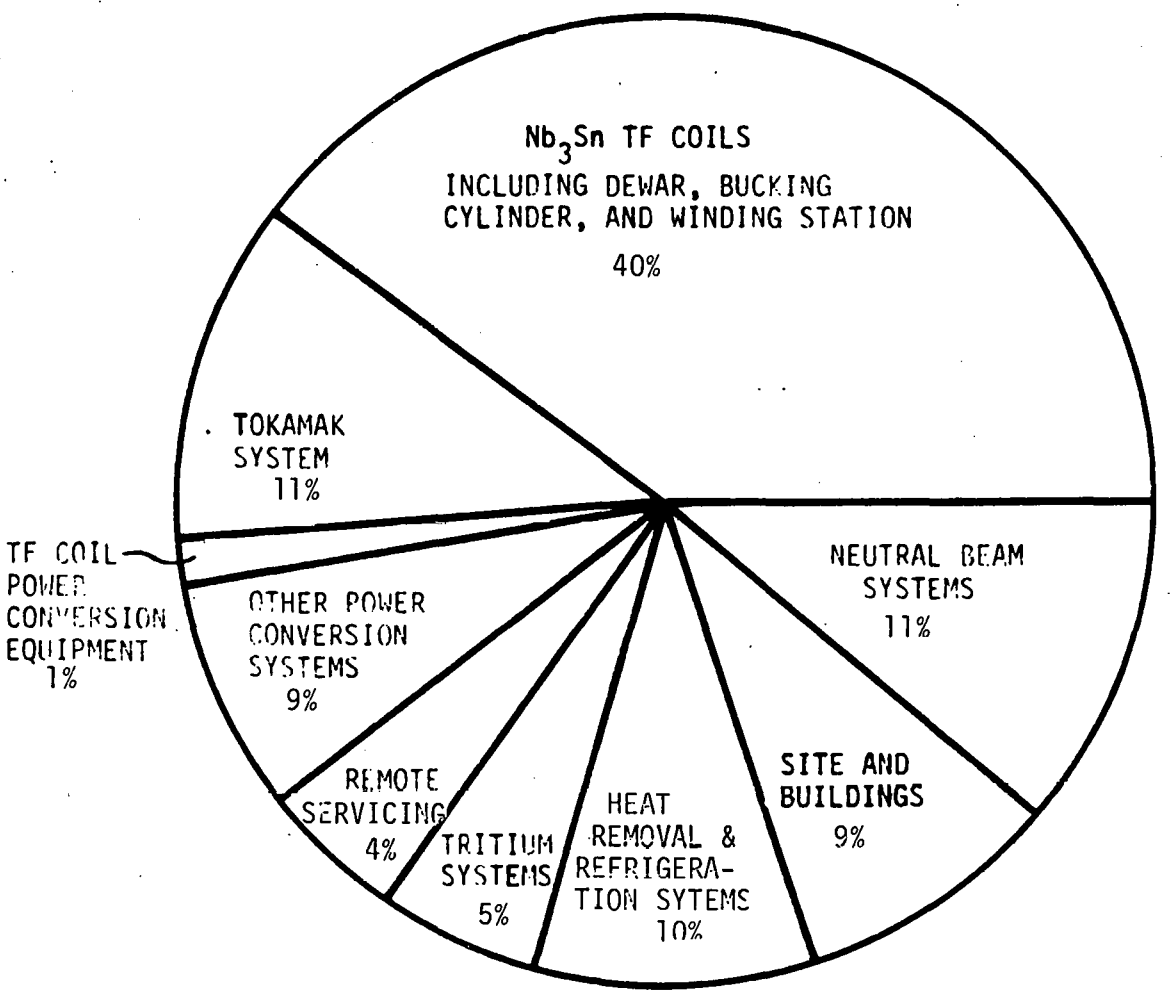

TOTAL COST, BUILDINGS & EQUIPMENT = $388M

a = 1.2 m, R_o = 5.0 m, Elongation = 1.6, B_{max} = 10.9 T

Figure 4-8. Cost Distribution by System for TNS-4, An Nb_3Sn TF Coil Device

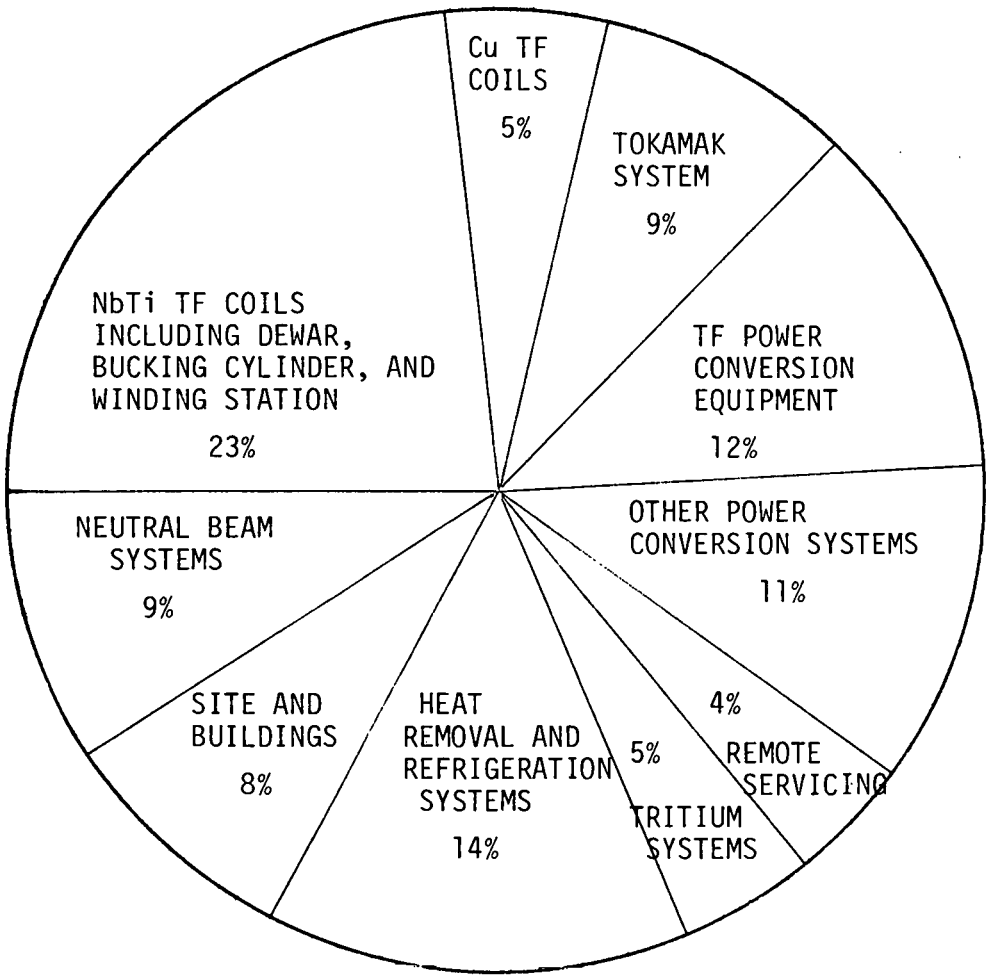

TOTAL COST, BUILDINGS & EQUIPMENT = $436M

a = 1.0 m, R_o = 4.5 m, Elongation = 1.6, B_{max} = 9.7180 T

Figure 4-9. Cost Distribution by System for TNS-5, A Cu/NbTi "Hybrid" TF Coil Device

As can be seen from Figure 4-6 for the Cu TF coil device, the two largest cost items are the power conversion equipment to run the TF coils and the TF coils themselves. Together they constitute about 39% of the total cost. The next largest cost items are the neutral beam systems and power supplies, the reactor site and buildings, the other power conversion systems for the OH and EF coils, and the tokamak system which includes the vacuum vessel, liner, structure, shielding, OH and EF coils, etc. Together these four items account for about 44% of the total. The remaining 17% of the cost is made up of the tritium handling systems, remote servicing systems, and the heat removal and refrigeration systems.

For the superconducting NbTi and Nb_3Sn, Figures 4-7 and 4-8, the largest cost item, at 35-40% of the total, is the TF coils, which also includes the dewars, bucking cylinder and winding station. Other large cost components are the tokamak system, neutral beams, reactor site and buildings, heat removal and refrigeration systems, and the OH and EF power conversion systems. Note that the TF coil power conversion equipment cost is very small for the superconducting devices. The cost of the tokamak support systems is considerably higher for the NbTi device, due to the larger refrigeration (heat removal) systems cost to run the NbTi at $\sim$10T.

The hybrid Cu/NbTi device tends to have higher costs because it requires the most expensive systems of each technology type. For example, it needs superconducting coils and their support systems while also requiring expensive power conversion equipment to run the Cu TF coils.

There are several obvious differences in the cost components for the various devices. The TF coils are less expensive for the Cu; however, together with their power supplies they account for about the same fraction (40%) of the cost as do the superconducting coils, dewars, etc., for the NbTi and Nb_3Sn devices. The heat removal and refrigeration systems are larger for the NbTi and Nb_3Sn due to the cryogenics involved. Other components, such as the tokamak system, neutral beams, OH and EF power supplies, and reactor site and buildings, account for about the same fraction of the cost in both the Cu and superconducting devices.

4.8.2 ANNUAL UTILITY AND FUEL COSTS

The key annual utility and fuel costs for the four reference point designs are summarized in Table 4-10. Included are the costs to run the copper coils (PF in all four cases and TF in the case of TNS-1), the cooling and refrigeration systems, and the tritium systems.

The total cost for the copper TNS-1 design is ∿4.0 M$ per year with the largest cost item being the cost to operate the TF coils. The total cost for the two superconducting designs is less primarily because there is essentially no cost to operate the TF coils. However, the cooling and refrigeration costs for these designs is significant relative to the cooling cost required for the TNS-1 copper design. Note that in all cases, the annual cost for fuel (tritium) is ∿1.0 M$.

TABLE 4-10

ANNUAL UTILITY - FUEL COSTS (M$)

	Cu TNS-1	NbTi TNS-3	Nb_3Sn TNS-4	Cu/NbTi TNS-5
POLOIDAL FIELD COILS	0.13	0.13	0.1	0.17
COPPER TF COILS	2.47	0.00	0.00	0.84
TRITIUM SYSTEMS	1.00	1.08	1.05	1.02
COOLING SYSTEMS	0.45	1.78	0.78	0.34
TOTAL ANNUAL COST	4.05	2.98	1.99	3.37
RELATIVE ANNUAL COST	1.0	0.74	0.49	0.83

5.0 REFERENCE SYSTEM GENERIC DESIGN FEATURES

The four reference point designs described in Section 4.0 each contain a number of tokamak and support systems and subsystems. Since, in general, many features of these systems are the same for each of the four designs, these systems are discussed separately in this section of the report. Included in this discussion are the following:

- Vacuum Vessel
- Impurity Control
- Nuclear Shielding
- Toroidal Field Magnet System
- Poloidal Field Magnet System
- Electrical Systems
- Heat Transport Systems
- Tritium Systems
- Plasma Heating - Neutral Beam System
- Remote Servicing Systems
- Plant Facilities
- Torus Vacuum Pumping System

5.1 VACUUM VESSEL

The reference system vacuum vessel for TNS is shown in Figure 5-1. The vessel concept uses 316 stainless steel elliptical segments having a shallow I-beam cross section. The segments, each spanning 6° of the torus, are joined together to form a ring stiffened shell defined by the inner flanges of adjacent I-beams.

The design of the TNS vacuum vessel was guided by Section III, Division 1 - Nuclear Power Plant Components of the ASME Boiler and Pressure Code for the following reasons:

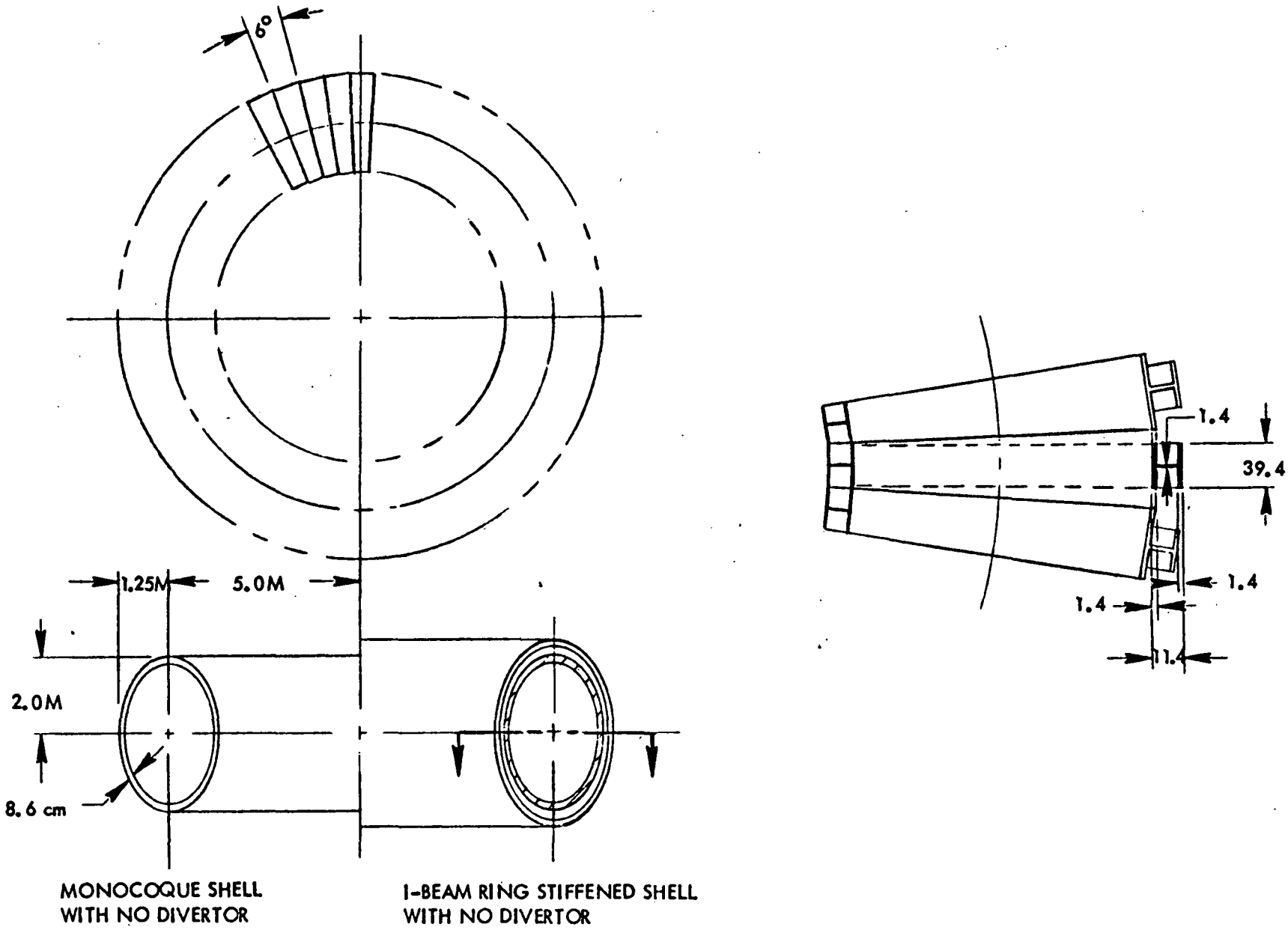

Figure 5-1. Combined First Wall and Vacuum Vessel

- Compliance with a widely used and accepted safety code assures a reasonable degree of conservatism and consistency in applying the design rules
- Deviation from the Code could highlight new and unanticipated conditions which will require special consideration
- Non-compliance with the Code may be necessary and may indicate areas where revision or extension of the Code can be profitably begun in anticipation of its application to future power reactors

The design procedure ultimately to be used on the TNS vacuum vessel is iterative finite element analysis, with the size of the elements and the gradation of physical properties adjusted locally to provide the degree of precision necessary for confidence in the adequacy of the design. This procedure, however, is time consuming, costly, and presupposes considerable knowledge of the design. For preliminary design purposes, a simpler and more direct procedure was used, ideally one which takes design conditions as input and calculates the geometry of the vessel directly.

Since the vacuum vessel is externally pressurized, it can fail either plastically or by buckling; both modes of failures must be considered, so a straight forward design calculation is not possible. An analytical procedure[13], was developed at Lawrence Livermore Laboratory to predict the collapse pressure of underground structures which must survive or collapse predictably during underground weapons tests. In this procedure, material properties and vessel geometry are reasonably well separated and the output is the collapse pressure for a vessel having the specified overall geometry and materials properties, with the thickness of the wall the only variable. Sufficient precision in the calculation is possible using a solid-state calculator to determine by a few iterations and interpolation the wall thickness required for a specific collapse pressure, as shown in Figure 5-2. This procedure was used in the design of the vacuum vessel.

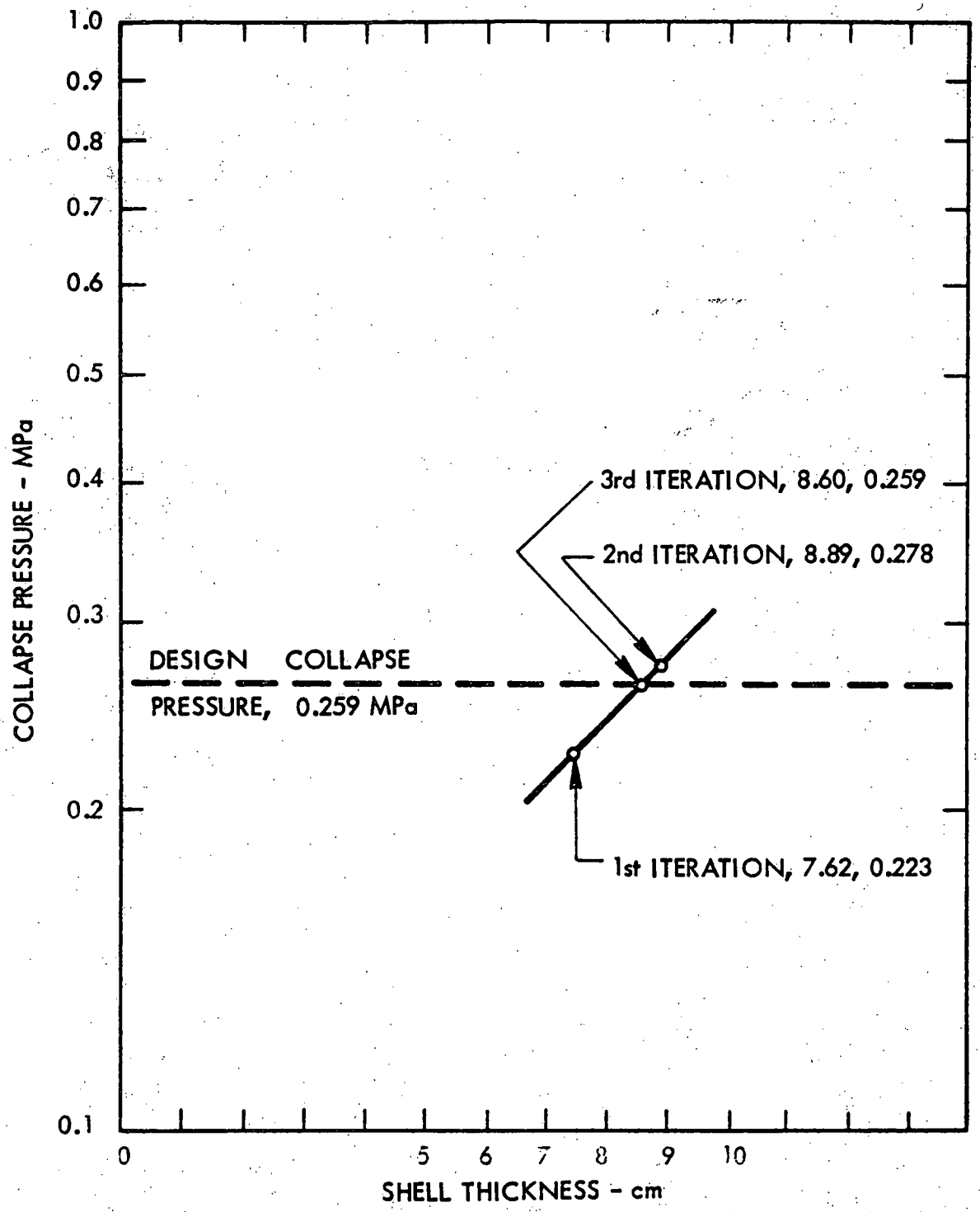

Figure 5-2. Determination of Elliptical Shell Thickness (2.50 m x 4.00 m Ellipse)

Once the required thickness of the wall of a uniformly thick wall vessel has been determined, design variations can be examined. The simplest variation is to replace the thick wall with an I-beam ring. The flange width is approximately the chord across 6° of the inner equator of the torus. The thickness of the flanges (and for convenience the web thickness also) is the thickness required to make the full width of the flange effective, when both shear lag and compressive buckling are considered. The height of the beam, which is determined by an iterative calculation, is whatever is necessary to make the moment of inertia the same as that of the uniform wall spanning 6° of the outer equator of the torus. The vacuum vessel consists of sixty of these I-beam elliptical rings, for strength, with the vacuum boundary formed by extending the inner flanges toroidally and welding them together; these flange extensions are not effective in increasing the strength of the I-beams.

Section III of the Code limits the design pressure to one-third of the collapse pressure. The first approximation of the collapse pressure is therefore three atmospheres. The highest atmospheric pressure recorded,[14] is 1000 millibars, i.e., 0.018 MPa. The collapse pressure required by the Code would thus be 0.324 MPa. The calculational procedure, however, specifically accounts for eccentricity, which in establishing the Code requirements[15], permits reducing the collapse pressure by 20%. Accordingly, the design pressure for the vacuum vessel was set at 0.259 MPa.

The design temperature for the vacuum vessel was set at 500°C. The design temperature is judged high enough to permit vacuum bake-out, plasma discharge cleaning, and normal cyclic operation. The vessel cooling system must be designed to keep the vessel below the design temperature during all these operations.

The Code limits the thermal stress function, $E\alpha\Delta T$, to one-half the allowable stress taken from the applicable fatigue curves. If the mean stress at some location is assumed to be the yield stress, for a large number of cycles, the variable stress component can be no more than the yield stress. It is, therefore, of interest to determine what temperature difference will cause a thermal stress equal to the yield stress. The results for Type 316 stainless steel for base temperatures up to the design temperature are presented in Figure 5-3. Local temperature excursions exceeding 40°C to 50°C will cause significant thermal stresses.

Figure 5-1 shows the simplest vessel configuration considered, a monocoque shell with no divertor chambers, which encloses a 2.5 m x 4.0 m (vertical) ellipse; the required shell thickness is 8.6 cm and the temperature difference radially through such a thick shell is sufficient to cause melting of the inner surface. The same figure shows the equivalent I-beam ring stiffened shell. The thickness of the inner flange (and therefore the vacuum shell wall) is 1.4 cm and the temperature difference radially through the vacuum shell is about 450°C.

Figure 5-4 shows a more complex vessel configuration having the same size plasma cavity but with divertor "burial chambers" above and below the plasma cavity. To provide space for the divertors, the vacuum vessel height was increased from 4.0 m to 5.6 m. The cavities are defined by a free-standing uncooled liner positioned by the elliptical vacuum shell. A monocoque shell would be 14.9 cm thick. An equivalent I-beam ring stiffened shell would have the same flange width and material thickness as in Figure 5-1 (shese are determined by the torus dimensions and the shear-lag considerations) but the height of the I-beam is increased from 11.4 to 23.4 cm to provide the required stiffness.

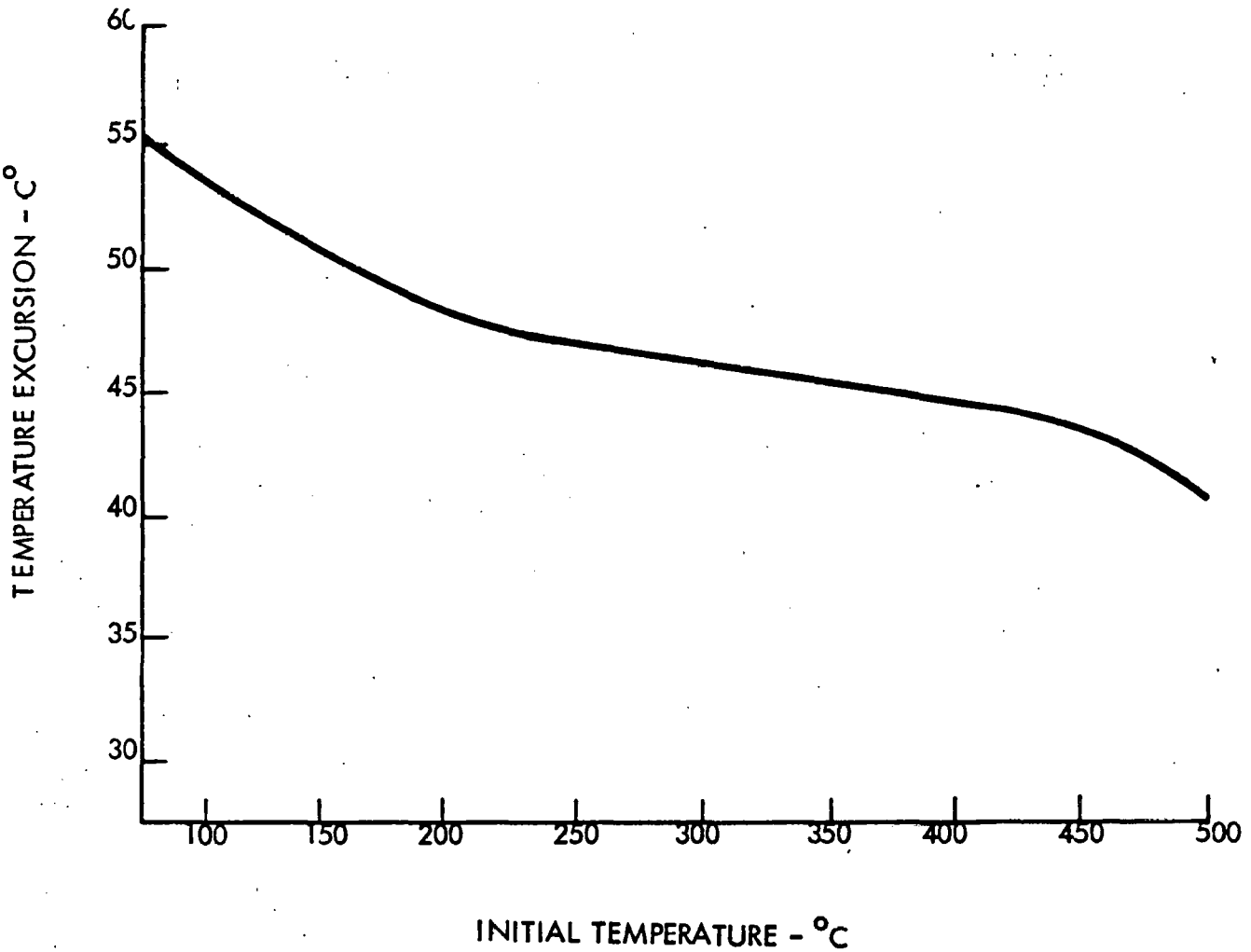

Figure 5-3. Temperature Difference to Cause Thermal Stress Equal to Yield Stress in AISI Type 316 Stainless Steel

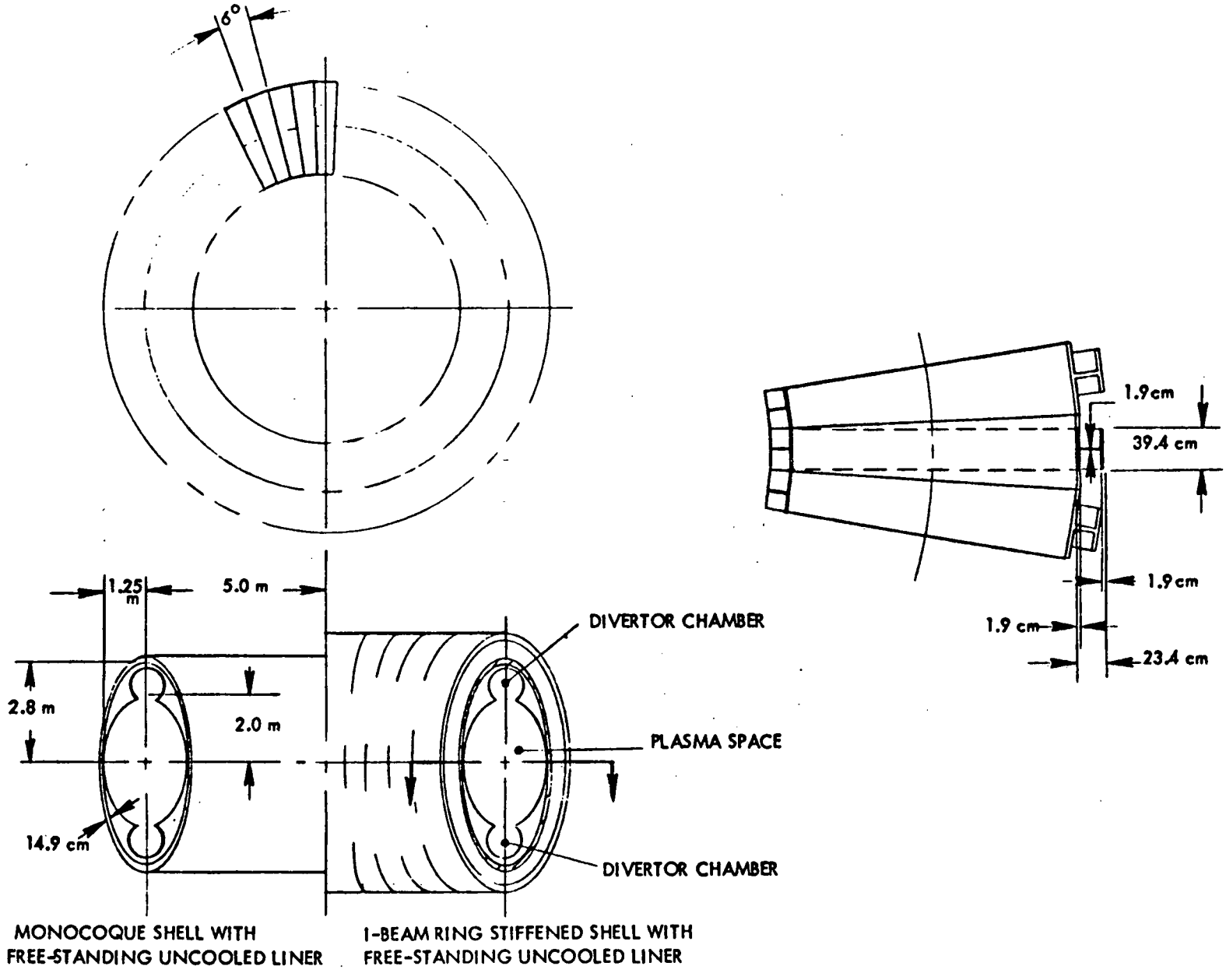

Figure 5-4. Vacuum Vessel with Free Standing Liner

An analysis was performed to define the basic design characteristics of the coolant channel networks required for cooling the first-wall/vacuum vessel system both with and without an effective poloidal divertor system. The coolant, selected to be low pressure water with an inlet temperature of 72°C and a maximum discharge temperature of 102°C, is supplied to the tokamak device from the test cell basement and is distributed toroidally by a ring manifold at the bottom of the device external to the shielding. From this manifold, coolant is supplied to each vacuum vessel segment by a separate nozzle whose flow is in turn distributed by small toroidal coolant headers spanning the width of the segment. Coolant channels are provided to blanket all surfaces of the I-beam structure (see Figure 5-5), and are arranged with poloidal orientation to allow coolant inlet at the bottom of the vessel, and discharge at the top. Such a channel orientation minimizes manifolding on the vessel itself, eliminates discontinuities in the vessel temperature distribution, provides an attractive coolant channel length of one-half of the poloidal circumference, and requires no segment-to-segment hydraulic connections. The coolant discharge lines from the vessel are essentially symmetrical to the inlet lines and are located at the top of the device.

Functionally, two different channel configurations are required. The channel network at the inner face of the inner I-beam flange must serve as the first wall. It must, therefore, provide sufficient coolant flow to remove both the neutron and gamma heating within the vessel flange, assumed to be 45 W/cm^3, and also the incident heat load from the plasma to the first wall surface, which will vary between about 85 W/cm^2 and 28 W/cm^2, depending on the design of plasma divertor and limiter systems. All other channel networks must be sized only to remove neutron/gamma heating within the associated vessel material.

Although the design of coolant channel networks will be seriously impacted by penetrations and the vessel toroidal geometry, the channel design can be well

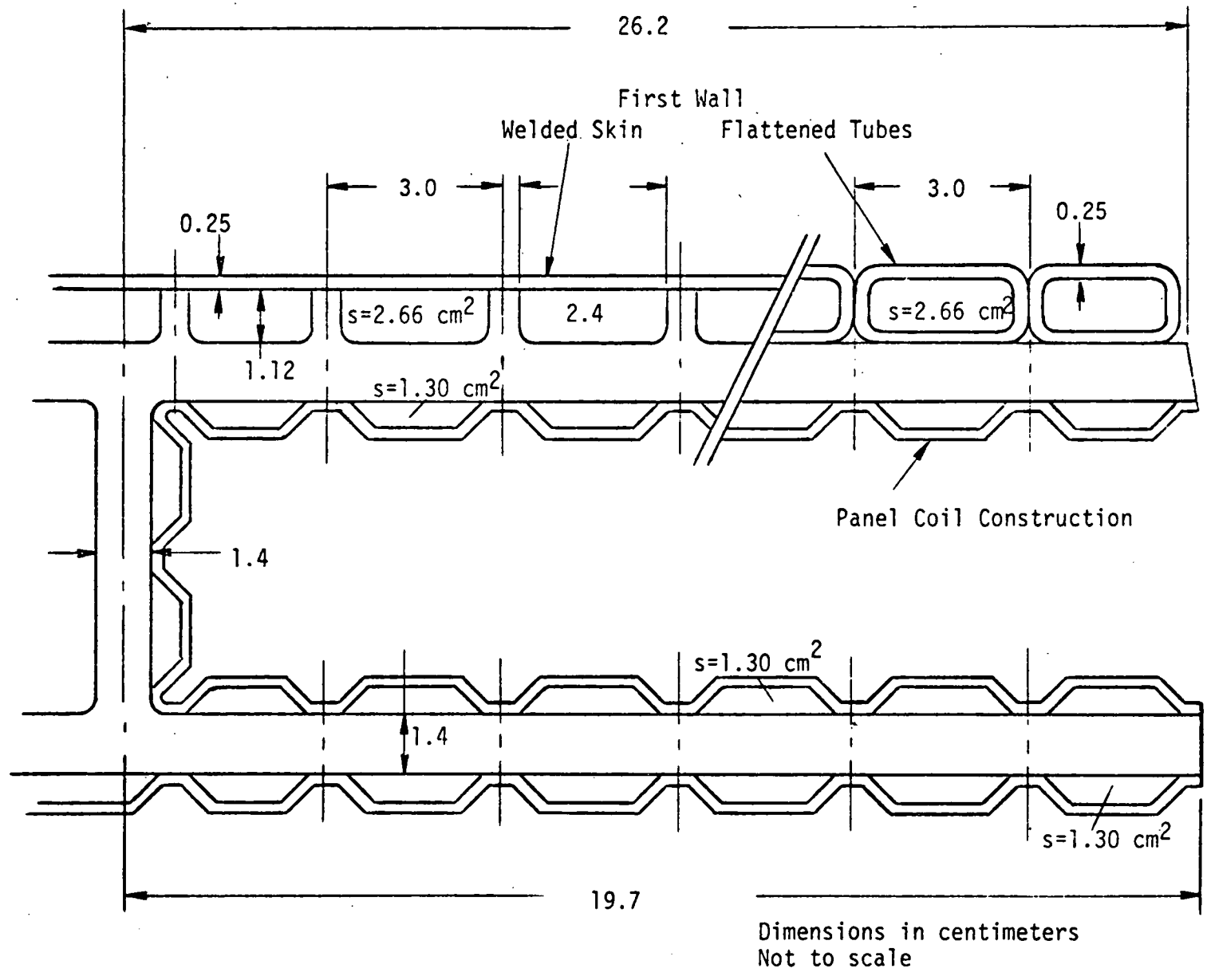

Figure 5-5. Cross Section of Vacuum Vessel I-Beam Segment Showing Typical Coolant Channel Configuration

characterized by examining idealized cylindrical segments corresponding to the average toroidal segment width with no penetrations. Table 5-1 summarizes the thermal hydraulic characteristics of such an idealized segment, and associated coolant network geometries for the various segment surfaces. The selection of the particular channel dimensions were based on a desire for uniform heating of first wall and non-first wall areas, maintenance of reasonable flow velocities, pressure drops, and heat transfer coefficients, provision of tolerable thermal stresses through the vessel cross section, and some judgement in regard to manufacturability.

5.2 IMPURITY CONTROL

There are potentially major deleterious effects due to impurities and helium in ignition devices including enhanced radiation losses, reduction of the reacting fuel ion density for a fixed plasma pressure, deterioration of the energetic neutral beam, modification of the current profile, high surface heat loads on the liner or first wall, and an increase in the $n\tau$ required for ignition.

In the TNS studies described in this report, it was assumed that impurity control would be accomplished by a passive wall treatment which in practice might be accomplished by liner geometries (honeycombs, etc.), low Z or low sputtering liner materials, or a gas blanket. Since the purpose of the current studies was to examine various TF coil technologies over a rather broad design space, this decision not to include an active impurity control system in designs employed in the trade studies was judged acceptable. The judgement was also made that this decision would not bias the outcome of the trade studies. However, in conjunction with the trade studies, a parallel investigative study was conducted in which magnetic divertor designs were examined and developed. The following section briefly summarizes a compact poloidal divertor design developed for TNS application.

TABLE 5-1

THERMAL/HYDRAULIC CHARACTERISTICS* OF REFERENCE VACUUM VESSEL DESIGNS

	No Divertor	With Divertor
OVERALL SEGMENT CHARACTERISTICS		
Number of Segments	60	60
Average Inner Flange Width (cm)	52.4	52.4
Average Outer Flange Width (cm)	39.4	39.4
Depth of Web	8.6	8.6
Poloidal Circumference (cm)	1200	1200
First Wall Surface/Segment (m^2)	6.29	6.29
Surface Heat Flux (W/cm^2)	85.0	28.0
Surface Heating/Segment (MW)	5.34	1.76
Segment Volume (m^3)	0.241	0.241
Nuclear Heating Rate (W/cm^3)	45.0	45.0
Nuclear Heating/Segment (MW)	10.84	10.84
Total Heating/Segment (MW)	16.18	12.60
Water Volume Flow/Segment (m^3/s)	0.129	0.100
Total Vacuum Vessel Head Load (MW)	970.8	756.0

	First Wall		
CHANNEL NETWORK CHARACTERISTICS	No Divertor	With Divertor	Non-First Wall
Channel Pitch (cm)	3.0	3.0	3.0
Channel Width (cm)	2.4	2.4	2.4
Channel Depth (cm)	1.11	0.73	0.54
Flow Area/Channel (cm^2)	2.66	1.75	1.30
Wetted Perimeter (cm)	7.02	6.26	5.88
Hydraulic Diameter (cm)	1.52	1.12	0.88
Coolant Velocity (m/s)	7.0	6.0	5.0
Velocity Pressure (kPa)	24.2	17.8	12.3
Reynolds Number	193,000	122,000	79,800
Friction Factor	0.02	0.02	0.02
Friction Pressure Drop (kPa)	191	190	168
Heat Transfer Coefficient** (W/cm^2K)	2.51	2.36	2.14
Heat Transfer Coefficient*** (W/cm^2K)	5.88	4.93	4.12
Coolant Film Temperature Differential (K)	22.1	14.8	10.7
Total Heat Load (MW)	8.17	4.59	8.01
Water Volume Flow/Segment (m^3/s)	0.065	0.036	0.064

*Heating rates are based on an early TNS reference design.

**Based on channel wetted area.

***Based on overall network covered area.

5.2.1 A COMPACT POLOIDAL DIVERTOR DESIGN FOR TNS

This study concentrated on the "so-called" natural poloidal divertor configuration where the divertor and equilibrium field (EF) coils are inside the toroidal field (TF) coils. It is generally conceded that to operate a tokamak at steady state, or for long burn times, a divertor with a high efficiency particle trapping system may be necessary to reduce the impurities and fusion ashes. Aside from impurity control, a divertor will also be required to handle the fuel throughput if recycling is shown to be impractical. The concern here, assuming a magnetic divertor is proven to be necessary, was to find a design approach which is theoretically feasible and within the present day design technology. Considerable attention has been focused on poloidal divertors and their advantages and difficulties have been discussed by other investigators. The advantages are: 1) that the poloidal divertor is a natural result of having a poloidal field to maintain plasma equilibrium; and 2) that it will maintain the axisymmetric configuration of the tokamak. The disadvantages are: 1) the power deposition on the particle collecting surfaces tend to be very high; 2) the engineering problems associated with the divertor coils and particle collection tend to be very difficult; and 3) auxiliary pumping requirements are still very high. In the current study, a major focus was to develop a concept and a design to provide sufficient collecting area to maintain the average power deposition below 3 MW/m^2 and at the same time minimize the height of the divertor system.

PHYSICAL CONCEPT

The key plasma parameters chosen for the divertor study were from an early TNS tokamak design. The MHD equilibrium calculation of the flux pattern and the other analyses were based on the early design parameters. While this early design differs from the current reference point designs, the parameters were similar and the divertor design is easily adapted to the current designs. From stability considerations, a D-shaped plasma cross section was found to be desirable and in the process of determining the required distribution of windings it was found

that a particular arrangement of turns led to a natural poloidal field divertor configuration with fluxes near the null point of the D-cross section.

The principle of the compact poloidal divertor concept is shown in Figure 5-6. In this concept, an array of opposing coil sets is used to define a magnetic flux channel. The net current of these coil sets is designed to be zero so that they have negligible effect on the plasma. The lower set of coils has positive currents, in the same direction as the current I_{EF-D}, which form a plane passing through the original divertor coil. The upper set of coils has an equivalent negative current. The angle of the current plane with the horizontal is arbitrary and is about 20°, as shown in the figure, to provide maximum utilization of the space. The objective of this design was to form a channel between the two coil sets by compressing the flux instead of expanding it vertically (the usual way to gain area). The height is reduced, but the width is increased to use as much of the available space as possible.

The burial chamber is located inside this channel which looks like a dished washer with thickness d and width w. In this model, d = 0.3 m, w = 1.5 m, and the total current in each coil set is I_D = 3.0 MA. The poloidal field intensity B_p in the burial chamber is about 1.55 T. Based on the above design parameters, the design concept and orientation of the divertor with respect to the tokamak is shown in Figure 5-7.

Particle Collection Methods

Two methods have been investigated for particle collection; these are 1) flowing liquid lithium and 2) solid metal collectors. These methods are illustrated in Figure 5-8. The flux lines in the burial chamber as sketched in Figure 5-8a are viewed from the top. If this flux slab is divided into 48 bundles, the method of collecting the particles is to intercept the oncoming particle stream with lithium-wetted screens as shown by Figure 5-8b which is the enlargement of a flux bundle AB of Figure 5-8a. The space behind the screen is available for structure, pumping ports, and a lithium circulating path. The lithium screens would also be placed on the top and bottom of the collecting horn to increase the

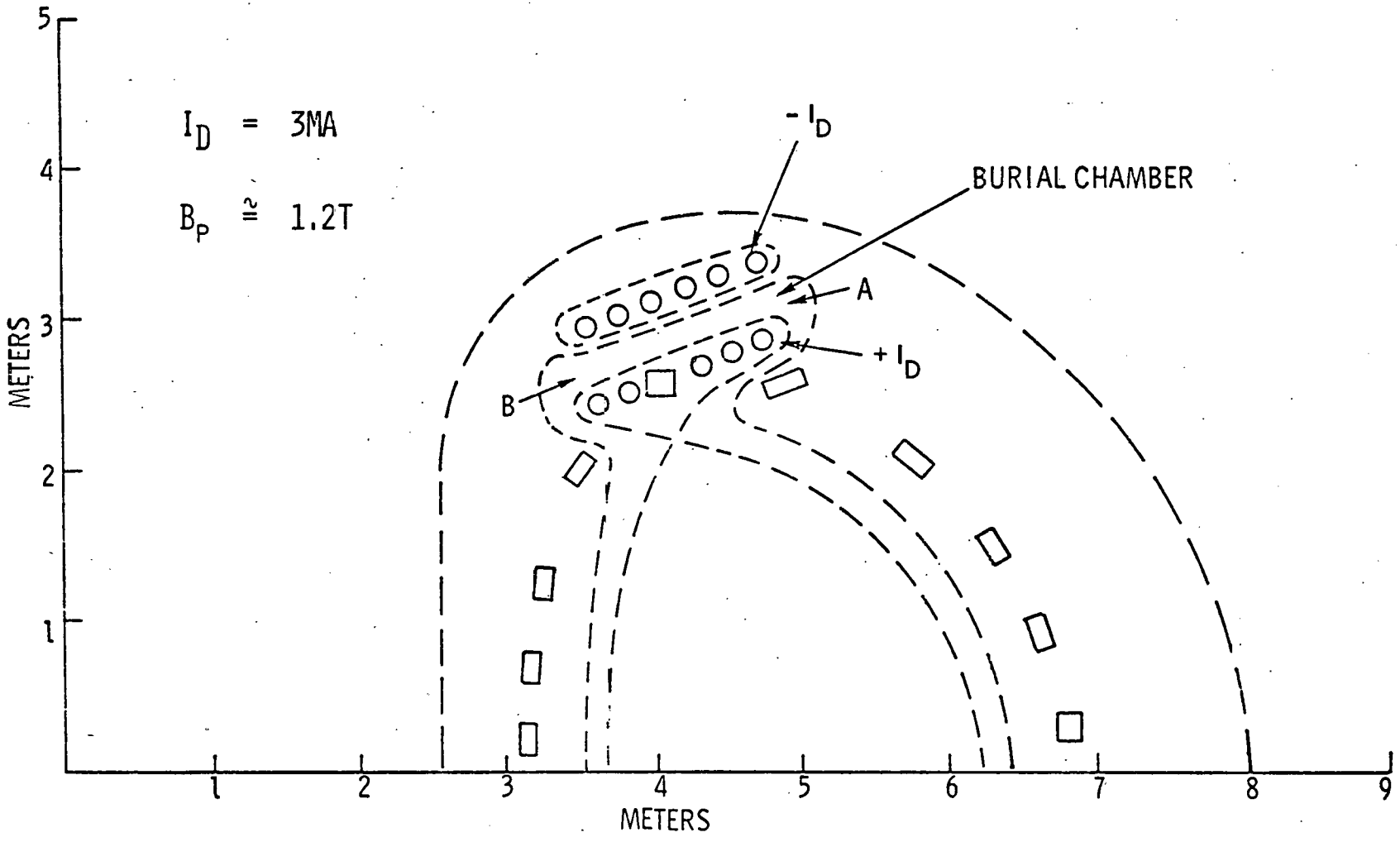

Figure 5-6. Proposed Divertor Design; Flux in the Chamber is Compressed by Two Sets of Coils.

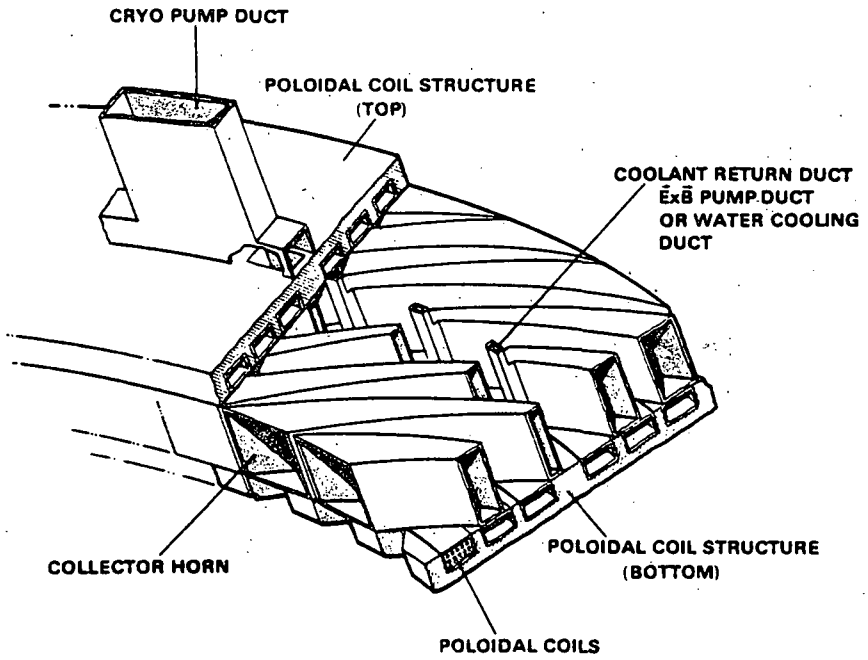

5-7(a)

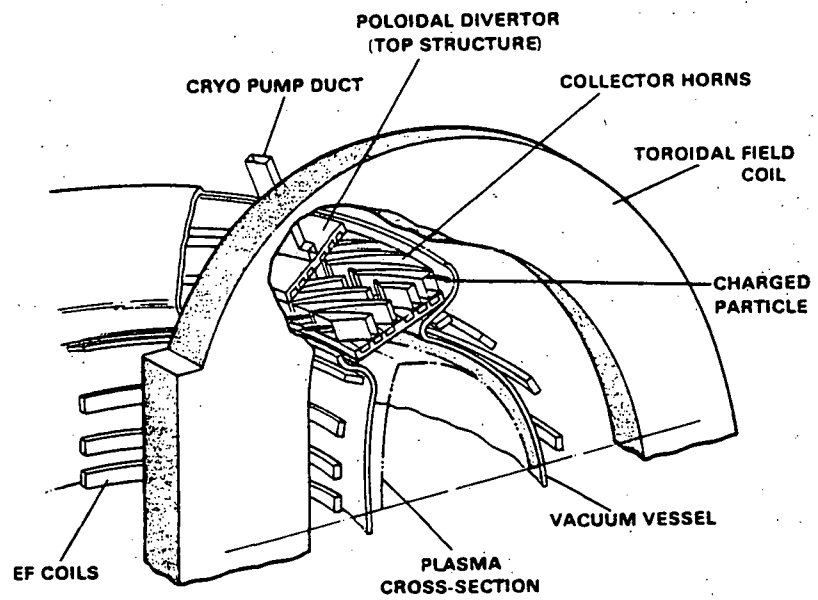

5-7(b)

Figure 5-7. The Sectional Trimetric Views of the Poloidal Divertor (a) Assembly and Its Implementation in TNS (b)

5-8(a)

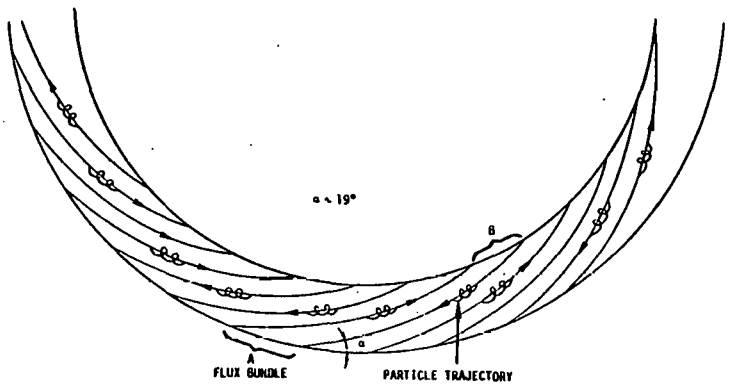

5-8(b)

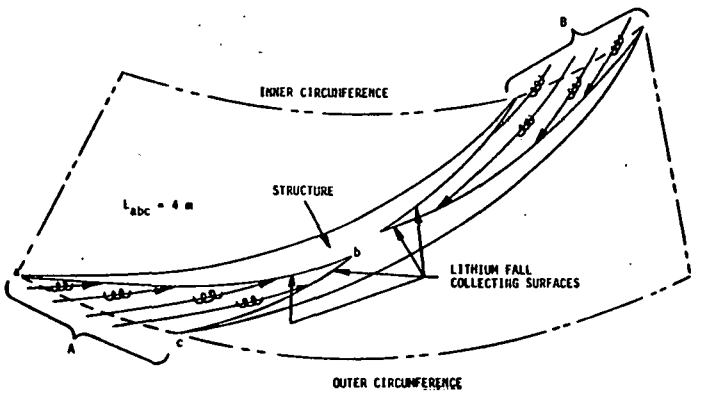

5-8(c)

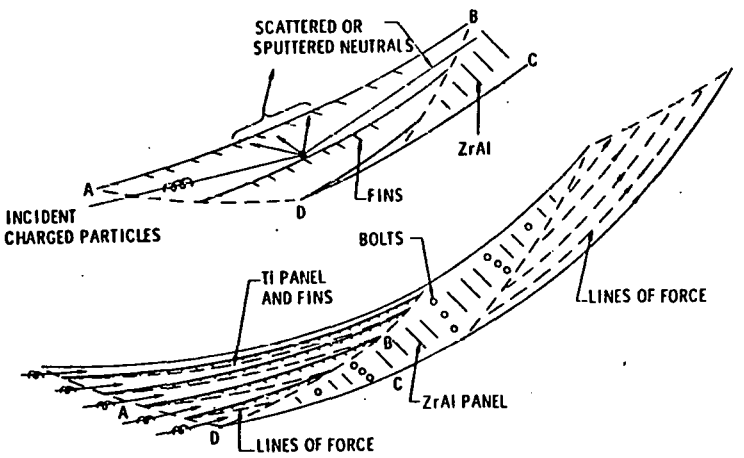

Figure 5-8. Illustrations of the Methods of Particle Collection Using Liquid Lithium Film or Solid Metal Collector Panels

collecting area. All of the structures and coils are protected from the particles by the lithium-wetted screens formed in the shape of a "horn". There are a total of 192 horns which give a total collecting area of $\approx$ 320 m^2. For solid getters a much larger surface area is needed to reduce the thermal load and particle flux. For this purpose, each of the 48 flux bundles is divided into six channels as shown in Figure 5-8c. The collecting panels are indicated by solid lines with fins. The fins are shadowed by the panels from the incident charged particles and serve only as traps for scattered or secondary neutral particles. This is again illustrated by the enlarged segment. There are no backside walls in these horns so that the neutrals that escape trapping on the fins will enter and be gettered by the Zr/Al panels located behind the horns. Therefore, the power density is reduced to 0.5 MW/m^2 which can be easily handled. The charged particle collector panel is chosen to be titanium.

The flowing liquid lithium system is complicated and contains unknown physical uncertainties. The pumping requirement for helium alone is too high to handle, even with the most optimistic assumptions. The fact that the removal of helium is one of the main purposes of the divertor led to a serious look at the use of solid metal getters.

The principle and methods for using solid getters to achieve an ultrahigh vacuum are well-known and such getters are commercially available. However, the use of solid getters to collect particles in the divertor burial chamber has not been seriously investigated.

The mechanisms involved in collecting ions by solid metal are ion entrapment, atom diffusion and, in some cases, channeling is important. Practical applications are found in ion pumping. In fact, the entrapment of positive ions in solids is the only significant mechanism for pumping rare gases such as helium. The trapping coefficient ranges from zero to nearly unity depending on the incident ion, its energy, target material, and its temperature.

The divertor pumping system must be capable of maintaining a high vacuum while handling a large flux of very energetic particles diverted from the scrape-off zone of the plasma. Thus, the collector must have the capacity for both the particle and thermal loads. What is desired is a high sticking probability, a low sputtering yield, and at the same time, the capacity for gettering large numbers of particles (hydrogen and helium). The other physical characteristics which are of interest are the melting point, the density per mole, and thermal stress. The metals with high melting points investigated for this gettering application are surveyed and tabulated in Table 5-2. The temperature range given represents the range in which the sticking probability is greater than 0.8. The capacity of the getter materials is defined as the fluence before saturation occurs. The saturation fluence, sticking probability, and capacity increases with incident ion energy. Titanium has a wide and suitable temperature range, high sticking probability and high saturation fluence for hydrogen and a low sputtering yield for light ions.

As shown in Table 5-2, zirconium has a slightly higher sputtering yield with hydrogen of 3% (as compared to $\sim$ 1% for titanium), but the optimum operating temperature range extends to about 390°C (as compared to 280°C for titanium). The cooling water required is therefore less than that for titanium plates. The trade-off is a 2% in sputtering yield between these two materials against the cooling water requirement. Titanium and zirconium are hence two good candidates as solid getters for the divertor.

The high heating load on the leading edge of the collection needs careful evaluation. By rounding off the corners and curving the edges into the horn interior, the thermal load can be designed to be below 3 MW/m^2 concentrated on a 1 mm strip. Niobium or tungsten inserts could be used to protect the leading edges.

TABLE 5-2

COMPARISON OF IMPORTANT THERMOPHYSICAL PROPERTIES OF SOLID GETTER MATERIALS

(1) Sticking Probabilities for a Given Target Temperature Range. The Lower Sticking Probabilities are the Values at the Low and High Ends of the Temperature Range.

(2) Saturation Doses and Sputtering Yields for Several Metals are for H^+ or D^+ at Normal Incident Energy Ranging from 1 to 5 keV

Element	Melting Point °C	Density g/cm^3	Atomic Weight g	Optimal Temperature Range °C	(1) Sticking Probability		(2) Saturation Dose cm^{-2}	Reemission Constant k	(2) Sputtering Yield %
					lower	max			
Er	1400	9.16	167.3	160-650	0.8	0.92	-	-	3.0
Mo	2620	10.20	95.94	-	0.8	-	$\sim 10^{17}$	4.3×10^{-3}	-
Nb	2415	8.57	92.90	(-70)-230	0.8	0.96	2×10^{17}	-	< 0.9
Ta	2996	16.60	180.95	-	0.9	-	10^{18}	-	-
Ti	1725	4.50	47.90	(-50)-280	0.8	0.96	10^{18}	-	< 1.0
W	3410	19.40	183.85	-	0.8	-	5×10^{16}	-	-
Zr	1857	6.49	91.22	(-10)-390	0.8	0.96	10^{18}	-	3.0

CONCLUSION

The evaluation of the major aspects of the divertor concept presented indicates that it is a viable approach. This design will make most economical use of the space inside the TF coil array and provide very large particle collection suface areas which allows the use of solid collectors. Approximately 60% of the helium ions can be trapped by the solid metal panel, hence, the auxiliary pumping requirement for helium is significantly reduced.

The divertor proposed here can be accommodated within the clearance already existing in the TNS design configuration examined. Regardless of which toroidal field coil technology is chosen, it appears that the compact divertor approach can be implemented with minimal impact on the overall machine size.

A more comprehensive discussion of the design development of this concept and the supporting rationale and analyses is contained in Reference 16.

5.3 NUCLEAR SHIELDING

D-T plasma operation in any of the TNS options will produce large quantities of 14.1 MeV neutrons. These very high energy neutrons plus the secondary radiation they generate in the form of both gamma rays and lower energy neutrons will cause damage to materials and represent a personnel hazard. Each of these requires that adequate shielding be provided within the design. For the various TNS options, several assumptions were made regarding the radiation shielding and the manner in which it can be scaled in size, the most important of which are given below:

- The shield material will be 65 v/o stainless steel and 35 v/o borated water (1 boron atom per 68 water molecules). This material attenuates the neutron flux by one decade for each $\underline{\sim}$ 18.5 cm thickness.
- The stainless steel will be in the form of balls about 1 cm in diameter. The borated water also serves as a coolant for the shield.

- The thickness of the device shielding located between the vacuum vessel and the poloidal windings will be determined by limiting the dose at the poloidal windings to $\leq 10^{10}$ rads over the lifetime of the device. The dose of 10^{10} rads is the threshold for radiation damage to the PF winding insulation which is epoxy resin bonded, mineral filled, laminated glass fiber.

- An analytic expression, based on the results of one-dimensional transport analyses (ANISN), was used to scale the thickness of shield material required between the vacuum vessel and the poloidal field coil as a function of the neutron wall loading.

- The thickness of shield between the vacuum vessel and the TF coils will be selected so that the total time averaged nuclear heating rate in the superconducting TF coils will be $\leq$ 20 kW (about one-third of the total pulse average heating rate in the TF coils). An analytic expression similar to that used to calculate the shield thickness for the poloidal windings was used to scale the thickness.

- A 0.05 m thickness of lead surrounds the primary shield for all TNS configurations that use superconducting TF coils.

- The total device shielding thickness will be the thickness required to attenuate the neutron flux (in the reactor cell) by $\sim$ 3.5 decades. Additional bulk shielding would not be very effective since $\sim$5% of the surface area of the torus is associated with ports and penetrations through the shielding.

- Ordinary concrete was used as the structural material for the walls, ceiling, and floor of the reactor cell.

- The thickness of the concrete walls, ceiling, and floor of the reactor cell were scaled by analytic expressions to limit the radiation doses to personnel to the following values:

Restricted Areas on Site	Design Objective
Annual	1000 mrem
Quarterly	600 mrem
Unrestricted Areas on Site	
Annual	100 mrem
Site Boundary	
Annual	5 mrem

- Shielding of thickness 0.3 m was required on the exterior surface of the neutral beam injector ducts.

The expressions developed for size-scaling the various nuclear shielding features of the design in the trade studies which have been performed are the following:

1) The thickness, t_{EF}, of borated-water cooled, steel shielding required to reduce the integrated radiation dose to the insulation on the EF coils to D_{EF} is given by

$$t_{EF} = 0.0808 \ln \left(5.60 \times 10^5 \frac{J_W \cdot N_T \cdot T_L}{D_{EF}}\right) \quad \text{(meters)}$$

where J_W is the neutron wall loading in MW m^{-2}, N_T is the total equivalent number of full power pulses, T_L is the effective time, in seconds, at peak power during a pulse, and D_{EF} is the permissible lifetime radiation dose in rads.

2) The thickness, t_{TF}, of borated-water cooled, steel shielding required to reduce the time-averaged nuclear heating rate in superconducting TF coils to P_{NTF} is given by

$$t_{TF} = 0.08095 \ln \left[14.6 R_o \cdot J_W \cdot (a + \Delta + 0.75) \cdot \frac{T_L \cdot P_{NTF}}{T_C} \right] \quad \text{(meters)}$$

where

R_o is the major radius in meters,

J_W is the neutron wall loading in MW m^{-2},

a is the horizontal minor radius of the plasma in meters,

Δ is the distance from the outside of the plasma to the interior surface of the shield in meters,

T_L is as previously defined,

P_{NTF} is the permissible time-averaged heating rate in the TF coils in kilowatts, and

T_C is the pulse period in seconds.

A thickness of 5 cm of lead must be added outside t_{TF}.

3) The thickness t_D, of borated-water cooled, steel shielding required to attenuate the neutron flux by 3.5 decades is $t_D = 0.65$ meter.

4) The thickness of ordinary concrete required to reduce the annual dose outside the reactor cell walls to 100 mrem for 1000 full energy pulses is given by

$$t_{wall} = 2.86 + 0.13 \ln \frac{P_F}{1570} \quad \text{(meters)}$$

where P_F is the peak D-T fusion power level during the pulse. This relationship assumes that the device shield provides 3.5 decades of neutron attenuation.

5) The thickness of ordinary concrete required for a flat ceiling and for the floor of the reactor cell are given by

$$t_{ceiling} = t_{floor} = 2.26 + 0.13 \ln \frac{P_F}{1570} \quad \text{(meters)}$$

6) The neutron wall loading is given by

$$J_W = \frac{2.25 \times 10^{-18} \bar{n}_D \bar{n}_T \langle \sigma v \rangle \delta a}{\sqrt{2 (1 + \delta^2) + 4 (1 + \delta)\left(\frac{\Delta 2}{a}\right) + 4\left(\frac{\Delta 2}{a}\right)}}$$

where	$\bar{n}_D$	is the deuteron density,	(m^{-3})
	$\bar{n}_T$	is the triton density,	(m^{-3})
	$\langle \sigma v \rangle$	is the Maxwellian averaged fusion cross-section,	$(m^3 s^{-1})$
	δ	is the plasma elongation factor,	
	a	is the horizontal minor radius of the plasma, and	(m)
	Δ_2	is the distance from the edge of the plasma to the first wall	(m)

A schematic cross section layout of the vacuum vessel and shield for the reference TNS with copper TF coils is given in Figure 5-9. A cross section layout of the shield design for the reference TNS with NbTi TF coils is given in Figure 5-10.

5.4 TOROIDAL FIELD MAGNET SYSTEM

The primary objectives for assessing the TNS options were device performance and cost which are significantly impacted by the TF coil configuration. It was considered desirable to select a coil configuration that was at least near term state-of-the-art as far as each coil type was concerned.

5.4.1 COIL SHAPE AND SUPERCONDUCTOR DESIGN PARAMETERS

The TF coils for the TNS were selected to be the pure tension D-shape design with trapezoidal cross section. The inner legs of the coils are wedged against a bucking cylinder to resist the centering forces. The central ohmic heating coils are located inside the bucking cylinder and are enclosed by an inner common dewar. The outer portion of each TF coil is enclosed by a separate dewar. The individual outer dewars mate with the central dewar outside the vertical legs of the coils.

A thermal-hydraulic analysis was completed for both the NbTi and Nb_3Sn superconductors for a toroidal field coils for TNS-3 and TNS-4, respectively, to determine the thermal and fluid flow characteristics of the conductor channels under normal and faulted conditions. An analysis for cooling the bobbins of the coils was also considered. The overall dimensions for the NbTi and Nb_3Sn coils used in performing these analyses are given in Table 5-3. These parameters are similar to those finally selected as the TNS reference point designs for TNS-3 (NbTi) and TNS-4 (Nb_3Sn).

For the superconductors, a multifilamentary and cabled design was selected. Copper is used as the stabilizing matrix. The cables are encapsulated by a thin stainless steel jacket. The conductors are cooled by forced flow supercritical helium through the interstices of the strands. The conductors are pancake-wound around

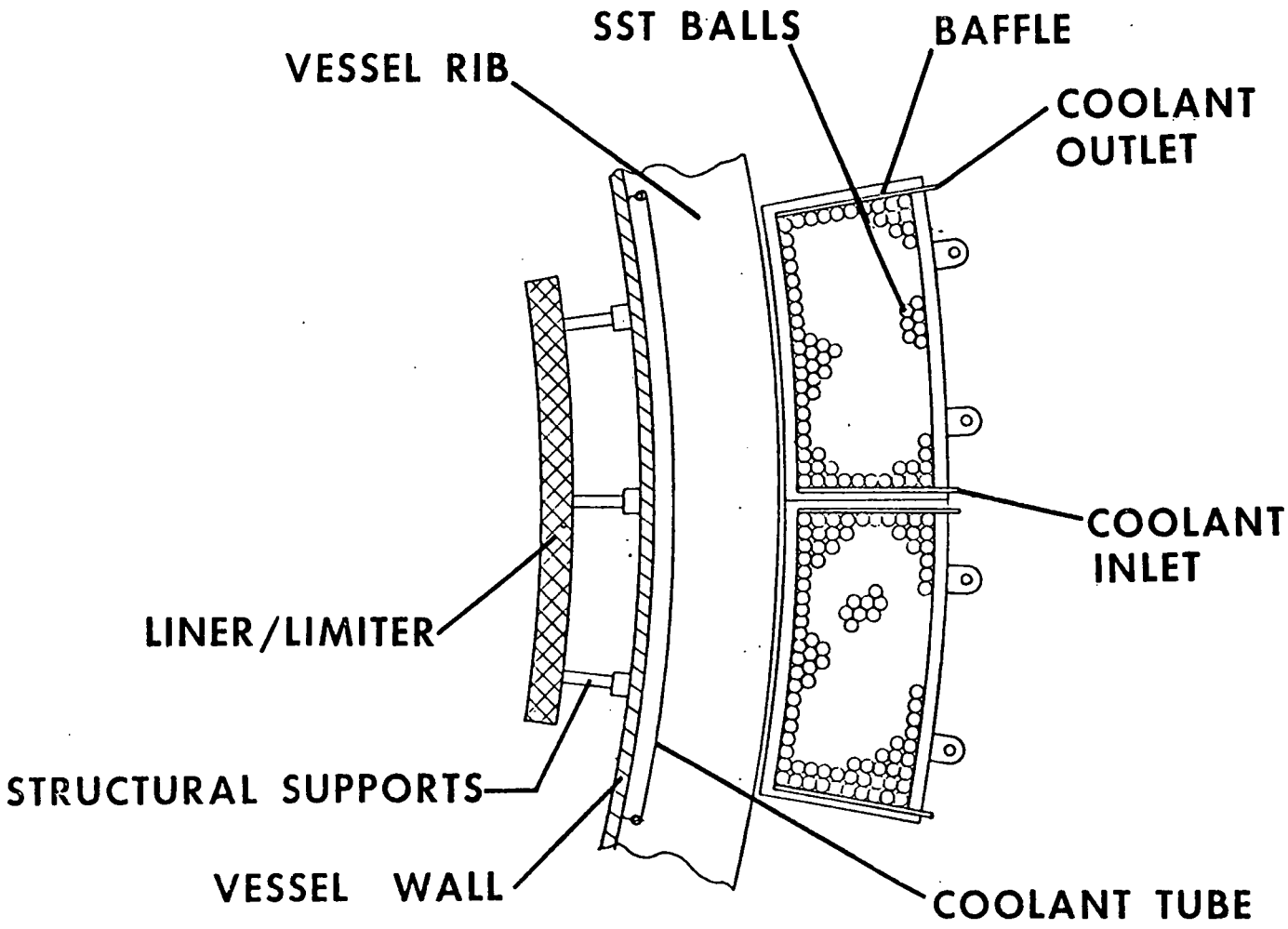

Figure 5-9. Vessel and Shield Schematic for TNS with Copper TF Coils

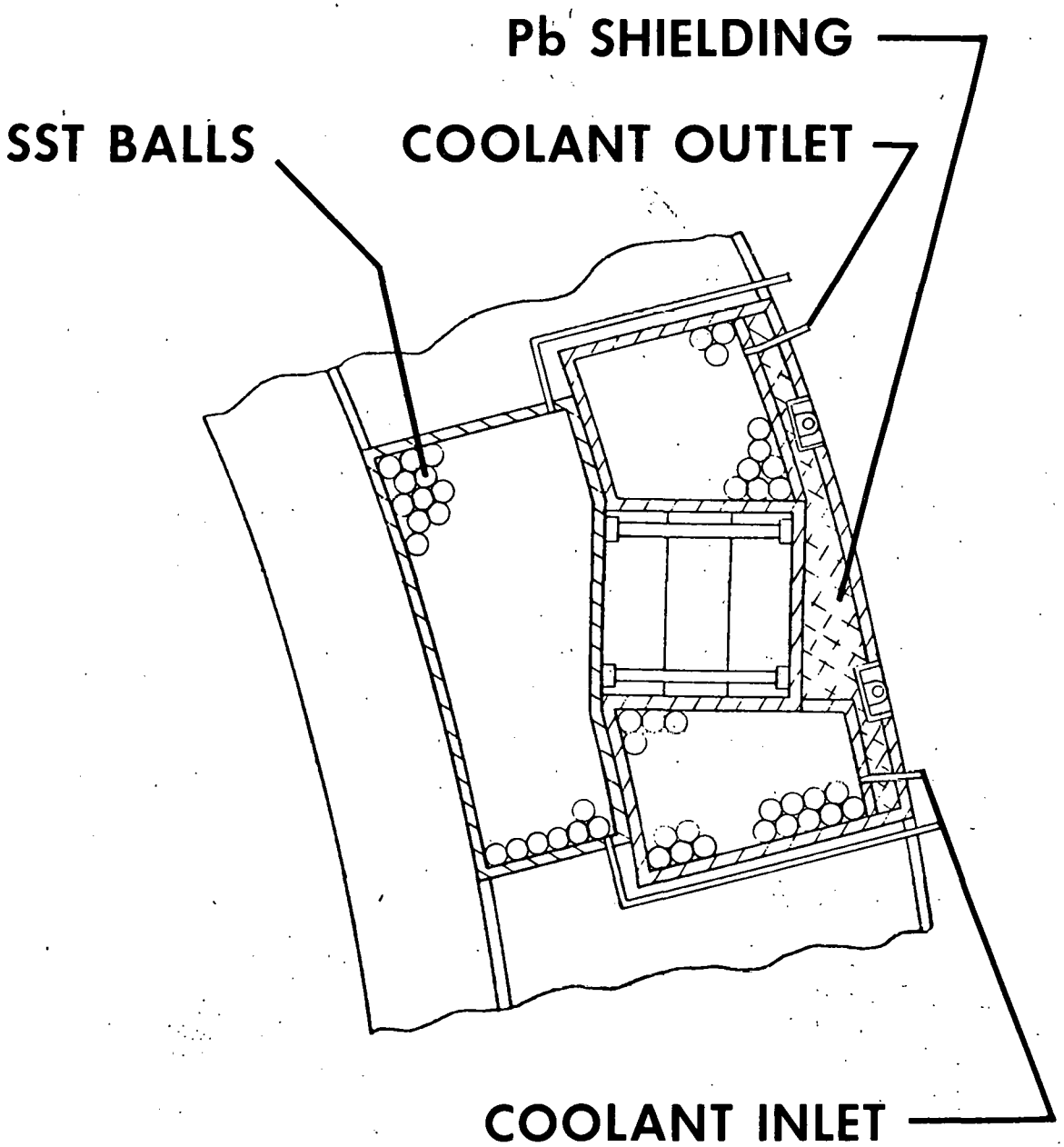

Figure 5-10. Shield Schematic for TNS with NbTi TF Coils

TABLE 5-3

MAJOR DESIGN PARAMETERS OF THE NbTi AND Nb_3Sn TF COIL OPTIONS FOR TNS
(VALUES SELECTED FOR THERMAL ANALYSIS)

	TNS-3 (NbTi)	TNS-4 (Nb_3Sn)
Major Radius, R_o, m	5.50	4.75
Minor Radius, a, m	1.2	1.0
Peak Field at Winding, B_m, T	8.3	11.6
Field at Axis, B_t, T	4.3	5.8
No. of Coils	20	20
Horizontal Bore, m	5.2	4.9
Vertical Bore, m	7.4	7.8
Mean Coil Circumference, m	22.8	23.8
Outer Radius of Vertical Leg, m	3.1	2.6
Radial Build of Coil, m	0.63	0.82
Coil Cross Sectional Area, m^2	10.8	11.6
Volume of Conductor, m^3	99	100
Volume of Structure, m^3	118	217
Stored Energy, MJ	8900	14000

the stainless steel coil support bobbins. This type of superconductor design and cooling method have been shown to be viable for large scale magnetic coils in various analyses and experiments. References 17 and 18 are two examples. The cabled design provides a large heat transfer surface area to strand volume ratio to enhance heat transfer. Forced flow cooling provides flexible control of coolant flow rate to assure cryogenic stability, in spite of the added power requirement for coolant pump work. The major design parameters of the superconductors are shown in Table 5-4.

The cross sections of the two superconducting coil options are shown in Figure 5-11. Multiple conductors are wound in parallel along the spiral slot in a bobbin, but are in series with those in the next bobbin. As shown in the figure for the TNS-3, there are five slots in a bobbin with four NbTi superconductors in a slot. The conductors are not graded radially.

For TNS-4 there are eight slots in a bobbin with three Nb_3Sn superconductors in a slot. The conductors are graded into three radial zones to reduce the cost of superconductors. The conductors in the same slot are to be cooled by a system of parallel hydraulic channels. The coolant would enter the parallel channels near the innermost turn of the coil where the magnetic field is the highest and exit at the outermost turn into a common plenum. One difficulty in this type of parallel channel cooling would arise when one conductor within a parallel flow system is driven to a normal state while the others in the same system remain superconducting. The transition from superconducting to normal increases the resistance to the coolant flow to the faulted channel. The total system coolant flow will be redistributed with the faulted channel receiving less than the design flow and the others receiving more coolant flow. The cryostability analysis to determine the coolant channel inlet flow rate in order to meet the stability requirement should therefore be performed based on a parallel channel fluid flow analysis.

5.4.2 STABILITY ANALYSIS

For superconducting TF coils, the superconductor and the cooling system are designed to be cryostable. The cryogenic recovery capability of a given conductor

TABLE 5-4

MAJOR DESIGN PARAMETERS OF THE NbTi AND Nb_3Sn SUPERCONDUCTORS FOR THE TNS-3 AND TNS-4 COIL OPTIONS (VALUES SELECTED FOR THERMAL ANALYSIS)

	TNS-3 (NbTi)	TNS-4 (Nb_3Sn) Zones		
		1	2	3
Nominal Peak Field, T	8.0	12.0	9.8	7.0
Overall Average Current Density x 10^7 A/m^2	2.86	2.85	3.75	4.65
S/C Operating Current Density, x 10^9 A/m^2	0.25	0.65	1.25	2.40
Conductor Plus He Area, x 10^{-4} m^2	3.72	5.26	4.0	3.23
Superconductor Area, x 10^{-4} m^2	0.4	0.23	0.12	0.0625
Void Fraction	0.4	0.3	0.35	0.4
Cu:Bronze:Nb_3Sn Ratio	4.6:1(1)	12:3:1	17.7:3:1	27:3:1
Strand Configuration	3 x 7 x 7		3 x 7 x 19	
Strand Diameter, mm	1.39	1.084	0.911	0.786
Wetted Perimeter, m	0.524	0.947	0.859	0.793
Percent Compactness	20	30	25	20
Hydraulic Diameter, mm	1.14	0.67	0.65	0.65
Nominal Channel Length, m	120	45	50	102
Coolant Inlet Temperature, K	4		5	
Approximate Total No. of Parallel Channels	2280		1233	
Estimated Refrigeration Load(2)	88 @ 4 K		38 @ 5 K	

NOTE: (1) Value indicates copper-to-NbTi ratio for TNS-3

(2) Includes pumping power with 50% efficiency, nuclear heating, ac losses and heat leakages.

	TNS-3 (NbTi)	TNS-4 (Nb_3Sn)
Total MA - T	118.5	137.4
I, kA	10	15
Conductor/Coil	292.4	457.9
Bobbin/Coil	29.6	19.1
Slots/Bobbin	5	8
Conductor/Slot	4	3
Structural/SC Area Ratio	1.19	2.16

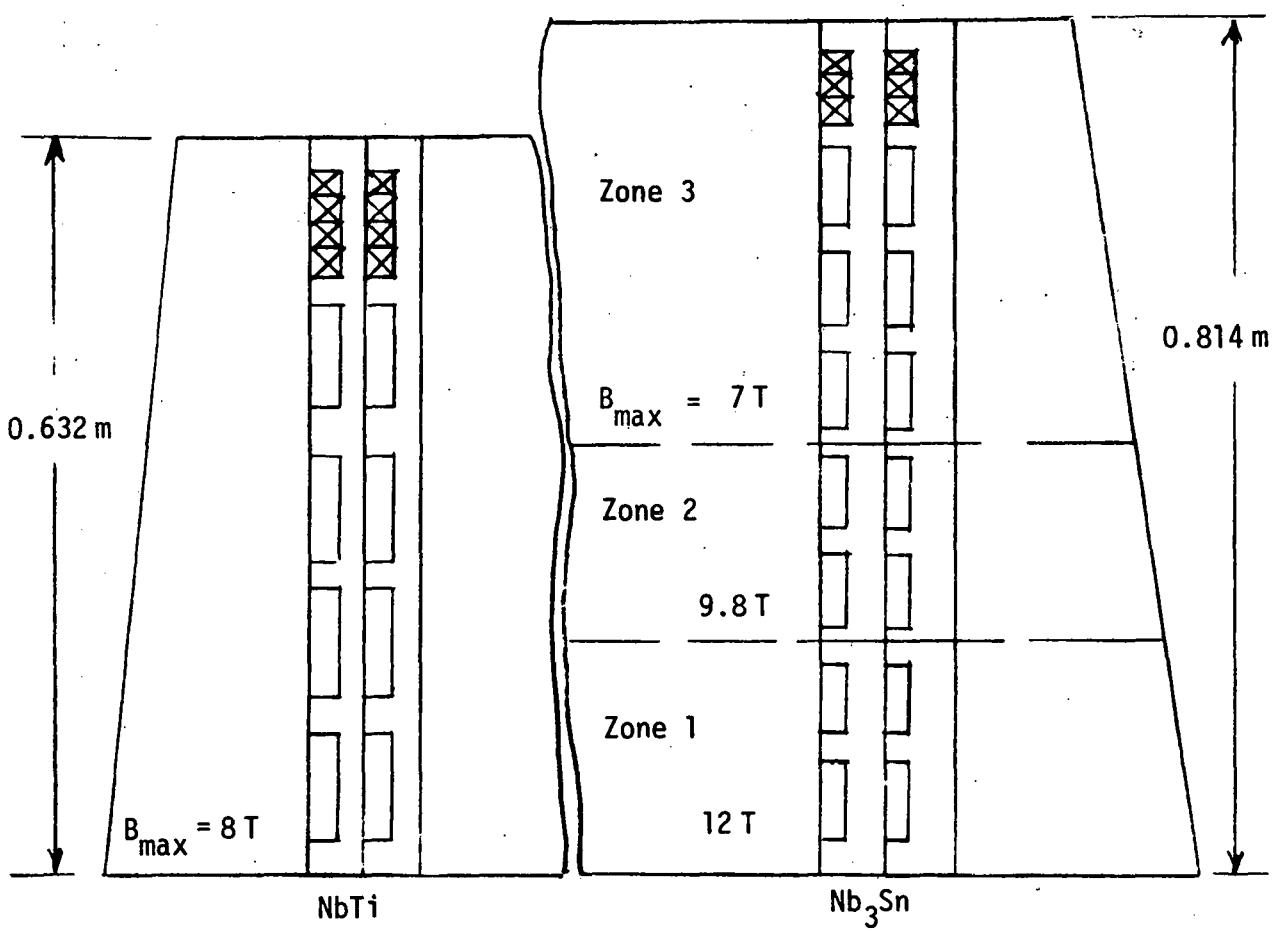

Figure 5-11. Pancake-Wound TF Coil Cross Sections of TNS-3 and TNS-4

design is defined as the ability to recover to a fully superconducting state from an initially imposed normal zone temperature (driven to that temperature by a sudden heat deposition in the conductor) over a given normal zone length.

The superconductor cryogenic stability analyses were performed for the NbTi and Nb_3Sn superconductors to determine stability and the cooling requirements. The resulting recovery capabilities of the superconductors from a temperature excursion into the normal resistive state are shown in Figure 5-12. The present stability requirement groundrule specifies that the superconductors shall be able to recover to their fully superconducting state after an event in which an amount of energy of 10^5 J/(m^3 of conductor plus He volume) is suddenly deposited in half of a turn of the conductor winding. Figure 5-12 indicates that the NbTi design can meet the requirement with a coolant flow mass velocity of 7.4 g/s-cm^2 per conductor and that the Nb_3Sn design can meet the requirement with a very small flow rate. However, in order to maintain a turbulent flow in the Nb_3Sn conductor channels, a flow mass velocity of 2 g/s-cm^2 per conductor was selected. At this mass velocity the stability margin of the Nb_3Sn superconductors is more than 3×10^5 J/m^3. The refrigeration requirements with the selected flow rates for the two superconductor designs are given in Table 5-4.

5.4.3 COIL FORCES

The TF coil centering forces are reacted by coil nose wedging for the TNS-1 copper option. The TNS-3 design utilizes a bucking cylinder, whereas TNS-4 considers a combination of bucking cylinder and coil wedging to minimize the thickness of the bucking cylinder and provide reasonable wedging stresses. Figure 5-13 illustrates this arrangement for TNS-4 (Nb_3Sn). The TNS-5 copper/NbTi hybrid option contains concentric rings of TF coils with the copper coils generating the high field inside the bore of the superconducting coil. The centering forces on the superconducting coils are reacted through a bucking cylinder. Completely independent of this system of forces, the centering forces on the copper coils are reacted against each other through the wedging faces on the copper coils. Figure 5-14 illustrates this arrangement for this hybrid design.

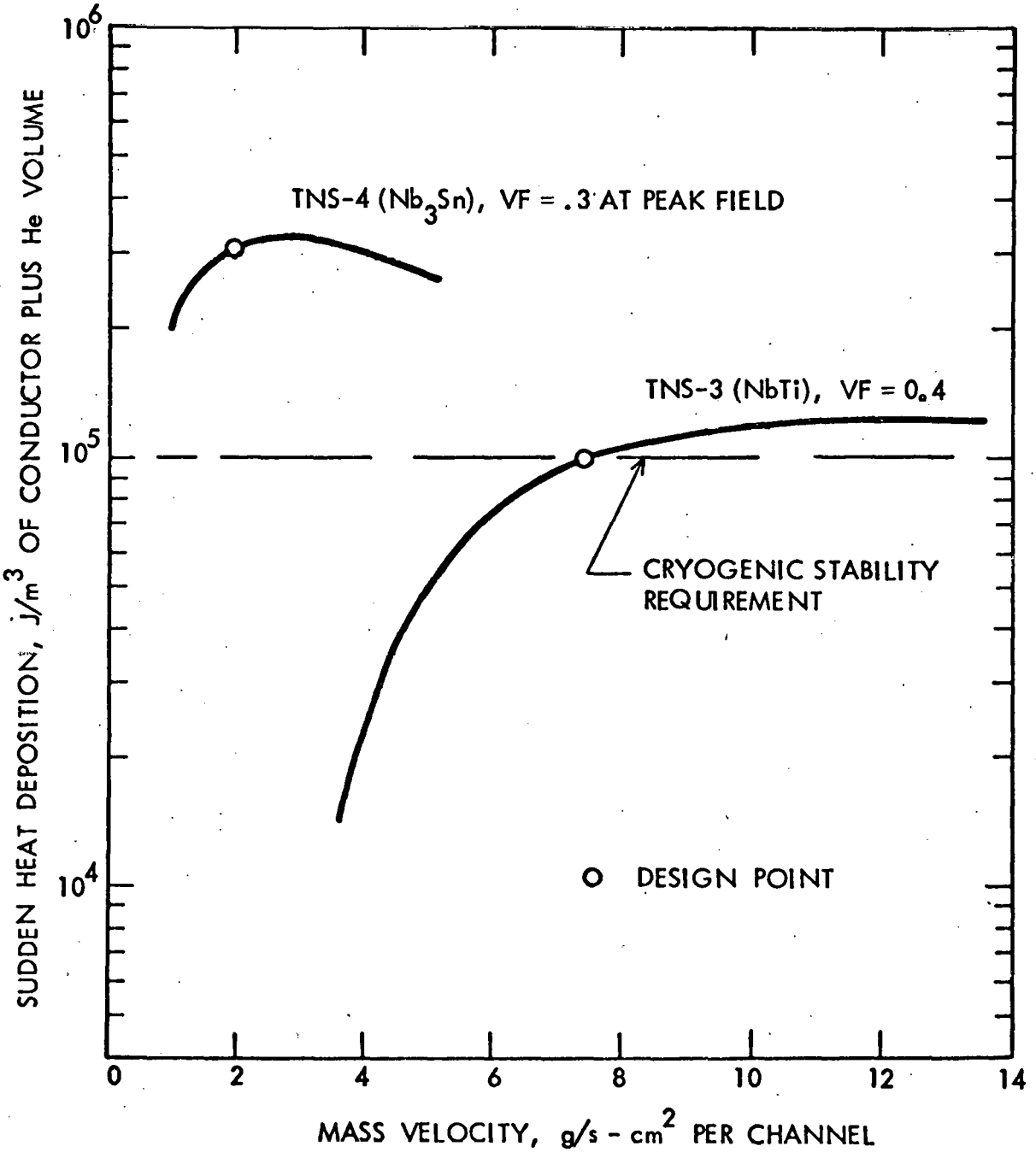

Figure 5-12. Recovery Capability of TNS Superconductors

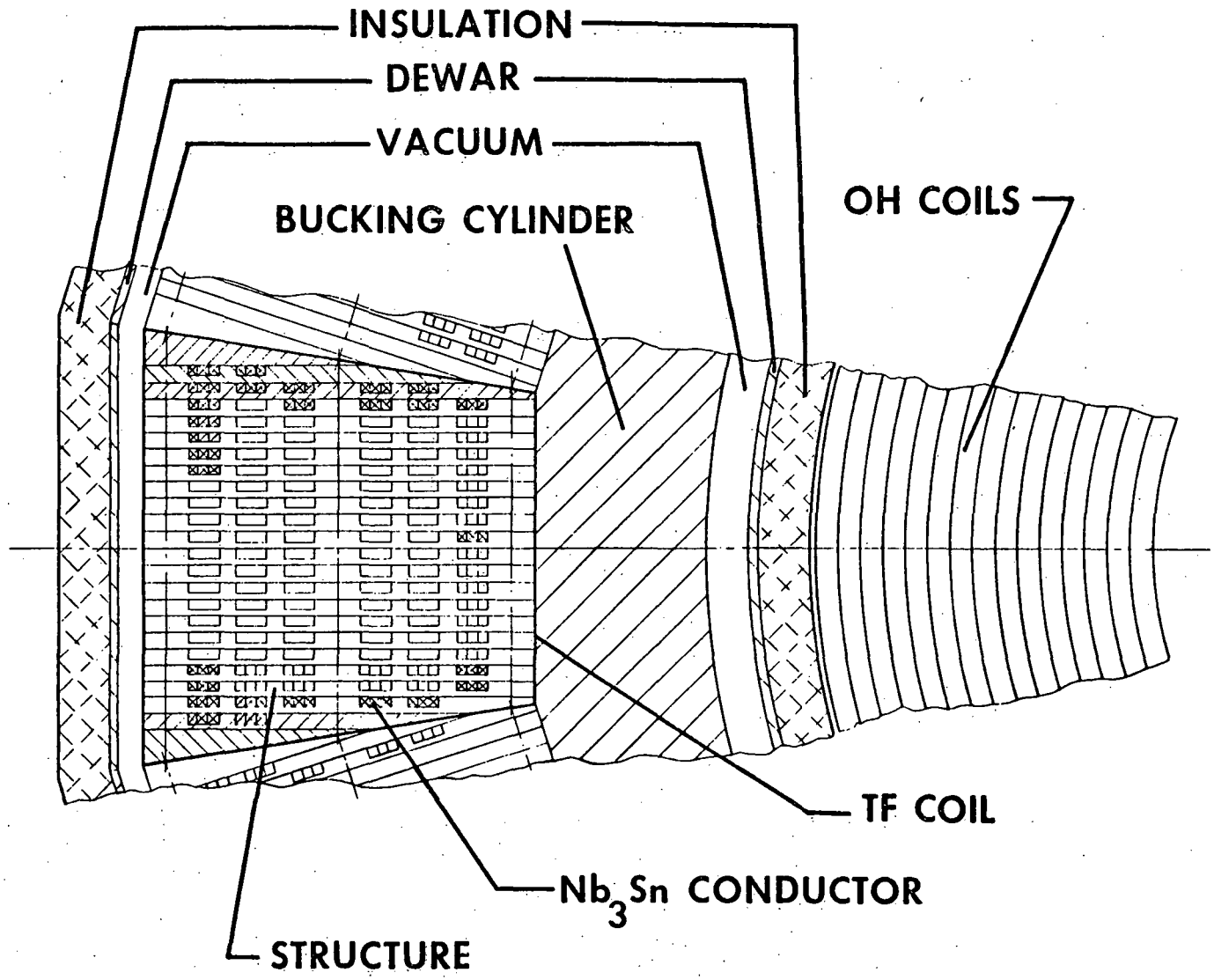

Figure 5-13. TF/OH Coil Cross Section - Reference TNS with Nb_3Sn TF Coils

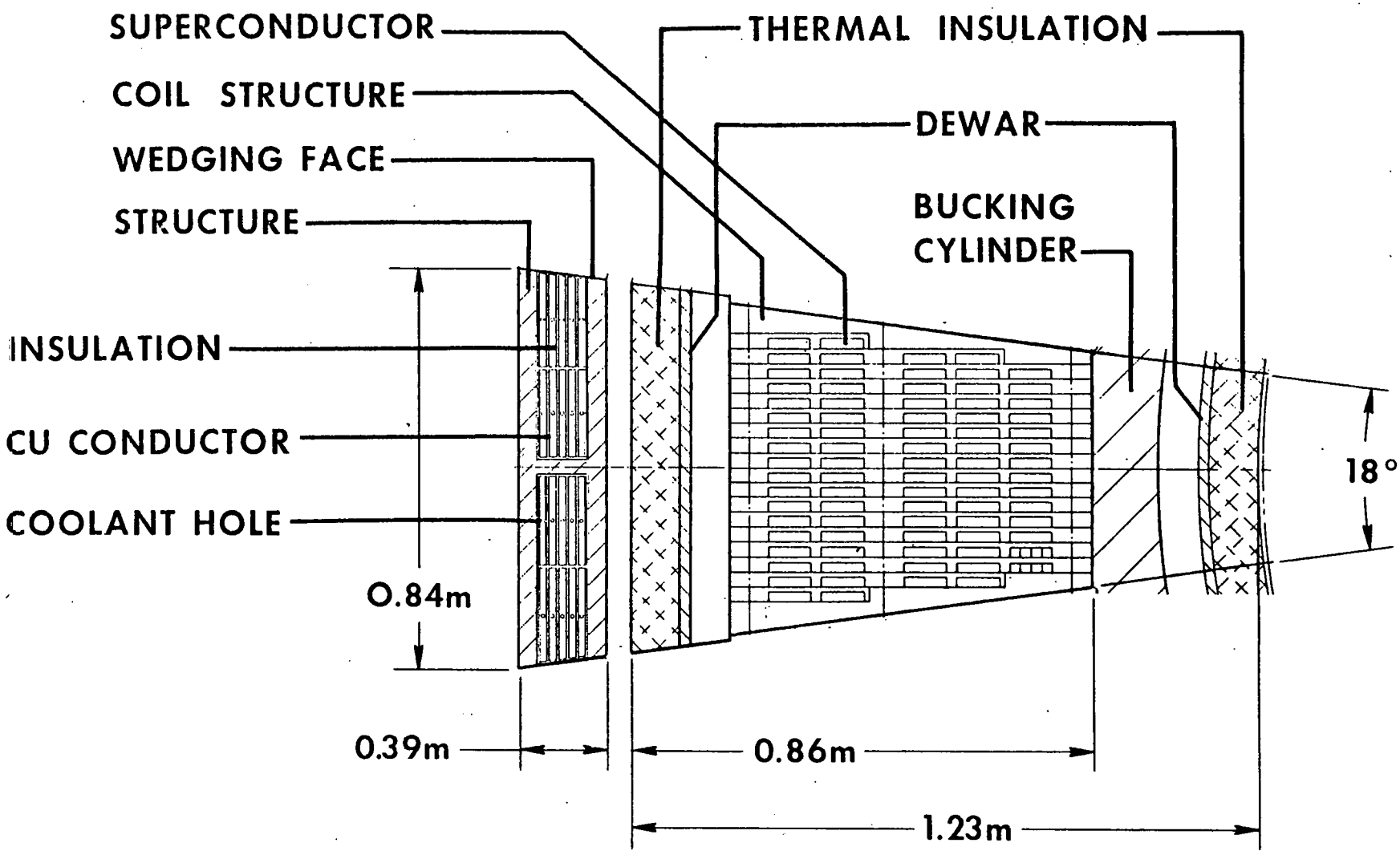

Figure 5-14. TF Coil Cross Section - Reference TNS with Hybrid Copper/NbTi TF Coils

To minimize heat losses, all of the superconducting coils are enclosed in a nitrogen cooled common vacuum dewar. The bucking cylinder, which resists the coil centering forces and the coil noses are enclosed in the common central portion of the dewar. Individual dewars surrounding each coil outer leg are connected to the large central portion of the dewar. The dewar with approximately a 0.9 cm vacuum gap is covered on the outside with $\approx$ 9 cm of foam insulation. Figure 5-15 illustrates this arrangement for the reference TNS with NbTi TF coils (TNS-3).

A spoke supported concept is utilized to transmit the vertical coil out-of-plane loads to the outer legs of the dewar. The coil support members carry the out-of-plane forces and the coil weight. The coil is supported around the circumference by the spokes (except in the wedging nose section) which are perpendicular to the coil plane and run from a mounting plate on the coil to the dewar wall opposite the mounting plate. Since the spokes are relatively long, bending stresses are minimized if there is relative in-plane motion between the dewar and the coil structure. The dewar-to-coil spoke arrangement is shown schematically in Figure 5-16.

A structural analysis of a spoke support system was performed considering the effects on a coil adjacent to a faulted coil; considering the combined effect of the loads from a faulted coil, the field, and bending of spokes due to coil in-plane displacement; and considering the thermal stresses due to a differential contractions of the coil, dewar, and spokes, due to cooldown to operating conditions. It was determined that 16 spokes of 1.59 cm diameter would be required to support the vertical load. A total load carrying area of 2032 cm^2 per coil is required to support the lateral loads. A total number of 380 spokes (equaling the 2032 cm^2 cross section) of various sizes are distributed along the curved portion of the D-coil to react the lateral forces.

5.5 POLOIDAL FIELD MAGNET SYSTEM

The poloidal field coils are used to provide the initial flux swing to produce current in the plasma, elongate the plasma, produce a double poloidal null for the divertor, and hold the plasma in place both horizontally and vertically. The poloidal field coils are divided into the ohmic heating (OH) coil set,

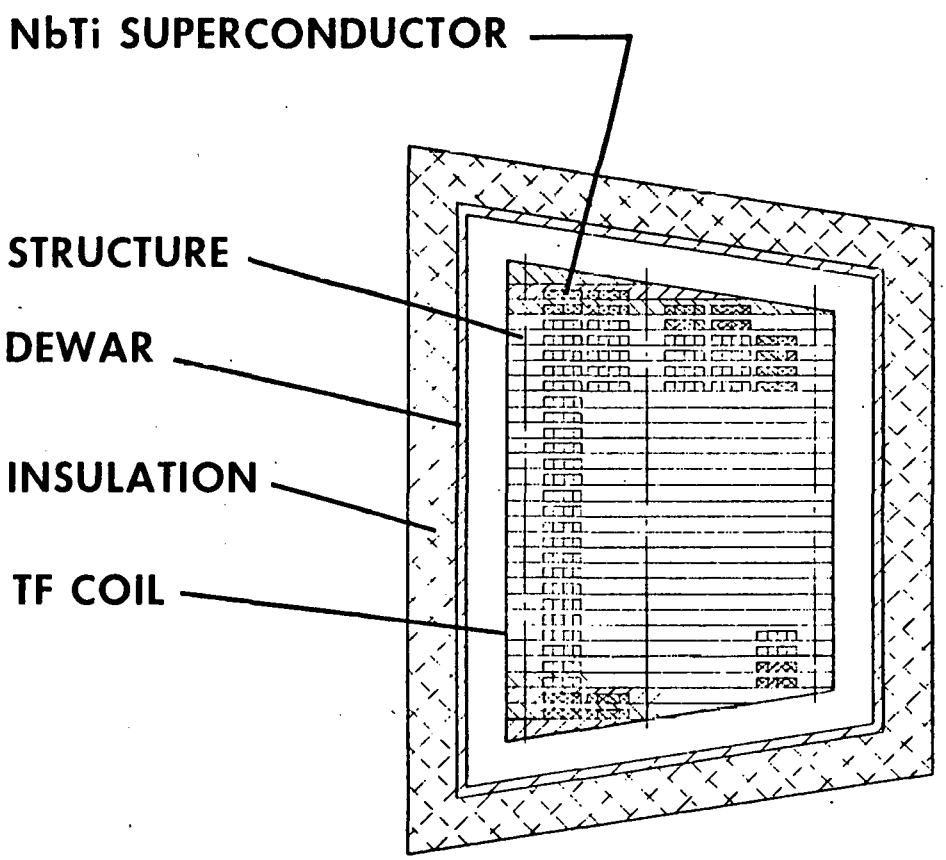

Figure 5-15. Dewar/TF Coil Cross Section Reference TNS with NbTi TF Coils

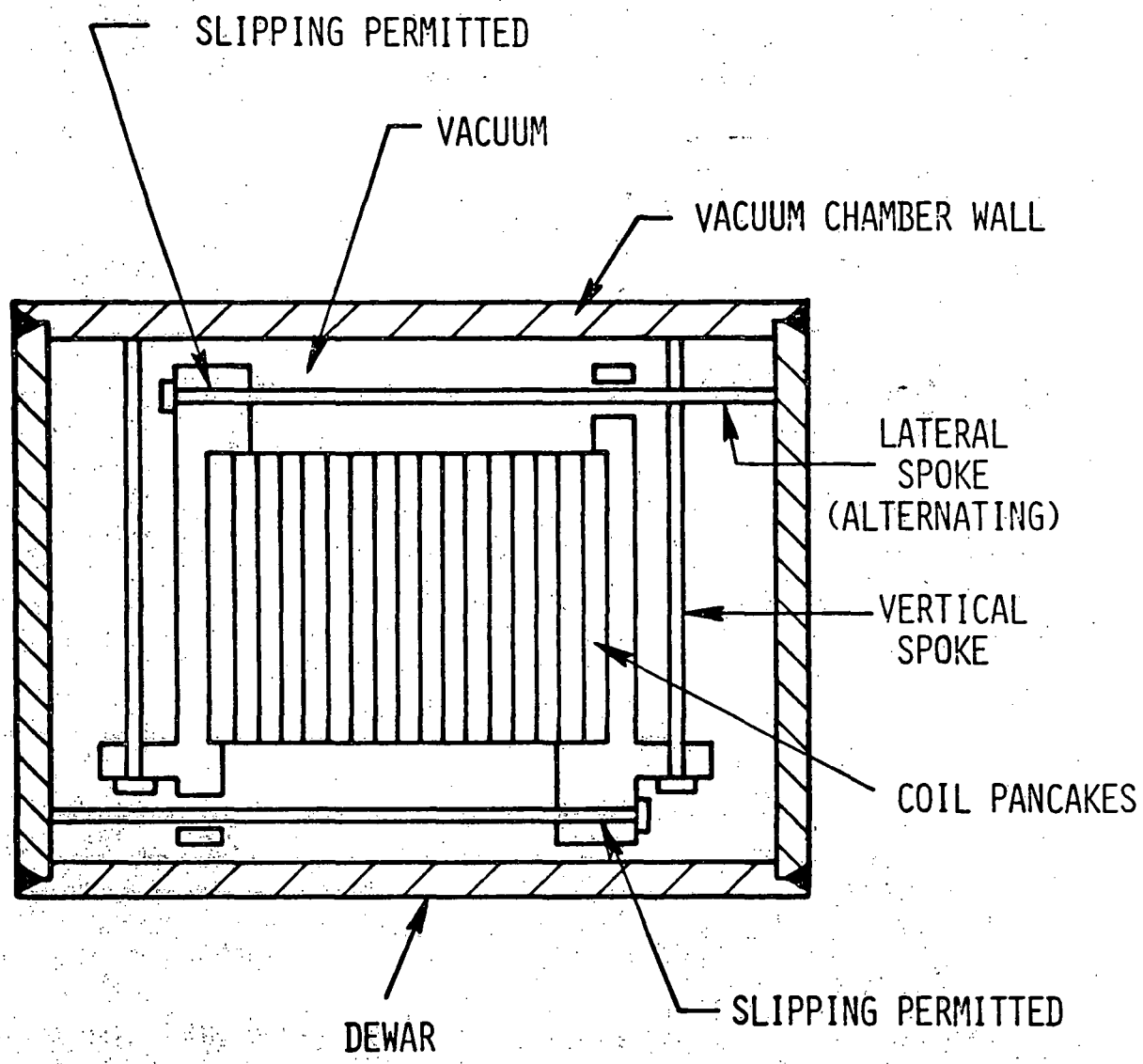

Figure 5-16. Schematic of Dewar-Coil Spoke Support Arrangement

which initiates the plasma current, and the equilibrium field (EF) coil set, which provides the remaining functions and provides a part of the flux swing.

The OH coil set provides a change in magnetic flux enclosed by the plasma in order to ensure breakdown in the plasma and produce the required plasma current. The OH coil set provides a continuing smaller change in the flux during the pulse to maintain the plasma current. The variation in OH flux over the plasma must be held to a low value in order not to disrupt the plasma.

The equilibrium field coils must provide a vertical field to maintain radial stability. The same coil set elongates the plasma moderately to an elongation of 1.6 and potentially provides a double poloidal null for the divertor.

As previously indicated no divertor system was employed in the TNS trade studies.

The poloidal field coil locations are as shown in Figures 4-2 through 4-5. The conductors are water cooled OFHC copper, insulated in typical fashion with layers of fiberglass or polyester tape epoxy impregnated and overwrapped with mylar. Alternate conductor materials were considered, but these materials proved unattractive for various reasons compared to the OFHC copper.

While both ohmic heating (OH) and equilibrium field (EF) coils were included in poloidal winding studies, major effort went into establishing OH coil feasibility especially in the bore, where the OH coils are stacked to form a solenoid unique to the tokamak design.

A study was performed to provide methods for improving engineering design solutions for ohmic heating solenoids. Solutions were provided to perform detailed structural analysis of every conducting turn in the radial build of the solenoid. A computer program was developed to perform this structural analysis for both the ideal approximation and the actual, more realistic, relationship between conductor stress and solenoid flux.

Placement of the coils of the EF coil system is an important consideration for a flux-conserving tokamak such as TNS. Their purpose is to maintain plasma

equilibrium during the heating phase of the cycle, at which time the plasma expands and becomes non-circular. The location of the coils relative to the plasma significantly influences plasma stability and power consumption in the coils. For these reasons, the coils that provide this shaping control (designated as SF coils or EF-I coils) are located within the bore of the TF coil array, as near to the plasma as design constraints would allow.

This location results in significant design problems. These can be attributed principally to the proximity of the windings to the plasma radiation source and the limited access between the vessel and the TF coil bore. Evaluation studies of design and maintenance issues associated with the coil location, clearly revealed that the single most complex operation identified was the remote maintenance of the coils installed in the annular space between the vacuum vessel wall and the bore of the TF coil array. A variety of methods have been proposed to permit maintenance and repair of these coils; however, the problem of coil design and service will not be advanced until reliable joint designs and remote maintenance techniques have been successfully demonstrated.

5.5.2 POLOIDAL FIELD (PF) COIL OPERATING CONSIDERATIONS

In the trade studies which were performed, a number of key assumptions were made to permit evaluation of the PF coil current and voltage requirements thereby facilitating the definition of the associated electrical circuit requirements and selection of components. The electrical circuit and component requirements are discussed in Section 5.6. It was assumed that the currents in the EF-I, EF-D, and EF-O coils are proportional to the plasma current, I_p, during the entire operating pulse. Recall that the EF-I coils are those PF coils located inside the plasma major radius, the EF-D coils are those located above and below the horizontal midplane which correspond to divertor-like locations, and the EF-O coils are those PF coils located outside the plasma major radius. All of the EF coils are located within the bore of the toroidal field (TF) coils. The OH coils (solenoid) are located within the bore of the device. As previously indicated, all PF coils in the present study were assumed to be manufactured from normal copper.

In the present trade studies, the voltage and current profiles were established for a specified plasma current time profile. In performing the plasma startup evaluation, the concept of a small radius startup was arbitrarily employed. It was assumed that during breakdown and initiation of the plasma that the minor radius of the plasma would be some fraction of the final full radius. Further, it was assumed that the breakdown and plasma initiation would occur during the first 50 ms of the pulse with the initiation voltage constant during the first 5 ms. During this initial 50 ms interval, the originally very high resistivity of the plasma will rapidly decrease, the plasma current will ramp up from zero to a fraction of the full startup current and the plasma voltage will decrease as the plasma resistivity decreases. Between 50 ms and 1 s, it was assumed that the plasma radius would linearly increase to the full radius value. During this interval, the plasma resistivity would continue to decrease, the plasma current linearly increases to the full startup current and the plasma voltage also continues to decrease. It should be noted that the time intervals 0 - 5 ms, 5 ms - 50 ms, and 50 ms - 1 s were selected based upon engineering judgement. In performing the calculations in COAST, the duration of these three intervals can be arbitrarily varied to determine sensitivity of the results and this was done in the present trade studies. Figure 5-17 schematically portrays the time dependent variation of the plasma current, voltage, resistivity, and radius during the initiation phase of the pulse.

During the plasma initiation period ($t = 0$ to t_2) the plasma radius is held constant at a minor radius ($= a_1$). The plasma current increases linearly from 0 to a value given by

$$I_p\ (t = t_2) = \frac{5\, a_1^2\, s^2\, B_t}{q_{in}\, R_o}$$

where s is the plasma shape factor, B_t is the value of toroidal field on axis, q_{in} is an initial value of the safety factor (selected to be 2.0 during this time interval) and R_o is the major radius. The plasma inductance is

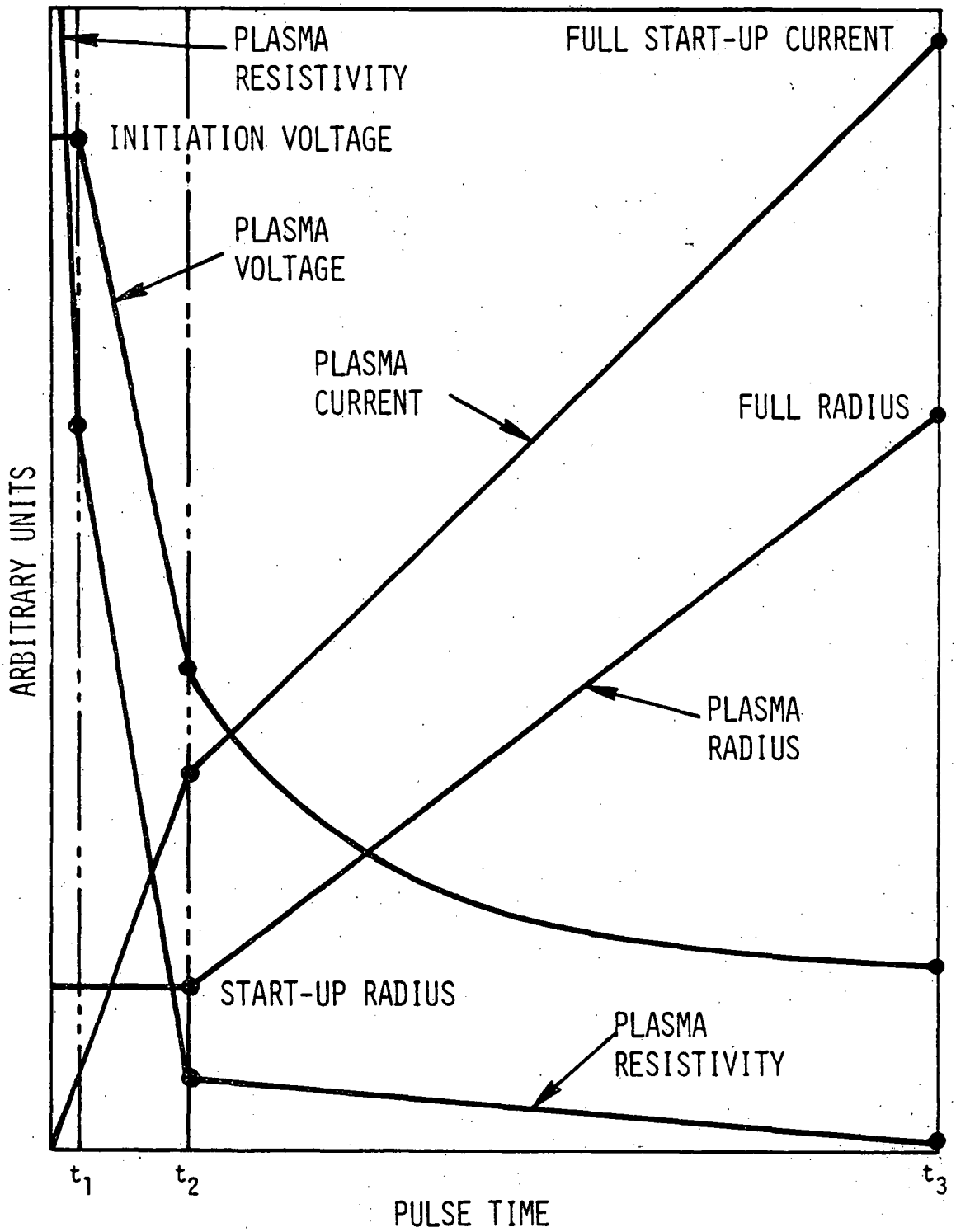

Figure 5-17. Plasma Start-up Calculation in COAST

calculated for the radius a_1 and the plasma resistivity at $t = t_2$ is proportional to $T_e^{-3/2}$ and T_e is specified.

As indicated, the EF coil currents are assumed proportional to I_p over the pulse interval. The OH coil current is determined on the basis of zero flux through the plasma. The OH current is adjusted to account for plasma resistive volt-seconds and assuming a 0.5 bias on the OH current.

The various coil voltages are calculated so as to include all inductance voltages (including all mutual and self-inductive terms) and including all restrictive voltages.

A precise flux map for a single circular coil element proved useful in determining the mutual inductance between pairs of coplanar coils as well as between the coil pairs and the plasma. A graphical construction method was developed to also permit determination of mutual impedances for non-coplanar coil pairs. Based upon this graphical method, families of curves were developed relating various mutual impedance ratios. These curves were then analytically fit to result in explicit formulae to determine all of the poloidal coil mutual impedances. Although a more sophisticated approach would be employed in the design of a given system, this approach was highly desirable and useful considering the large design space under investigation during these TNS studies.

The resulting inductance matrices for the four reference point designs summarized in this report are given in Tables 5-5 through 5-8 for TNS-1 through TNS-5, respectively.

Based upon the time dependent assessment of voltages and currents in each coil of the PF coil system, the capability requirements imposed upon the various electrical power supply components (switches, rectifiers, etc.) were determined. The features of the poloidal field coil electrical circuits are described in the following section.

TABLE 5-5

TNS-1 (COPPER

INDUCTANCE MATRIX

(Values on a Single Turn Basis in μH)

	PLASMA	EF-I	EF-D	EF-O	OH	R (μΩ)
PLASMA	7.58	2.92	2.79	6.83	0.575	——
EF-I	2.92	4.99	1.74	1.89	0.575	2.32
EF-D	2.79	1.74	9.12	2.72	0.575	19.71
EF-O	6.83	1.89	2.72	12.74	0.575	4.09
OH	0.575	0.575	0.575	0.575	0.544	0.123

TABLE 5-6

TNS-3 (NbTi)

INDUCTANCE MATRIX

(Values on a Single Turn Basis in μH)

	PLASMA	EF-I	EF-D	EF-O	OH	R (μΩ)
PLASMA	11.99	6.01	5.33	10.94	1.61	———
EF-I	6.01	8.51	4.11	3.99	1.61	4.14
EF-D	5.33	4.11	15.28	5.11	1.61	32.20
EF-O	10.94	3.99	5.11	17.06	1.61	5.92
OH	1.61	1.61	1.61	1.61	1.58	0.358

TABLE 5-7

TNS-4 (Nb_3Sn)

INDUCTANCE MATRIX

(Values on a Single Turn Basis in μH)

	PLASMA	EF-I	EF-D	EF-O	OH	R (μΩ)
PLASMA	9.74	4.38	3.97	9.03	0.688	——
EF-I	4.38	6.86	2.77	2.87	0.688	2.97
EF-D	3.97	2.77	12.39	3.86	0.688	24.12
EF-O	9.03	2.87	3.86	15.48	0.688	4.72
OH	0.688	0.688	0.688	0.688	0.664	0.169

TABLE 5-8

TNS-5 (Cu/NbTi)

INDUCTANCE MATRIX

(Values on a Single Turn Basis in μH)

	PLASMA	EF-I	EF-D	EF-O	OH	R (μΩ)
PLASMA	9.17	3.99	3.68	8.16	0.233	——
EF-I	3.99	6.20	2.59	2.62	0.233	3.17
EF-D	3.68	2.59	11.11	3.55	0.233	25.70
EF-O	8.16	2.62	3.55	13.88	0.233	5.00
OH	0.233	0.233	0.233	0.233	0.201	0.034

5.6 ELECTRICAL SYSTEMS

An early judgment was made to consider only water-cooled copper for the poloidal field coils in these trade studies, although investigations of superconducting systems were planned for a later phase of the study. As discussed in Section 5.5 for the poloidal field system, two types of coils were specified. Equilibrium field (EF) coils were specified to position and stabilize the plasma. In order to explore the possibility of high β operation and moderate elongation, the EF coils were placed inside the TF coils and were further subdivided into independently-driven inner (EF-I), outer (EF-O), and divertor type (EF-D) coils. The ohmic heating (OH) coil system, placed outside the TF coils, provided volt-seconds for the establishment, heating and maintenance of the plasma current. The EF coils were specified to have a net number of ampere-turns equal to the plasma current at all times. This constraint minimizes pulsed heating and overturning moments in the TF coils. This mode of operation for the EF coils also contributes a substantial fraction of the required plasma volt-seconds, reducing requirements on the OH coil system.

The ground rules for selection of toroidal field circuits depended primarily on whether the toroidal field coils were superconducting or resistive. For superconducting TF coil systems, such as the TNS-3 (NbTi) and TNS-4 (Nb_3Sn) machines, the power supply requirements are relatively modest. The desire to have a reasonably short system-start-up time, while requiring the low voltage from the TF power supply led to a ground rule that the electrical system should be capable of charging the TF coils to full current in 1/2 hour. Coil current was held to the conservative present state-of-the-art level of 10 kA. In order to ensure equal current in all coils, all TF coils are connected in series. In event of a fault, the low-voltage power supply is to be disconnected from the coil and the coil energy is to be dumped through external resistors.

For a TF system using copper TF coils, such as the TNS-1 (all copper) and TNS-5 (hybrid copper and niobium-titanium) machines, it was assumed that the copper coil currents would have to be pulsed and that motor-generator-flywheel sets would be necessary to buffer the TF coil power from the utility line. The current in the TF copper coils was to be charged, sustained and run down by a

single controlled power supply. Since the proposed pulses were of a sufficiently long duration ($\sim$ 30 second TF current flat-top times, $\sim$ 45 second charging times) to allow generator field control, a low-power exciter control and an uncontrolled diode bridge on the generator armature were selected as the controlled voltage source, instead of a more expensive controlled rectifier supply. The pulses are also sufficiently slow that a substantial portion of this pulse can be supplied directly from a stiff electrical grid, without buffering. Since this option is site dependent, it was modeled, but not selected in the costing studies.

5.6.1 SUPERCONDUCTING TF COIL POWER CONVERSION SYSTEM

While the specifics of the TNS superconducting toroidal field (TF) coil design are tentative, a power conversion system was identified as a working conceptual design for use in the trade study sizing and costs evaluations. TNS-3 and TNS-4 have superconducting coils for the TF field. TNS-5 employs a hybrid TF coil and uses both copper and superconducting windings.

The TF coil will be built in n segments, where $12 \leq n \leq 28$. For preliminary purposes a value of $n = 20$ was selected. The value of n does not have significant impact on the power conversion system except where the bore of the coil is changed to maintain a fixed field ripple in the plasma region. This causes the total stored energy and certain power supply component sizes to decrease as the number of coils is increased.

The coil current level has been tentatively set at 10 kA, which represents a conservative superconducting cable size. This sets the current capacity for the power conversion system.

It is desirable to connect all the coil segments in series electrically to provide for inherently identical currents in all coil segments. For larger systems, it may be necessary to go to series-parallel if the energy dump requirements result in too high a voltage. The coil segments could be parallel if the energy dump requirements result in too high a voltage. The coil segments could be subdivided into 2, 3, or 4 groups with each group having its own power conversion system and depend upon automatic control equipment to maintain

the currents equal. However, this increases cost, complexity and risk, so this approach would not be used unless some coil design problem such as insulation forces it. Accordingly, in the current TNS design trade studies, series connection of all coil segments was assumed.

The design for the coil system exhibits 128 H inductance. A reasonable time for bringing the TF coils up to full field is ∿30 min. This was selected as a compromise between taking hours to bring up the field, which would be satisfactory as a recovery time from a minor problem, and bringing up the field in very short times which would require very large power supplies. To get the field up in a 128 H coil system in 30 min. requires $\frac{10000\ A \times 128\ H}{1800\ s} = 711\ V$. Assuming that the power supply is ∿ 150 m (bus run) from the coil terminals, the total resistive drop in an air cooled copper bus and rectifier can be held to 12 - 15 V. The full current voltage requirement is about 725 V. Assuming 15% regulation loss in the rectifier, the open circuit voltage is ∿ 850 V.

In the event of loss of cooling, resistors are required to dump the current out of the coil system. The power supply cannot remove the current any faster than it built it up (30 min.) and this is judged to be too long.

The size of the resistors was estimated by allowing 500 V per coil segment for dumping (although a lower voltage may be adequate). At 10 kA, the resistors need to be ∿ 0.05 Ω which gives (for 20 segments) a total resistance of ∿ 1Ω across the power supply and a current drain at the peak value in the coil of 725 A (∿ 7% increase in power supply capability). The energy dumped in the resistors during startup will be 18.6×10^6 J. The energy dumped in the resistor from a coil dump is 6.4×10^9 J. Since the startup energy is less than 0.3% of the dump energy, the startup energy plays no role in sizing the resistors. Cast iron or steel resistors can be used with air cooling so that virtually no maintenance is required and no active systems are needed. To absorb the 6.4×10^9 J from 20 coils, or 3.2×10^8 J/resistor, requires 3.64×10^3 kg Fe/resistor assuming an allowable rise of 200 K. In a solid block, this would represent a volume of 0.43 m^3; with fins and connections each resistor will occupy a space several meters on a side.

Figure 5-18 illustrates the final TF circuit configuration for the superconducting designs with several features added. There is a grounding resistor connected from the center of the coil segment array to ground. This was selected to limit fault current under worst case conditions (during dumping) to 50 A, and is 100 Ω. Two isolation and grounding switches have been added to separate the coils from the power system. A saturable reactor will be required with the coil dump switch to allow clearing the arc over a wide range of currents. A solid state free-wheeling thyristor has been added across the power supply to provide a path for coil current to bypass the rectifier. This permits the coil current to free-wheel during the test so that there is no ripple voltage (ac) applied to the coil. The rectifier would otherwise cause a peak-to-peak voltage of over 800 volts at 360 Hz when its nominal output was zero. This thyristor can also be used to prevent damage to the rectifier components when ac to the rectifier is lost or when gate control is lost.

On the basis of reduced cost, reduced complexity, and reduced number of large electrical buses to be taken out of the reactor cell, the simplified version of the circuit given in Figure 5-18 is recommended for the TNS application.

5.6.2 COPPER AND HYBRID TF COIL POWER CONVERSION SYSTEMS

The TNS-1 design uses copper TF coils and will, therefore, require a flywheel generator as an energy storage system as shown in Figure 5-19. The generator will operate as a motor as it is brought up to speed with a variable frequency inverter which operates off a rectifier supplied by the 60 hertz line. Power will not be drawn from the line during an experiment.

At a predetermined time before plasma initiation, the phase control power supply will be turned on and the TF coil current raised to a prescribed value and maintained there until the end of the experiment at which time the current is driven to zero by operating the power supply as an inverter. This returns coil energy to the flywheel generator.

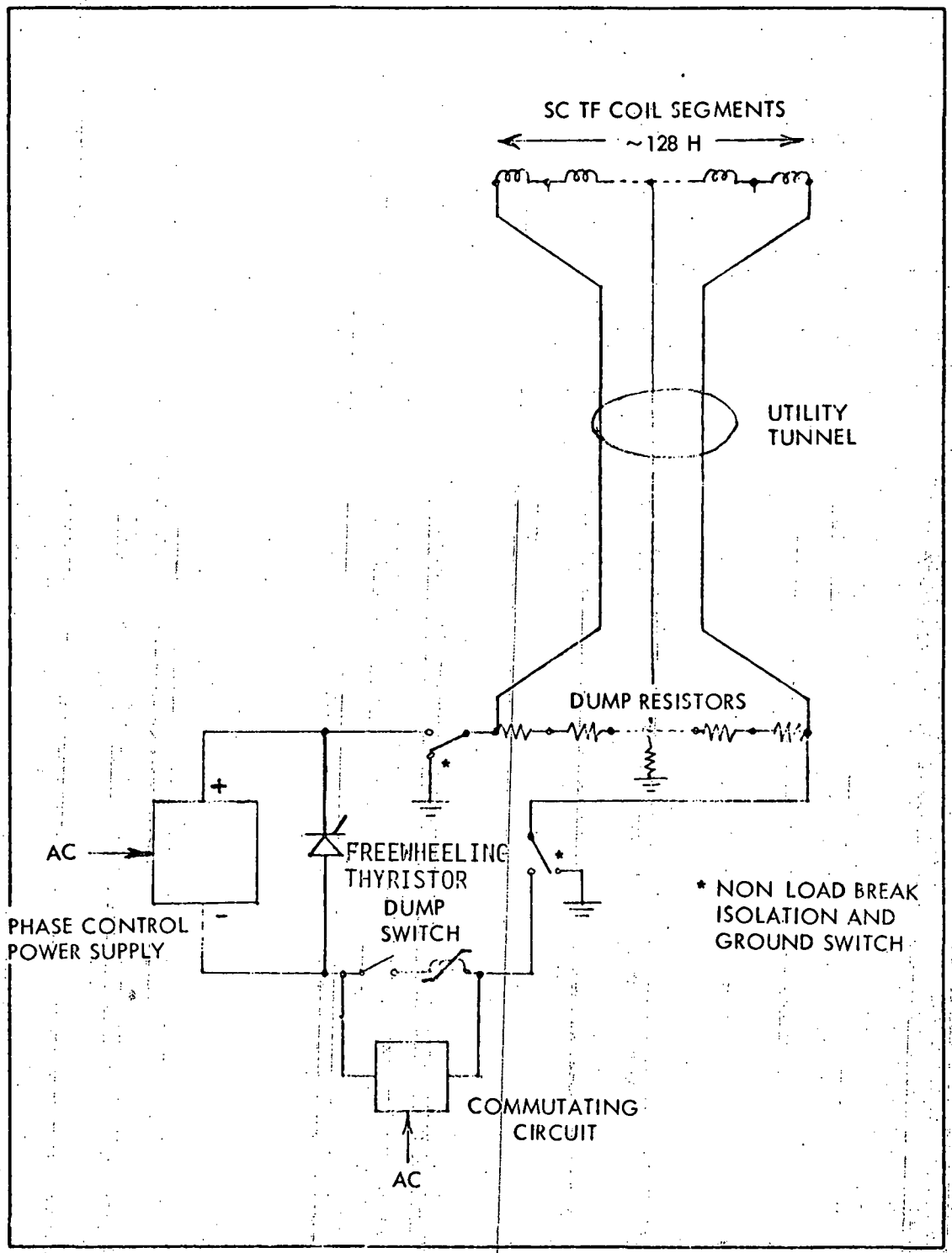

Figure 5-18. TF System Circuit (with SC Coils)

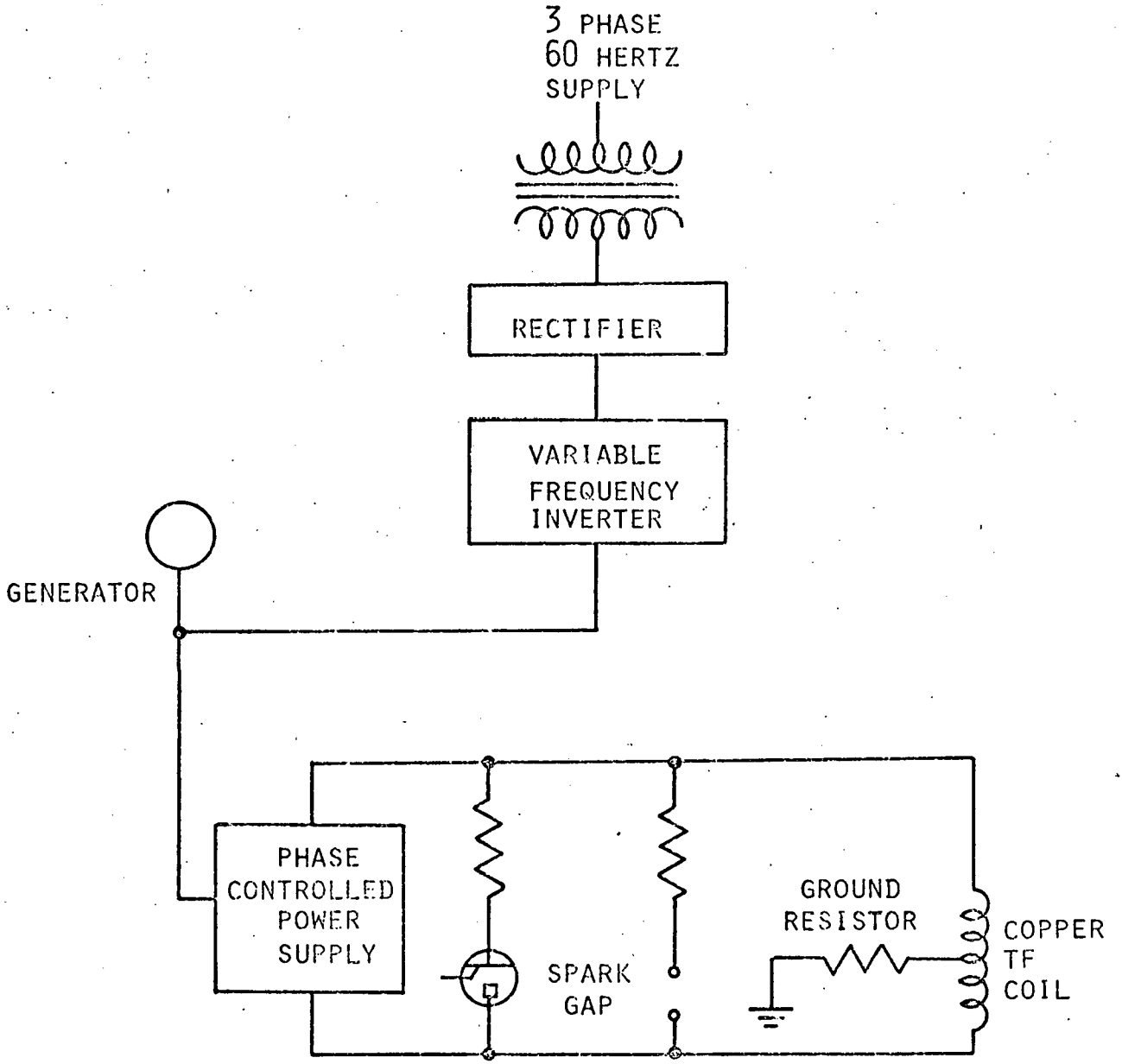

Figure 5-19. TF System Circuit
(Copper Coils)

Since the TF coil for TNS-5 is a hybrid, the superconducting coil will have its current maintained between experiments. However, the current of the copper coil will be raised to the required value for each experiment and then dropped to zero. Since the copper and superconducting coils are magnetically coupled, there will be an induced voltage in the superconducting coil. Therefore, the superconducting power supply must provide an equal and opposite voltage in order to maintain a constant superconducting coil current. TNS-5 will require a system as shown in Figure 5-19 for its copper TF coil and a system per Figure 5-18 for its superconducting coil.

5.6.3 THE OH POWER CONVERSION SYSTEM

Only copper OH coils were considered in the present trade study. Each of the four TNS options uses the same OH circuit configuration. However, the ratings, such as voltage and current, of the circuit components vary with the requirements of the individual TNS options.

An energy storage system is required to reduce the peak power drawn from the utility line. The OH energy storage device consists of an arc generator connected to complementary phase controlled SCR rectifiers. To achieve a minimum cost system no transformers are used. The circuit is shown in Figure 5-20. Since the rectifiers are usually operated at a fixed frequency, the effect of the varying generator speed on the commutating resistance was considered. The field excitation of the machine will not change significantly during the OH reversal. Therefore, the voltage and the frequency of the ac machines will vary together. The generator will be brought up to speed by operating it as a motor. It will be driven by a variable frequency inverter operating off the output of a rectifier fed from a 60 hertz supply. The same generator will supply pulse energy to the EF system, through rectifier-transformers.

Typical poloidal field coil system parameters associated with the OH system are given in column 4 of Tables 5-9 through 5-12 for TNS-1 through TNS-5, respectively.

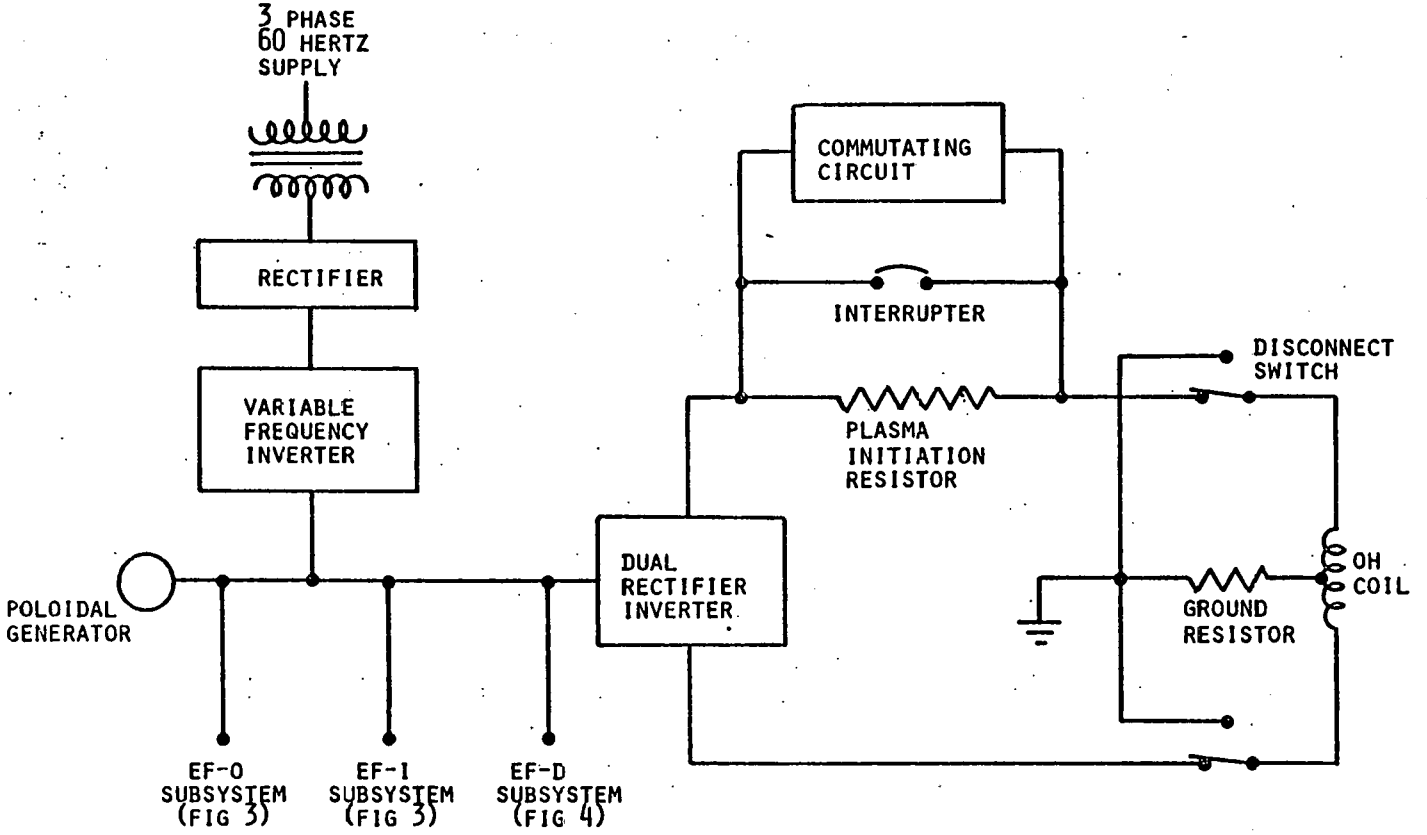

Figure 5-20. OH Power Conversion System Circuit

TABLE 5-9

POLOIDAL FIELD COIL SYSTEM PARAMETERS

TNS-1 Copper COAST Edition 3, 8/5/77 a = 1.00 m No Marg Field at Cond = 10.39 T

R_o = 4.00 m B_{max} = 10.39 T Bt (5.78 T) + Margin (-0.00 T) = 5.78 T

	EF-I	EF-D	EF-O	OH
MA-Turns at Initiation	-1.100E-03	1.760E-04	-1.520E-03	1.567E+01
MA-Turns at Begin of Startup	-1.991E-01	3.186E-02	-2.752E-01	4.784E+00
MA-Turns at End of Startup	-1.731E+00	2.769E-01	-2.392E+00	-9.550E+00
MA-Turns During Steady State	-1.833E+00	2.933E-01	-2.534E+00	-1.601E+01
Volts/Turn at Initiation	-2.270E+02	-2.204E+02	-2.337E+02	-2.111E+02
Volts/Turn at Begin of Startup	-4.829E+01	-4.200E+01	-5.423E+01	-4.328E+01
Volts/Turn at End of Startup	-5.887E-01	1.433E+01	-1.188E+01	3.516E+00
Volts/Turn During Steady St.	-4.453E+00	5.578E+00	-1.056E+01	-2.158E+00
Maximum MA-Turns	-1.833E+00	2.933E-01	-2.534E+00	-1.601E+01
Maximum Volts/Turn	-2.270E+02	-2.204E+02	-2.337E+02	-2.112E+02
Max. Volt-Amp Capability	4.161E+02	-6.463E+01	5.922E+02	3.384E+03
MJ Delivered by Flywheel	2.529E+02	4.973E+01	8.276E+02	7.662E+02
Initial Stored Energy (MJ)				6.671E+01
Self Induct. (H(-6))	4.990E+00	9.119E+00	1.274E+01	5.436E-01
Resistance (ohm(-6))	2.318E+00	1.971E+01	4.089E+00	1.227E-01
Number of Turns (-)	49	8	68	118
Coil-Pl Mutuals (-6)	2.918E+00	2.793E+00	6.832E+00	5.746E-01
I-D, D-O, I-O Mutuals (-6)	1.742E+00	2.723E+00	1.893E+00	

TABLE 5-10

POLOIDAL FIELD COIL SYSTEM PARAMETERS

TNS-3 S/C NbTi COAST Edition 3, 8/5/77 a = 1.20 m No Marg Field at Cond = 9.87 T

R_o = 5.70 m B_{max} = 9.87 T Bt (5.28 T) + Margin (-.00 T) = 5.27 T

	EF-I	EF-D	EF-O	OH
MA-Turns at Initiation	-7.045E-04	1.127E-04	-9.738E-04	6.084E+00
MA-Turns at Begin of Startup	-1.562E-01	2.500E-02	-2.160E-01	1.484E+00
MA-Turns at End of Startup	-1.597E+00	2.555E-01	-2.207E+00	-4.329E+00
MA-Turns During Steady State	-1.691E+00	2.705E-01	-2.337E+00	-6.273E+00
Volts/Turn at Initiation	-3.296E+02	-3.252E+02	-3.330E+02	-3.218E+02
Volts/Turn at Begin of Startup	-6.155E+01	-5.499E+01	-6.612E+01	-5.930E+01
Volts/Turn at End of Startup	2.000E+00	2.218E+01	-8.575E+00	6.940E+00
Volts/Turn During Steady State	-7.184E+00	8.524E+00	-1.401E+01	-2.430E+00
Maximum MA-Turns	-1.691E+00	2.705E-01	-2.337E+00	-6.273E+00
Maximum Volts/Turn	-3.296E+02	-3.252E+02	-3.331E+02	-3.221E+02
Max. Volt-Amp Capability	5.573E+02	-8.797E+01	7.784E+02	2.020E+03
MJ Delivered by Flywheel	3.706E+02	7.044E+01	1.002E+03	3.607E+02
Initial Stored Energy (MJ)				2.930E+01
Self Induct. (H(-6))	8.507E+00	1.528E+01	1.706E+01	1.583E+00
Resistance (ohm(-6))	4.139E+00	3.220E+01	5.917E+00	3.582E-01
Number of Turns (-)	45	8	62	78
Coil-Pl Mutuals (-6)	6.005E+00	5.332E+00	1.094E+01	1.611E+00
I-D, D-O, I-O Mutuals (-6)	4.109E+00	5.113E+00	3.989E+00	

TABLE 5-11

POLOIDAL FIELD COIL SYSTEM PARAMETERS

TNS-4 S/C Nb_3Sn COAST Edition 3, 8/5/77 a = 1.20 m No Marg Field at Cond = 10.95 T
R_o = 5.00 m B_{max} = 10.95 T Bt (5.28 T) + Margin (-.00 T) = 5.28 T

	EF-I	EF-D	EF-O	OH
MA-Turns at Initiation	-8.025E-04	1.284E-04	-1.109E-03	1.391E+01
MA-Turns at Begin of Startup	-1.780E-01	2.848E-02	-2.460E-01	3.457E+00
MA-Turns at End of Startup	-1.819E+00	2.910E-01	-2.514E+00	-9.754E+00
MA-Turns During Steady State	-1.926E+00	3.082E-01	-2.662E+00	-1.429E+01
Volts/Turn at Initiation	-2.894E+02	-2.840E+02	-2.941E+02	-2.759E+02
Volts/Turn at Begin of Startup	-6.218E+01	-5.474E+01	-6.824E+01	-5.774E+01
Volts/Turn at End of Startup	2.143E+00	2.109E+01	-1.000E+01	6.858E+00
Volts/Turn During Steady State	-5.904E+00	7.248E+00	-1.275E+01	-2.586E+00
Maximum MA-Turns	-1.926E+00	3.082E-01	-2.662E+00	-1.429E+01
Maximum Volts/Turn	-2.894E+02	-2.840E+02	-2.942E+02	-2.762E+02
Max. Volt-Amp Capability	5.575E+02	-8.753E+01	7.831E+02	3.948E+03
MJ Delivered by Flywheel	3.485E+02	6.834E+01	1.043E+03	8.720E+02
Initial Stored Energy (MJ)				6.424E+01
Self Induct. (H(-6))	6.860E+00	1.239E+01	1.548E+01	6.642E-01
Resistance (ohm(-6)	2.969E+00	2.412E+01	4.719E+00	1.684E-01
Number of Turns (-)	51	8	71	91
Coil-Pl Mutuals (-6)	4.376E+00	3.974E+00	9.028E+00	6.883E-01
I-D, D-O, I-O Mutuals (-6)	2.767E+00	3.864E+00	2.865E+00	

TABLE 5-12

POLOIDAL FIELD COIL SYSTEM PARAMETERS

TNS-5 Hybrid COAST Edition 3, 8/5/77 a = 1.00 m No Marg at Cond = 9.70 T
R_o = 4.50 m B_{max} = 9.70 T Bt (5.78 T) + Margin (-.00T) = 5.78 T

	EF-I	EF-D	EF-O	OH
MA-Turns at Initiation	-9.776E-04	1.564E-04	-1.351E-03	3.932E+01
MA-Turns at Begin of Startup	-1.770E-01	2.832E-02	-2.446E-01	1.181E+01
MA-Turns at End of Startup	-1.583E+00	2.461E-01	-2.126E+00	-2.435E+01
MA-Turns During Steady State	-1.629E+00	2.607E-01	-2.252E+00	-4.030E+01
Volts/Turn at Initiation	-2.551E+02	-2.492E+02	-2.601E+02	-2.173E+02
Volts/Turn at Begin of Startup	-4.806E+01	-4.217E+01	-5.269E+01	-3.978E+01
Volts/Turn at End of Startup	-9.104E-01	1.511E+01	-1.082E+01	3.332E+00
Volts/Turn During Steady State	-5.374E+00	6.495E+00	-1.147E+01	-1.542E+00
Maximum MA-Turns	-1.629E+00	2.607E-01	-2.252E+00	-4.030E+01
Maximum Volts/Turn	-2.551E+02	-2.492E+02	-2.602E+02	-2.175E+02
Max. Volt-Amp Capability	4.157E+02	-6.498E+01	5.860E+02	8.764E+03
MJ Delivered by Flywheel	2.698E+02	5.144E+01	7.952E+02	1.366E+03
Initial Stored Energy (MJ)				1.551E+02
Self Induct. (H(-6))	6.201E+00	1.111E+01	1.388E+01	2.007E-01
Resistance (ohm(-6))	3.173E+00	2.570E+01	5.004E+00	3.393E-02
Number of Turns (-)	43	8	60	115
Coil-Pl Mutuals (-6)	3.990E+00	3.680E+00	8.156E+00	2.332E-01
I-D, D-O, I-O Mutuals (-6)	2.591E+00	3.551E+00	2.615E+00	
R Volt, Seconds (I, SU, TOT)	2.456	3.757	9.511	

5.6.4 THE EF POWER CONVERSION SYSTEM

The reasons for the separation of the EF coils into three independently driven systems arises from a requirement to achieve a high-β system. The high-β approach selected for these TNS studies makes explicit use of the flux conserving properties of the fully developed plasma. To enhance and maximize this effect, the inner coil currents and the outer coil currents do not individually track the plasma current during neutral beam heating. The sum of the two, plus the divertor current, does track the plasma current. Individually, the outer current rises faster than the plasma current and the inner current decreases during auxiliary heating.

The EF-O circuit and the EF-I circuit configurations are identical. The circuit configuration is shown in Figure 5-21. The energy storage element, either capacitors or homopolar generators, is switched into the circuit at the beginning of initiation. The three-phase controlled rectifier carries the coil current at all times and is conducting at its full rated voltage during initiation. The diode conducts automatically when the energy storage element voltage drops below zero, or the coil current can be commutated into the diode at any time, by dumping the capacitor through the ignition switch. (The start-up switch was solid-state for most of the studies but has been replaced by ignitrons.)

The EF-D circuit is different from the other EF circuits. Although the voltage induced in the EF-D circuit is the same as in the other EF circuits, the current has the same polarity as the plasma current. In other words, the EF-D coil regenerates power to the circuit during start-up. The EF-D circuit is shown in Figure 5-22.

Typical poloidal field coil system parameters associated with the EF-I, EF-D and EF-O circuits are given in the first three columns of Tables 5-9 through 5-12 for TNS-1 through TNS-5, respectively.

5.7 HEAT TRANSPORT SYSTEMS

The heat transport systems of TNS consist of two major systems: 1) water-cooling for the vacuum vessel, shielding, copper coils, neutral beam lines,

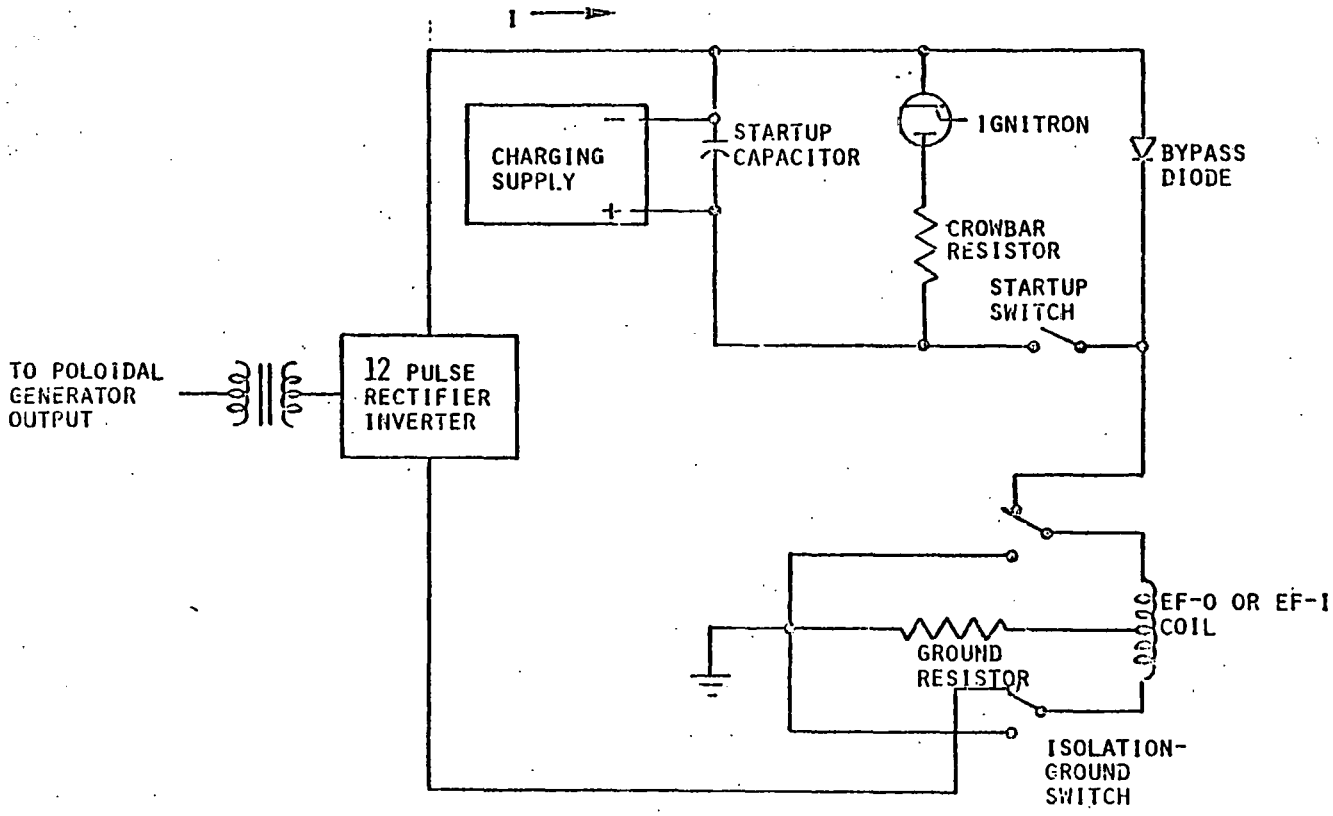

Figure 5-21. Circuit for the EF-0 and EF-1 Power Conversion Systems

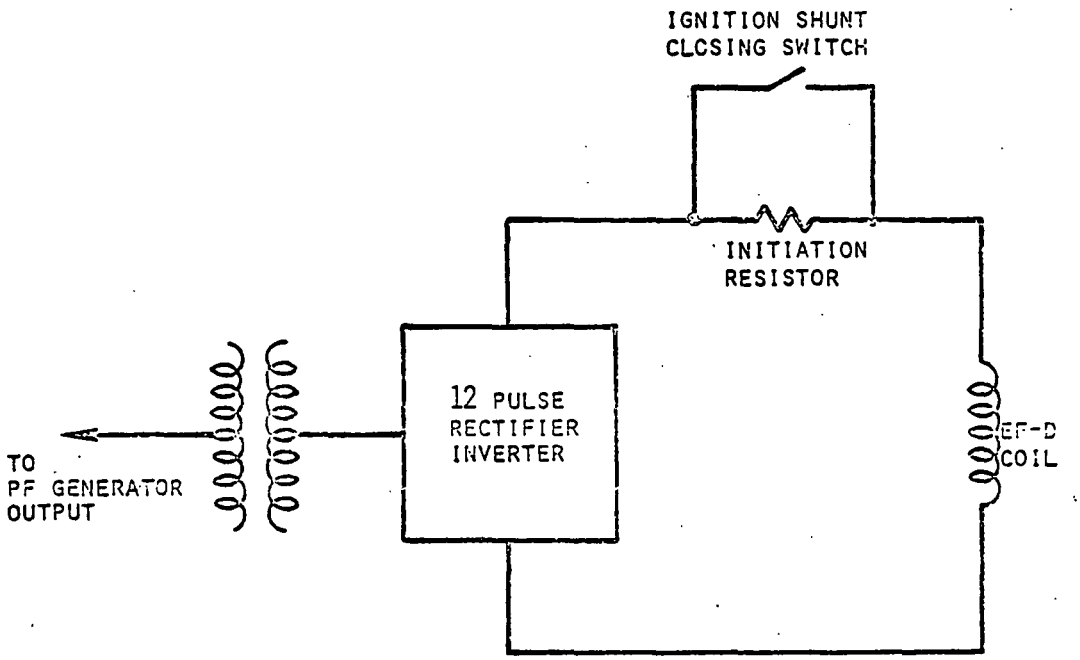

Figure 5-22. EF-D Power Conversion System Circuit

and power conversion equipment plus other minor requirements such as facility ventilation systems, etc., and 2) cryogen (LHe and LN_2) cooling of superconductors, dewars and cryopanels. The cooling water systems employ buffered heat transfer loops by means of intermediate heat exchangers. The cryogen systems employ cryogenic refrigerators to maintain required coolant temperatures. The final heat dissipation is by means of a common water cooling tower. The design features of the various cooling loops are shown in Figure 5-23. The individual systems are briefly discussed below.

5.7.1 VACUUM VESSEL COOLING SYSTEM CONFIGURATION

The heat loads on the vacuum vessel are from surface heat flux from the plasma and the neutron and gamma heating in the material. The total equivalent surface heat flux on the first wall is estimated to be 85 W/cm^2 without divertor and 28 W/cm^2 with a divertor. The vessel is cooled by low temperature, low pressure water in channels arranged along the poloidal direction. A description of the vessel and its cooling arrangement is given in Section 5.1. The design features of the heat transport system for the vessel cooling is shown on the top of Figure 5-23. Note that a closed intermediate cooling loop is interposed between the primary coolant and the plant circulating water for radiological safety. Thermal buffering is accomplished in this intermediate loop by active control of water flow to the primary and circulating water heat exchanger (IHX1 and IHX2). A design coolant temperature rise of 30 K is assumed in the heat exchangers. Due to the pulsing nature of heat load in the primary loop, the vessel inlet temperature is maintained constant at 345 K. The maximum vessel outlet temperature is 375 K. Coolant pressure at the vessel discharge is maintained at approximately 3 Pa by a blanket of hydrogen gas in a water column control tank. The flow of cold water from the elevated water tank to IHX1 is regulated to maintain a constant primary loop temperature at the vessel inlet. The intermediate loop flow will discharge from IHX1 at a nominally constant temperature and is collected in a ground level water tank. In turn, the water is pumped at a constant rate from the ground level tank, through IHX2, to recharge the elevated water tank. Hence, constant coolant inlet temperature is provided for the vacuum vessel, while a constant heat load is imposed on the plant cooling tower. The

DESIGN FEATURES

VACUUM VESSEL COOLING SYSTEM

- PRIMARY COOLANT IS LOW TEMPERATURE, LOW PRESSURE WATER.
- FIRST WALL COOLANT CHANNELS WILL BE THIN WALLED AND RESISTANT TO CYCLIC THERMAL FATIGUE DAMAGE.
- HYDROGEN BLANKET GAS PRESSURIZES LOOP AND PROVIDES DISSOLVED HYDROGEN TO SUPPRESS RADIOLYSIS OF WATER.
- PRIMARY COOLANT FLOW IS CONTINUOUS.
- VOLUME OF PRIMARY LOOP IS MINIMIZED BY LOCATION OF THE PUMPS, INTERMEDIATE HEAT EXCHANGERS (IHX1) AND AUXILIARY EQUIPMENT IN THE TEST CELL BASEMENT.
- COOLANT PURITY AND pH IS CONTROLLED BY USE OF SIDESTREAM FILTERS AND MIXED BED DEMINERALIZERS.
- BUFFER SYSTEM PROVIDES SECONDARY CONTAINMENT OF RADIOACTIVE PRIMARY COOLANT AS WELL AS LEVELING OF HEAT TRANSPORT TO THE PLANT CIRCULATING WATER SYSTEM.
- FLOW OF COOL BUFFER SYSTEM WATER FROM AN ELEVATED STORAGE TANK IS REGULATED TO MAINTAIN CONSTANT COLD LEG TEMPERATURE IN THE PRIMARY LOOP.
- WARM BUFFER WATER IS PUMPED CONTINUOUSLY FROM GROUND LEVEL STORAGE TANK, THROUGH THE CIRCULATING WATER HEAT EXCHANGER (IHX2) TO REFILL ELEVATED STORAGE TANK.

NEUTRON SHIELD COOLING SYSTEM

- CONFIGURATION IDENTICAL TO THE VACUUM VESSEL SYSTEM.
- BORATED WATER (1 B ATOM PER 64 H_2O) USED IN PRIMARY COOLANT LOOPS.
- PARALLEL SYSTEMS SLAVE EACH HALF OF THE SHIELDING.

NEUTRAL BEAM COOLING SYSTEM

- MAJOR THERMAL LOADS (BEAM DUMPS AND CALORIMETERS) ARE SERVED BY LOW TEMPERATURE, LOW PRESSURE WATER COOLING LOOPS SIMILAR TO THE VACUUM VESSEL SYSTEM.
- COOLING OF ELECTRICAL COMPONENTS (ION SOURCES, MAGNET SYSTEMS) IS PROVIDED BY A BRANCH OF THE COPPER COIL COOLING SYSTEM BELOW.

COPPER COIL COOLING SYSTEM

- SERVE: COPPER TOROIDAL FIELD COILS (TNS-1, TNS-5)
  OHMIC HEATING COILS
  EQUILIBRIUM FIELD COILS
  NEUTRAL BEAM ION SOURCES AND MAGNET SYSTEMS
  ELECTRICAL POWER CONVERSION EQUIPMENT
- COMMON THERMAL BUFFER SYSTEM SERVES ISOLATED PRIMARY LOOP FOR EACH MAJOR ELECTRICAL SYSTEM.
- MINIMUM COOLING WATER TEMPERATURES ARE OBTAINED BY DIRECT USE OF PLANT CIRCULATING WATER IN BUFFER SYSTEM.
- PRIMARY LOOPS UTILIZE FULL FLOW 25 MICRON FILTRATION AND SIDESTREAM DEMINERALIZATION.
- ALL PRIMARY LOOP EQUIPMENT IS CONTAINED IN TEST CELL AND BASEMENT.

HELIUM REFRIGERATION SYSTEM

- SUPERCRITICAL HELIUM COOLANT IS SUPPLIED FOR TF COIL CONDUCTOR AND BOBBIN COOLING AT 4.0 K (8 TESLA Nb_3Ti COILS) OR 5.0 K (12 TESLA Nb_3Sn COILS).
- PRIMARY SUPERCRITICAL HELIUM LOOPS ARE COOLED BY A LIQUID HELIUM BATH MAINTAINED AT 0.5 K BELOW THE REQUIRED COIL COOLANT TEMPERATURE.
- HELIUM BATH PROVIDES SUFFICIENT THERMAL CAPACITANCE TO ALLOW STEADY OPERATION OF REFRIGERATOR DESPITE VARIATIONS IN PRIMARY LOOP LOAD.
- LARGE, HIGHLY EFFICIENT HELIUM CIRCULATING PUMPS FOR OPERATION NEAR 4.0 K REQUIRE DEVELOPMENT.
- REFRIGERATION FOR CRYO-PUMPING PANELS WILL BE PROVIDED AT VARYING TEMPERATURES.

NITROGEN REFRIGERATION SYSTEM

- PROVIDES LIQUID NITROGEN AT 77 K FOR COOLING OF TF COIL DEWARS AND OTHER THERMAL SHIELDS.
- MAY BE USED FOR PRECOOLING IN HELIUM REFRIGERATION SYSTEM.

EXPERIMENTAL AREA VENTILATION SYSTEM

- COOLS, DEHUMIDIFIES, REHEATS, AND FILTERS AIR FOR ONCE-THROUGH VENTILATION OF THE EXPERIMENTAL AREA DURING NON-DT OPERATION.
- PROVIDES CLOSED SYSTEM COOLING OF THE TEST CELL ATMOSPHERE DURING D-T EXPERIMENTS.

AUXILIARY COOLING SYSTEMS

- SERVE BALANCE OF PLANT EQUIPMENT.

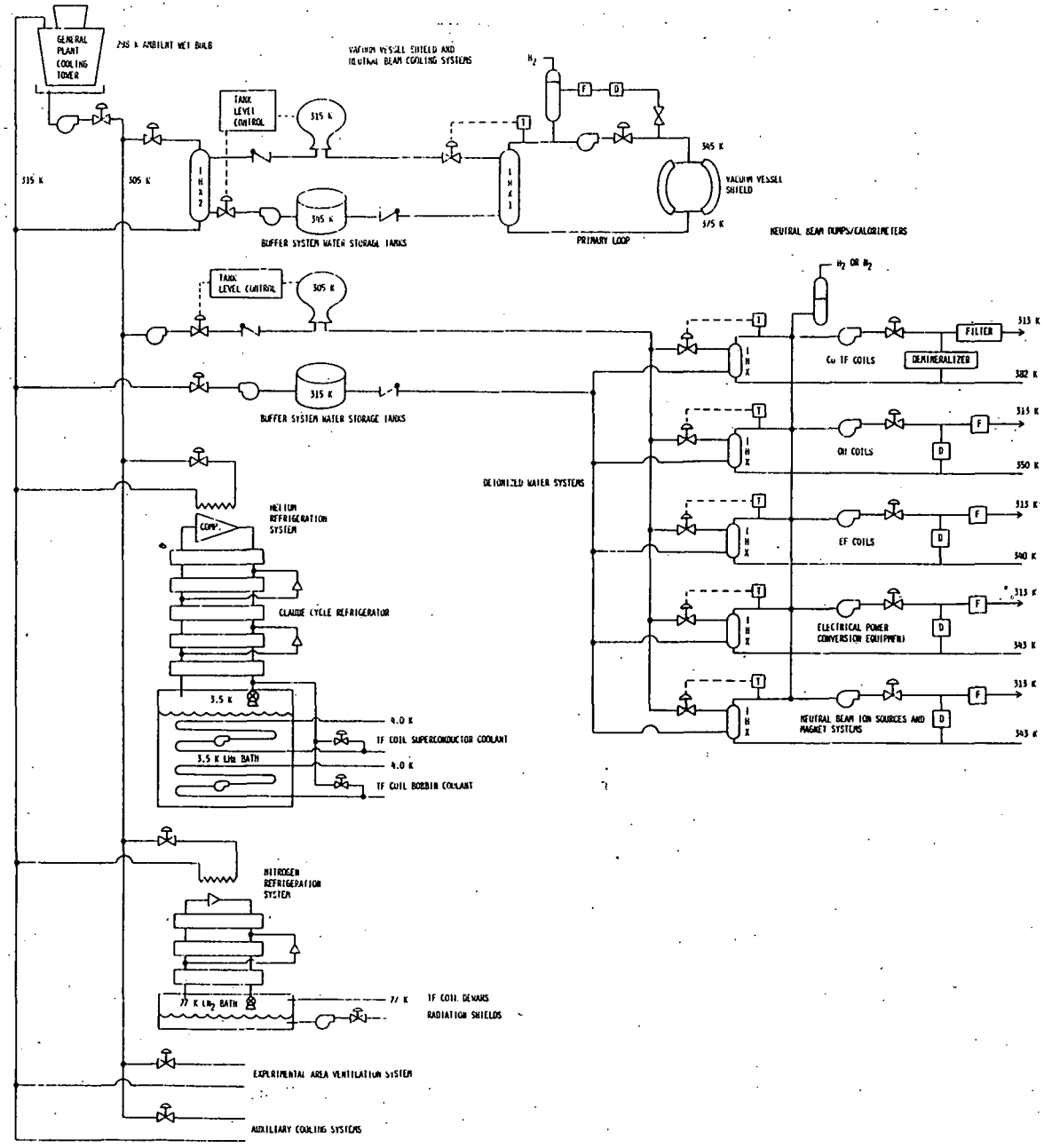

Figure 5-23. General TNS Heat Transport System Design Features

coolant temperature rise in the buffer loop is assumed to be the same as in the primary loop. The initial temperature difference in the primary/buffer heat exchanger will be equal to twice the primary loop temperature rise ($2 \times \Delta T = 60$ K). The temperature rise of the water tower side of IHX2 is assumed to be 10 K. The initial temperature difference in IHX2 is thus $\Delta T + 10$ K = 40 K.

Based on the heat transport system described above, the total required water flow rate in the primary loop is 8630 kg/s without divertor and 5920 kg/s with divertor, transporting a heat load of 971 MW and 756 MW, respectively. The capacity of the elevated tank will be set at twice the amount required to handle the normal energy per pulse, while the ground level tank capacity is set at 4 times the required value to allow draining of the entire buffer loop coolant volume to this tank.

A standard design of 2800 m^2 tube surface area for IHX1 was chosen. This allows variation of ΔT and number of parallel heat exchangers for the cooling requirements of various TNS components. This not only standardizes the loops design, but also facilitates the costing of the equipment.

The primary loop piping is assumed to be commercial grade 316 SS, schedule 40 pipes sized with a water velocity of 5 m/s. On the secondary side of IHX1, schedule 40 carbon steel pipe sized also for 5 m/s water velocity is assumed. Eight full flow stainless steel butterfly valves are allocated for each primary coolant loop for various control functions. One pump/motor combination serves each primary loop with an assumed pumping heat of 500 kPa. A single hydrogen pressurizer is allocated to the entire primary loop system with an initial pressure rating of 1 MPa. Sidestream coolant filters and mixed bed demineralizers are provided.

The components on the cooling tower side of the buffer loop are sized on the basis of mean thermal power with 50% margin for non-steady operation. A single buffer/circulating water heat exchanger (IHX2) serves the entire vacuum vessel primary loops. Carbon steel pipes of schedule 40 sized with a water velocity of 5 m/s are used in the loop. Six valves are allocated for flow control

functions on the buffer side of IHX2 and two valves are allocated on the cooling tower side. One pump-motor combination is used to pump buffer water from the ground level tank through IHX2 and up to the elevated tank. A total head of 850 kPa is assumed for this pump.

This gives a brief description of the cooling system for the vacuum vessel. It can be considered as a basic loop design. This arrangement has been employed as a basis for the cooling system for the other heat sensitive components of TNS with modifications to meet the different requirements of a particular component.

5.7.2 SHIELD COOLING SYSTEM CONFIGURATION

The character of heat input to the nuclear shield is similar to that of the vacuum vessel, but the total heat load will be about twice as great. It is judged reasonable, therefore, to assume that the shield cooling system must be equivalent to two vacuum vessel cooling systems, resulting in basic components of equivalent size. This was assumed the case in the present trade studies. The shield coolant is borated water, but this is assumed to have negligible impact on cost.

5.7.3 COPPER COIL COOLING SYSTEM CONFIGURATIONS

The copper coil cooling systems differ from the vacuum vessel system in thermal response characteristics, reduced concern for coolant radioactivity level and a requirement for lower coolant inlet temperature. For these reasons, a slightly different configuration was considered. In this modified system, the buffer loop heat exchanger (IHX2) is eliminated and the primary loop is divided into several loops. One serves the TF coils (TNS-1 and TNS-5), the others separately serve the EF coils, OH coils, neutral beam ion source, magnet system and the electrical power conversion systems. A common buffer system consisting of elevated and ground level water tanks (similar to that in the vacuum vessel system), serves all the primary loop heat exchangers (IHX).

The coolant temperature rise in the copper coils during a pulse varies considerably depending on the I^2R loss in each of the coil systems. The cooling channel inlet temperature of the coils is maintained at a constant temperature of 40K. The

circulating water is stored in the elevated buffer tank at 305°K and will experience a maximum of 10°K rise through the intermediate heat exchanger (ISX). The loop arrangement is shown in the middle section of Figure 5-23. The coolant temperature rise in the TF, OH and EF coils was estimated from a simplified analysis model based on adiabatic heating, considering a current density of 1500 A/cm^2. The temperature increases are 69, 37 and 27°K, respectively, for the TF, OH and EF coils. The maximum temperature rise for the electrical power conversion equipment, the neutral beam ion sources and magnet systems was assumed to be 30°K.

5.7.4 NEUTRAL BEAM ION COLLECTORS AND CALORIMETER COOLING SYSTEM CONFIGURATION

The heat loads on the ion collectors and calorimeters for TNS will be of the order of several kW/cm^2, much higher than that on the vacuum vessel, even though the pulse time is only about 6 seconds. A deionized water system pressurized to several MPa will be required. A buffered heat transport loop similar to that of the vacuum vessel, but with a high pressure primary loop, is employed. The primary loop water temperature should be maintained no higher than 308 K at the cooling channel inlet.

5.7.5 SUPERCONDUCTING COIL COOLING SYSTEM CONFIGURATION

Supercritical helium at 4 K (for TNS-3) and 5 K (for TNS-4) is required to cool the superconductors, the coil bobbins and various vacuum cryopanels. A common refrigeration plant is used to cool the various isolated primary loops for each component. A schematic for the TNS-3 helium refrigeration system is shown in Figure 5-23. The advantages of this system are: 1) individual coolant systems are isolated, providing great flexibility in choosing coolant flow rates for each loop, 2) combination of several pulsed heat loads will result in some leveling of refrigeration load. The main disadvantage is that the pump work added at low temperature will require more total power than use of a room temperature compressor. Cryogenic refrigeration equipment of the size required by TNS applications are still at the developmental stage, especially the required circulating pumps. This heat transport system would require detailed trade studies in cooperation with cryogenic equipment manufacturers.

The helium flow rate for TNS-3 (NbTi) was calculated to be about 25 kg/s and that for TNS-4 (Nb_3Sn) about 4 kg/s. For structural bobbin cooling, the coolant flow rate was estimated to be about 3 kg/s if the cooling channels are arranged in a circumferential direction. The flow rate would be considerably higher if the channels were oriented in a radial direction.

5.7.6 LIQUID NITROGEN REFRIGERATION SYSTEM

Liquid nitrogen is used to cool the TF coil dewars and the other thermal shields. The schematic of the refrigeration system is shown in the bottom of Figure 5-23 The LN_2 flow rate required for the dewars of a 20 TF coil configuration was estimated to be about 2 kg/s. The coolant flow requirement for the thermal shields depends on the detailed design of the various cryopanels and were not developed as part of the current study.

5.7.7 EXPERIMENTAL AREA VENTILATION SYSTEM

The major heat load of this system is for supply of dehumidified air at 293 K and 40% relative humidity to the reactor cell and the service system containment area (basement) on a once-through basis during non-operational periods and on a strictly recirculating basis during operational and abnormal periods with two changes of air per hour. A schematic of the system is shown in Figure 5-23 The circulating water side of the air treatment and conditioning system is connected to the plant water cooling tower. The heat load is estimated to be between 7 and 10 MW for each of the four TNS options.

5.8 TRITIUM SYSTEMS

The initial and principal objectives in evolving a configuration for the fuel handling complex was to provide a cost model for this system, in a general way accounting for variations in plasma and machine sizes as dictated by the four candidate TF coil design concepts being considered. Figure 5-24 shows the makeup of the fuel handling subsystems and the manner in which they interface with the reactor.

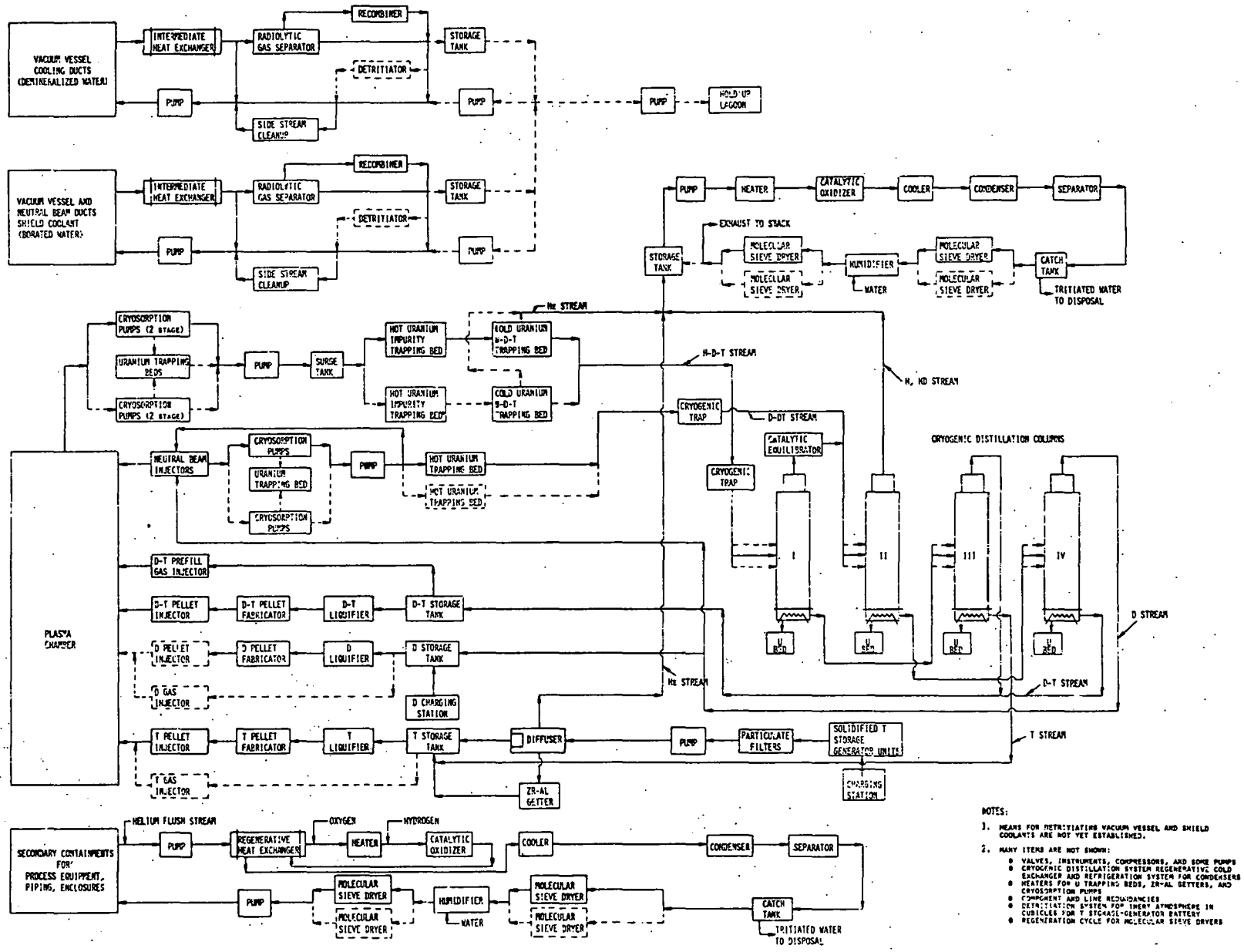

Figure 5-24. Preliminary Flow Schematic of TNS Fuel Supply and Treatment

5.8.1 SYSTEM FUNCTIONAL REQUIREMENTS

The functions of the TNS fuel handling complex include the following: 1) storage and delivery of the deuterium and tritium fuels to the device; 2) processing of the spent plasma from the vacuum and/or divertor systems to recover and recycle the residual fuel materials and dispose of the impurities; 3) isotopic enrichment required for proper adjustment of fuel mix and for eliminating helium generated and hydrogen produced from fusion and metal outgassing; 4) holding the escape of tritium into the facility and into the environment to acceptably low levels; 5) tritium trapping to ensure containment integrity in the event of emergencies such as power or cryogenic system failures or loss of vacuum; 6) detritiating of the reactor interior surfaces prior to opening the device for maintenance operations and the reactor cell atmosphere and walls in the event of substantial tritium releases to the cell atmosphere; and, 7) providing flow path and equipment redundancies in amounts adequate to insure facility operational continuity in the event of process equipment malfunctions.

Fuel handling capabilities potentially required in eventual fusion power reactors but not provided by the provisional TNS system include: 1) breeding of sufficient tritium to replace that destroyed by fusion and radioactive decay, fuel processing losses and depletions via transport into the plant metals; 2) reconstruction and recycle of tritium that has been converted to tritiated water; and 3) removal and recycle of tritium diffused into equipment coolants and power cycle energy transport media.

5.8.2 OPERATIONS MODE

As presently envisaged, the fuel reprocessing portion of the tritium system will operate on a batch basis rather than continuously. This option was chosen because the expected TNS operation with ignited plasmas will be limited to the equivalent of 1000 full power reference D-T pulses per year, or an average of about 100 such full power pulses per month. The amount of fuel associated with this operating schedule is relatively small, and continuous operation of the reprocessing facilities was not deemed justifiable. Accordingly, the

current concept involves accumulation of spent plasma followed by rapid batch-wise campaigning through the reprocessing cycle, perhaps about twice a month, treating spent materials from approximately 50 full power D-T pulse produced per campaign. During the accumulation period and during inactive periods of TNS operations, the cryogenic distillation columns, however, could be running under total reflux conditions in order to avoid the complications associated with start-up of multi-component cryogenic rectifiers. Typically, a spent plasma recovery campaign could be completed within one operating day. This degree of batch operation is not greatly different from that expected for eventual fusion power reactor fuel processing systems. Regeneration of cryo-pumps is by nature a batch operation, and it is anticipated that batch purification processes will be used even with large systems. The principal differences between the TNS fuel recycle system and that expected in eventual power reactors are in the duty cycle and in the coupling (through surge systems) primarily of batch purification systems with continuous isotope separation and feed systems.

5.8.3 GENERAL CAPABILITIES

General capabilities provided in the fuel handling system preconceptual design are listed below:

FUEL INJECTION

1. Streams of D-T, H, D, and T are available as separate additions for vacuum vessel gas prefill for both non-tritium experiments and tests involving tritium.
2. Pellets of solidified D-T, T, and D may be used for refueling during reactor operation.
3. D will be supplied to the high energy neutral beams, up to 150 MW and 250 keV.

SEPARATION OF HYDROGEN ISOTOPES FROM IMPURITIES

1. Depleted uranium hot and cold traps will remove most chemical impurities, including helium.
2. Particulate filters will be located downstream from uranium beds.
3. Zirconium-aluminum alloy getters will be used for small storage and surge systems.
4. Helium will be evacuated from uranium getter beds before regeneration, or prior to withdrawing tritium from storage-generator units.
5. Cryogenic trapping will provide additional purification of streams entering the distillation system.
6. Palladium-silver alloy diffusers will be used to remove helium from new tritium shipments or any fuel which has been on gas storage for extended periods.

SEPARATION OF HYDROGEN ISOTOPES

1. Cryogenic distillation will produce D-T, H, D, and T product and waste streams.

STORAGE OF TRITIUM

1. Bulk inventory storage will be in solid form as $UT_{2.8}$, utilizing depleted uranium.
2. Temporary holdup of larger quantities of H-D-T mixtures will be on uranium beds.
3. In-process storage of refueling streams of D, T, and D-T will be as liquids (assuming pellet feed).
4. Temporary holdup of small high-purity streams will use zirconium-alloy getters.
5. Emergency storage of cryodistillation column inventory will be on uranium beds.

STORAGE OF DEUTERIUM AND OTHER NON-TRITIUM GASES

1. Bulk inventory storage will be as presurized gases or on uranium beds.
2. Temporary or emergency storage of slightly tritiated D will be on uranium beds.

DETRITIATION OF ATMOSPHERES AND GASEOUS VENT STREAMS

1. Gaseous vent streams will be treated by catalytic thermal cracking of any tritiated hydrocarbons, oxidation on suspended precious metal catalysts, and adsorption on regenerable (and in some instances non-regenerable) desiccants.
2. Treatment of helium atmospheres of secondary containment systems and process piping jackets will include catalytic oxidation and desiccation for removal of hydrogen isotopes and cleanup of the helium streams.
3. The reactor cell atmosphere detritiation system uses catalytic oxidation and desiccation, with operation intended only for emergency situations.
4. Readying of the reactor vessel for opening for maintenance includes detritiation of gas from discharge cleaning by catalytic oxidation and desiccation.

DETRITIATION OF CONTAMINATED LIQUID STREAMS

1. Although several efforts are underway in the United States and Europe for eliminating tritium from water waste streams, no suitable economic technology currently exists for detritiation of streams such as the vacuum vessel and shield aqueous coolants; so as an alternative, lagoon storage is provided for long-term holdup.

5.8.4 SYSTEM CONFIGURATION GROUNDRULES

The essential features of the ground rules for the tritium systems are summarized below:

TRITIUM STANDBY STORAGE AND INVENTORY

1. Stored as solidified tritide on depleted uranium chips in three separate compartmented isolated generator storage units.
2. Storage-generator design is based on $UT_{2.8}$ with total storage capability of the uranium equivalent to 360 full power D-T pulses augmented by a 30% excess capacity. Also assume: bulk density of 2 g/cm^3; internal volume of interior body ten times that of the loosely packed uranium chips; interior body cylindrical configuration with a 2:1 height to diameter ratio.)
3. On-site standby tritium inventory, not including in-process and held-up materials is equivalent to a normal two months' supply, augmented by a 30% contingency, amounting to 260 full power total 42 second plasma duration full power reference D-T pulses.

SPENT PLASMA TRAPPING AND PROCESSING

1. Primary trapping by the vacuum system is by a compound cryopump using a 4.2 K chevron to pump D, T, and H and a 4.2 K molecular sieve panel to pump helium; the pump will immobilize and store all of the spent plasma components.
2. The quantity of material that leaves the system and enters the vacuum system during the plasma active pulse period (33 s duration) is negligible.
3. Hydrogen entry into the plasma is based on an outgassing rate of $\sim 10^{-10}$ torr-liters/s cm^2, and the effective surface area is estimated to be ten times that of the computed smooth internal area of an assumed elliptically shaped toroidal vacuum vessel.

4. Tritium processing losses (excluding radioactive decay) during recovery-recycle operations amount to 0.15% of the initial tritium content of the spent plasma products in the accumulated batch.

5. Processing-purification is accomplished by combinations of hot trap gettering, mechanical filtration, cold trap gettering, cryogenic trapping, cryogenic distillation, catalytic cracking-oxidation, adsorption-desiccation, and selective permeation-diffusion.

6. The cryogenic distillation complex has capability to produce adequately pure product streams of D-T, D_2, HD and T_2; additionally, this complex will accept a side stream from the contaminated deuterium collected on the cryoadsorbent panels of the neutral beam vacuum system for tritium removal. In principle, a pure tritium stream will not be needed if pellets can be made from D-T mixtures.

7. Normal operation on the upstream side of the palladium-silver alloy diffuser is not to exceed 650 K and 1.5 MPa ($\sim$ 230 psia).

8. The maximum pressure to be encountered in in-process gas holdup storage tanks is 0.4 MPa ($\sim$ 60 psia).

TRITIUM CONTAINMENT AND CLEANUP

1. Each of the three tritium storage-generator units is provided with its own dedicated heaters, coolers, controllers, inert gas blanketing, vault, and emergency protection system.

2. Pumps for tritium processing operations in general shall not have rotating mechanical seals; if this criterion cannot be met, complete containment of the pump in a separate sealed enclosure will be required.

3. All tritium processing equipment is to be doubly enclosed and the volumes enclosed by these jackets are to be continuously flushed by a circulating inert buffer-gas which is processed (by a cleanup system) to maintain a low cover-gas tritium level.

4. Tritium cleanup systems are to be provided for the off-gas holding tanks, vacuum vessel, reactor cell and the inert buffer gas of the secondary containments; sizing of these are to be based on cleanup periods of 120 hr following a major release into the reactor cell and 48 hr for the reactor vessel prior to reactor shut down and conduct of maintenance.

5. Ample storage capacity is provided for separate temporary holdup of all of the closed-circuit vacuum vessel and shield system aqueous coolants so these materials can be contained when the system must be drained for equipment maintenance.

6. Additional storage capacity is provided (tanks and lagoon) for long term holdup of tritium contaminated primary aqueous coolants and buffer water coolants of the heat dissipation system in the event that the latter become tritium contaminated.

5.8.5 SPECIAL REDUNDANCY AND SAFETY FEATURES

The need for special redundancy and safety features has been cited. In some instances the sizes and costs of hardware items are partially determined by the amount of safety and redundancy features incorporated. The nature of the more important redundancy systems included in the current facility design concept are outlined in the following tabulation:

1. Redundancy is provided for gas holdup tanks, in-process transfer lines, isolation/control valves, surge tanks, transfer pumps for matters of safety and operational continuity; additionally, to provide for operational continuity-flexibility duplicate equipment is provided for such crucial items as fuel pellet injectors, cryogenic distillation columns and diffusers.

The redundancies for the valves, lines, and pumps also allow means for alternate routing of materials.

2. Thick wall double jacketing is specified for the three tritium generator-storage units, with 2.5 cm cylinder walls and 4.0 cm heads, and 3.0 cm annular clearance between the interior and outer bodies.

3. Tritium generator-storage units are housed in sealed, inerted steel lined (2.0 cm thick lining) concrete (30 cm thick walls) separate cubicles. The cubicle configuration and particulars are: rectangular shape; 1.0 m clearance on all sides between outer body of generator-storage unit and cubicle wall; provided with inerted atmosphere (helium or argon), rapid cooling-quench system, tritium cleanup system with 0.06 m^3/min flow capability.

4. The tritium generator-storage units are supplied with particulate filters to prevent uranium fines carry-over, and diffusers to assist removal of radioactive decay generated He-3 after any long term storage. Evacuation of uranium beds before regeneration will usually provide adequate helium removal.

5. Timing of regeneration of the cryoadsorption panels of the vacuum will limit the maximum hydrogen isotope partial pressure in the associated volumes under full regenerating conditions to less than $\sim$ 10 torr. This pressure is only approximately 1/4 the lower combustibility limit for hydrogen and thus provides a 300% safety factor in the event of air inleakage into the vacuum equipment.

6. Housing of all gaseous prefill equipment in an inerted glove box.

7. Support systems required for tritium containment (such as clean-up systems, uninterruptible electrical power, cryogenic equipment) will be adequately protected against hazardous conditions, including fire, earthquake, tornado, and missiles.

8. An array of uranium traps and zirconium-aluminum getters are included, with capability to trap the entire contents of the cryoadsorption panels and cryogenic distillation system in the event of auxiliary equipment or complete electrical power failure.

5.8.6 PROCESS THROUGHPUT CONSIDERATIONS

The following TNS plant performance was selected to provide a basis for sizing the fuel processing equipment and scoping throughput rates:

Flow time through diffusers for D-T prefill gas, s	15
Regeneration time for vacuum system cryoadsorption panels, hr	1
Regeneration time for Zr-Al getter cartridges, hr	1
Duration of cryogenic distillation separation campaign, hr	1
Fill and adjustment time for gas measuring volumes, s	8
Reversible regeneration capacity of a Zr-Al getter (SAES C-500) cartridge, torr-liters	2500
D-T pellet injection duration for complete refueling, s	20
Number of Zr-Al getter cartridges per canister	6

5.8.7 TRITIUM SYSTEM PARAMETERS FOR THE FOUR REFERENCE OPTIONS

The trade studies have led to the tentative selection of the previously described reference point system designs for the four TNS options. Table 5-13 summarizes the more relevant fuel parameters associated with these designs. As shown in the table, TNS-1 which involves the smallest plasma volume also makes the smallest demand on the tritium systems.

TABLE 5-13

COMPARISON OF PRINCIPAL FUEL PARAMETERS FOR THE FOUR REFERENCE TNS OPTIONS

	TNS-1	TNS-3	TNS-4	TNS-5
TF Coil Conductor	Cu	NbTi	Nb_3Sn	Cu/NbTi
Plasma Minor Radius, m	1.0	1.2	1.2	1.0
Plasma Major Radius, m	4.0	5.7	5.0	4.5
Plasma Elongation	1.6	1.6	1.6	1.6
Plasma Volume, m^3	126	259	228	142
Torus Internal Smooth Surface, m^2	247	411	361	278
On-site Standby T Inventory, MCi	0.62	1.03	0.90	0.700
Peak On-site T Inventory, MCi	1.36	1.85	1.70	1.45
Monthly Required T Replenishment, kCi	52.9	74.9	66.1	59.1
U Charge in T Generator-Storage Units, kg	3.28	5.44	4.77	3.69
T Generator Internal Volume, cm^3	5470	9070	7950	6150
T Gaseous Prefill, Ci/Pulse	1517	2594	2275	1706
T Pellet Refueling, Ci/Pulse	869	1361	1194	977
Fusion Fraction	0.20	0.17	0.17	0.19
Reprocessing Quantity, gatm/campaign	7.9	13.3	11.7	8.9
Composition of Material Reprocessed, a/o*				
H	4.81	4.7	4.7	4.8
D	41.8	42.8	42.7	41.9
T	41.8	42.7	42.7	41.8
He-4	10.1	8.62	8.62	10.1
He-3	1.31	1.05	1.10	1.24

*Treated on a smeared basis.

5.9 PLASMA HEATING - NEUTRAL BEAM SYSTEM

The neutral beam (NB) system for heating the plasma to ignition conditions is based on neutralized beams generated from 150-keV D^+ atomic ions. The system of neutral beam arms for a given TNS option and size necessary to heat that plasma to the required temperature consists of a number of standard arms composed of 3 positive-ion sources which have a nominal current rating of 100 A each. Taking neutralization efficiencies and beam transmission efficiencies into account, each arm can provide 10.4 MW of 150-keV neutral particles (D^0) to the plasma. The selection of 150-keV neutrals for all TNS options and sizes is assumed to apply based on the injection of neutrals during a programmed start-up scenario in which the plasma density is brought up to the full density required for ignition during the injection period (see Section 5.2.2). Such a start-up allows the neutral beams to penetrate to the plasma center at the beginning of the injection period and takes into account the alpha-particle heating of the plasma center during the final period of NB injection. The injection period is approximately 6 seconds and all NB arms inject beams at the plasma horizontal mid-plane at an angle of $\gtrsim 16^0$ (where 0^0 injection is along a radius vector) in order to avoid the ripple trapping of the injected particles in the toroidal magnetic field. The injection geometry is shown in Figure 5-25.

The key features of the standard TNS neutral beam arm is shown in Table 5-14. The following is a list of the main NB arm components as well as the more important design parameters:

- Source/Accelerators - There are three 100-A sources per arm. Each source is assumed to be an ORNL-type source which has been scaled up from that for TFTR application (56 A, 120 keV, 20-cm diameter emitting area in a circular geometry) to 100-A, 150-keV, and 26-cm diameter circular emitting area. The NB pulse time is 6 s and the overall dimensions of each source are 1-m diameter x 1.5-m high. The fraction of the molecular component from each source is $\sim$0.1 of the total source current, and a D_2 gas throughput of $\sim$21 torr liter per second is required to operate each source (assuming a 50% gas efficiency). An isolation valve is provided for each source.

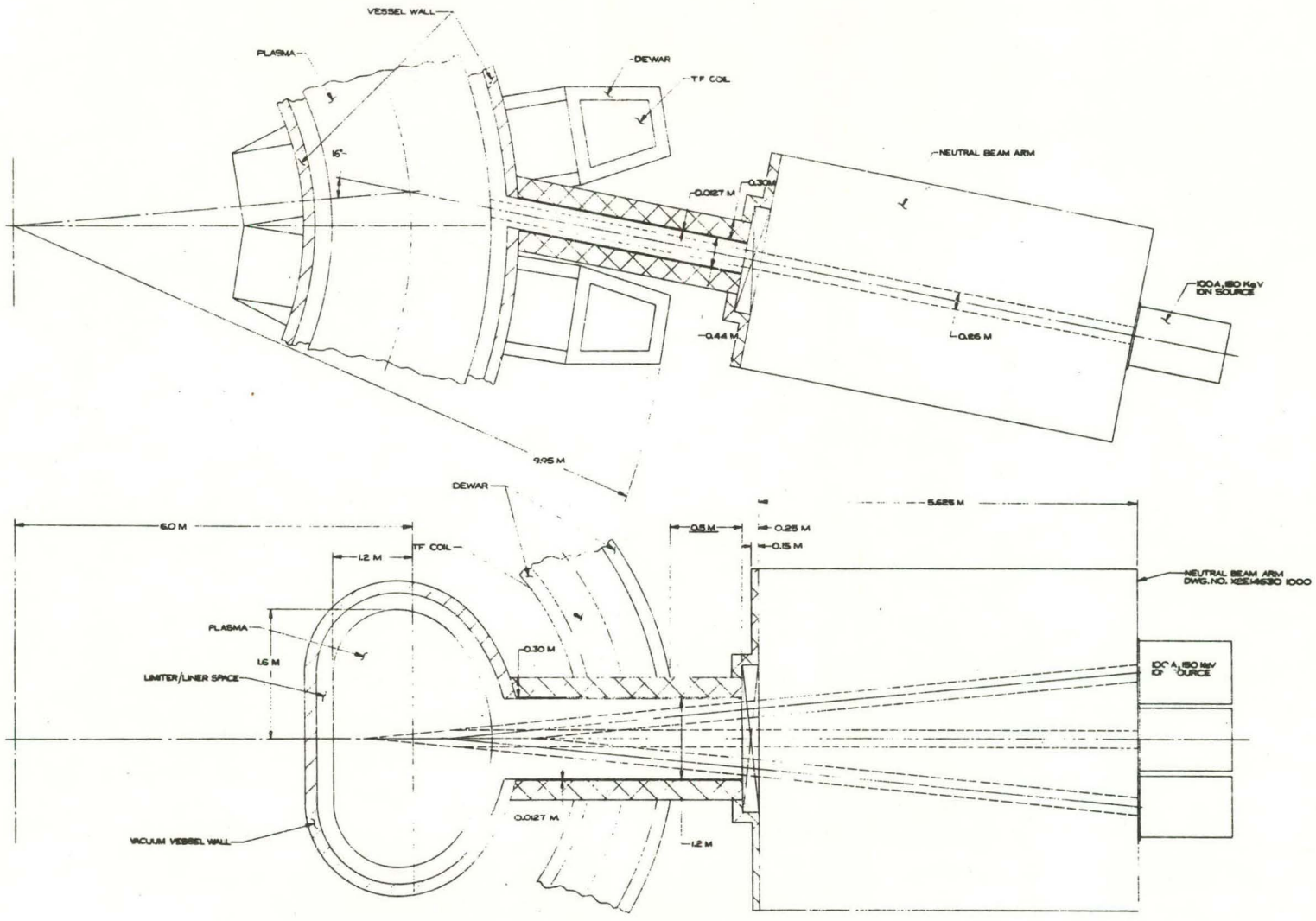

Figure 5-25. Neutral Beam Arm/Duct/TNS Toroidal Vessel Interface

TABLE 5-14

FEATURES OF STANDARD TNS NEUTRAL BEAM ARM

INJECTION ENERGY	150 keV
NB PULSE LENGTH	6 s
CHARGE STATE OF SOURCE IONS	+1
FRACTION OF SOURCE CURRENT DUE TO D^+ IONS	0.9
INJECTION ANGLE AT MIDPLANE□	$\gtrsim 16^o$
CURRENT PER SOURCE	100 A
SOURCES PER NB ARM	3
NB POWER TO PLASMA PER NB ARM (150 keV)	10.4 MW
TRANSMISSION COEFFICIENT THROUGH ARM	0.87
NEUTRALIZATION EFFICIENCY*	29%
SOURCE GAS EFFICIENCY	50%
CLEAR OPENING OF NB DUCT	0.44 m x 1.20 m
TOTAL ACCEL POWER PER NB ARM	45 MW
TOTAL ELECTRICAL POWER PER NB ARM	$\sim$ 55 MW
GAS THROUGHPUT PER ARM	$\sim$ 53 torr l s^{-1}
HV PUMPING SPEED PER ARM△	$\sim 5 \times 10^6$ l s^{-1}
OVERALL LENGTH OF NB ARM	7.5 m
OVERALL CROSS-SECTIONAL DIMENSIONS	3.3 m x 5.0 m

□ HORIZONTAL INJECTION

* 90% OF ASYMPTOTIC VALUE

△ BASED ON 50 M^2 OF CRYOPANEL

- Neutralizer Assembly - Each neutralizer duct is a 2-m long x 0.36-m I.D. copper duct which is water-cooled and provided with a ferro-magnetic shield outer tube. The assembly of three-ducts provides the capability to operate the neutralizers either in the coupled-mode (normal) or the decoupled-mode (source conditioning). A separate D_2 gas feed is provided to allow the gas pressure in the duct to be controlled.

- Ion Deflection - Electrons are removed from the unneutralized portion of the beam leaving the neutralizer duct by means of a mirror coil and the beam "blows up" due to the repulsion of the ions in the beam. To assure space charge blow-up of the beam, a system of high potential electrodes, similar to a design developed at Lawrence Livermore Laboratory for a direct conversion system is employed to maintain the beam channel free of electrons. The space charge blow-up concept has not been fully developed for TNS application. If a conventional system employing a bending magnet were used to remove the charged portion of the beam, there would not be a significant difference in the cost.

- Ion Collector - In addition to the ion deflector electrode system, an internal wall or bulkhead will also act as a particle collector. This wall has apertures to allow the neutral beam to pass through while the charged portion of the beam will spread out due to the defocusing of the beam as it passes through the electrodes. The ion collector consists of a water-cooled, tub-shaped structure fabricated of copper plates and supported in a frame of stainless steel structural components.

- Vacuum Pumping System - The main vacuum pumps consist of 50 m^2 of crysorption panels and have a total pumping speed of $\sim 5 \times 10^6$ l s^{-1}. The gas load during pulsing is estimated at $\sim$100 torr l s^{-1} taking into account desorption caused by the beams impacting the surfaces of the electrodes, particle collectors, etc., and gas loads from the sources and neutralizer ducts. The operating pressures are calculated to be $\sim 2.6 \times 10^{-5}$ torr in the source-neutralizer region and $\sim 1.8 \times 10^{-6}$ torr in the calorimeter region. The gas pressure x distance product between the neutralizer and plasma is sufficiently low such that the losses due to reionization of the neutral beam is $\sim$1%. The pumping panels will be required to be regenerated every 1000 pulses (approximately) to limit the hydrogen content held-up in the panels to a safe level with respect to an explosive situation.

The sizing model used in COAST for the neutral beams is based on the establishment of the neutral beam power requirements which in turn will establish the number of injector arms ($\sim$10 MW per arm). The NB power must exceed the power loss of the plasma in order to raise the temperature of the plasma to that required for ignition. If it is assumed that during the NB heating phase that

empirical scaling holds, it can be easily shown that the NB power is given by $P_{NB} \propto T_i R_o$, where Ti is the ignition temperature and R_o is the plasma major radius. From detailed calculations, it has been established that 50 MW of 150 keV D^o are required for R_o = 5 m and T_i = 13 keV. The 50 MW of power would thus require 5 neutral beam arms. From the above relation, the power requirements for each TNS option and size are calculated in COAST.

5.10 TORUS VACUUM PUMPING SYSTEM (TVPS)

The reference design for the TVPS consists of a number of high vacuum pumping modules each utilizing $2m^2$ of cryosorption panels of molecular sieve material maintained at 4K. The number of such modules required on a given device is a function of the vacuum vessel wall area as discussed later in this section.

Each module is located in the reactor cell basement approximately 7m from the toroidal vacuum vessel. With the pumps located in the basement, sufficient radiation shielding is provided so that nuclear heating of cryopanels is avoided. The pumps communicate with the main vessel via a 0.61-m diameter duct in which is located a large (0.61-m diameter) all-metal gate-valve. Taking the various conductances and specific pumping speeds (10^5 l s^{-1} per m^2 of panel for H_2) into account, the effective pumping speed per pumping unit is 10^4 l/s (H_2). For a specific design (used as a point reference in arriving at the main features of the TVPS), it was determined that 10 units were required to maintain an operating pressure of $\sim 1 \times 10^{-8}$ torr between plasma pulses in a toroidal vessel with 370 m^2 of smooth surface area. This pressure is based on the outgassing of hydrogen from the stainless steel vessel walls, as well as the various parts and appendages associated with essential beam ducts and plasma diagnostics. For the $\sim$400 m^3 vessel (R = 5 m, a x b = 1.45 m x 2.2 m) used in this point design, the characteristic pump-out time is 4 s.

The backing system (also located in the basement) is composed of a 30 l s^{-1} mechanical pump as well as a central Zr/Al getter pump station for use in cryopanel regeneration. The total quantity of gas which can be held up in a pump before a regeneration is required is $\sim 10^5$ torr liter per unit. A schematic of the reference TVPS is shown in Figure 5-26.

The basic functions of the TVPS are two-fold: 1) maintain the vacuum vessel at base pressure ($\sim 10^{-8}$ torr) between pulses, and 2) pumping the vessel after a pulse is quenched and before the initiation of the next plasma pulse. These functions are shown quantitatively in Figures 5-27 and 5-28.

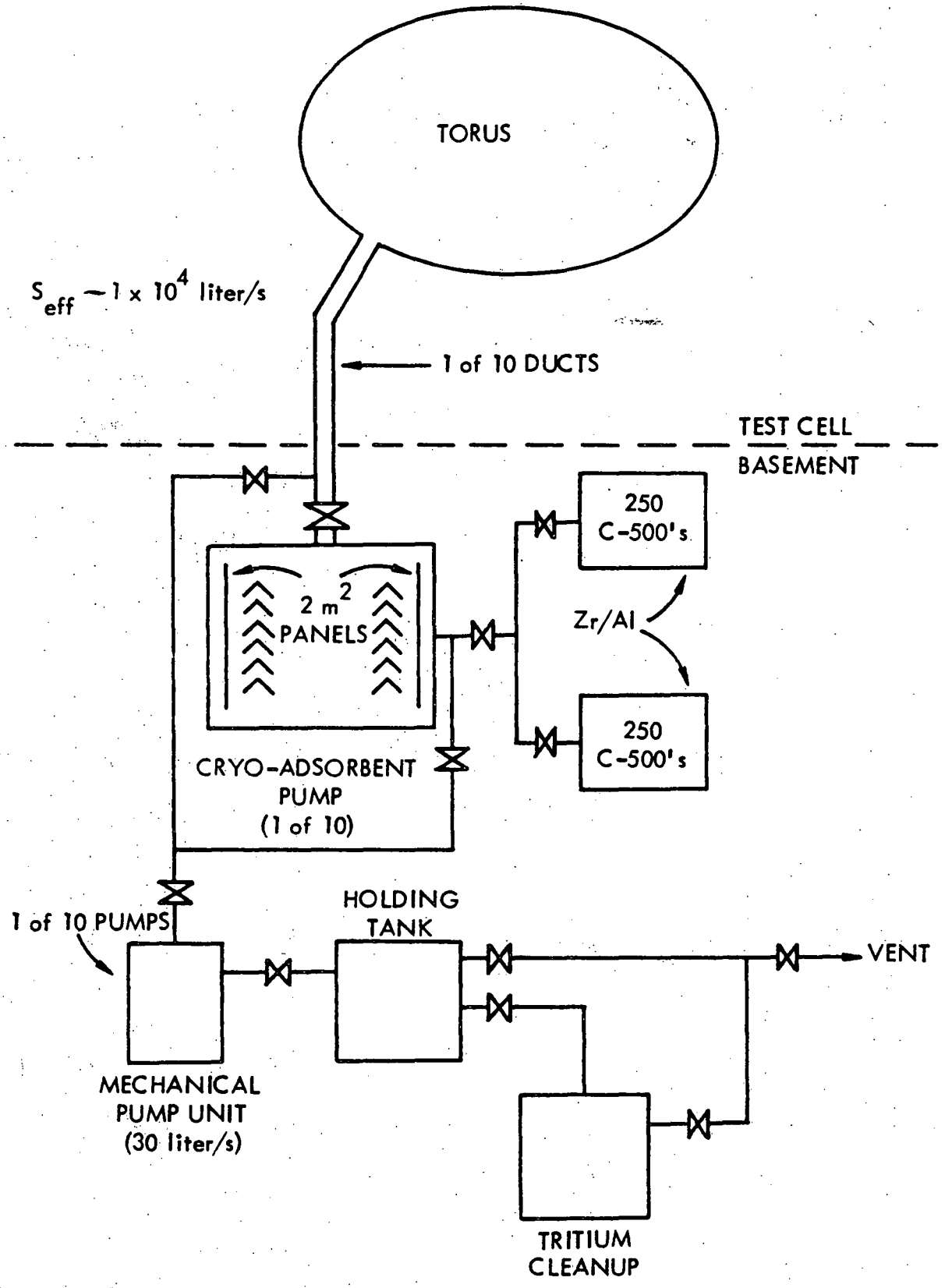

Figure 5-26. Possible Torus Vacuum Pumping System for TNS

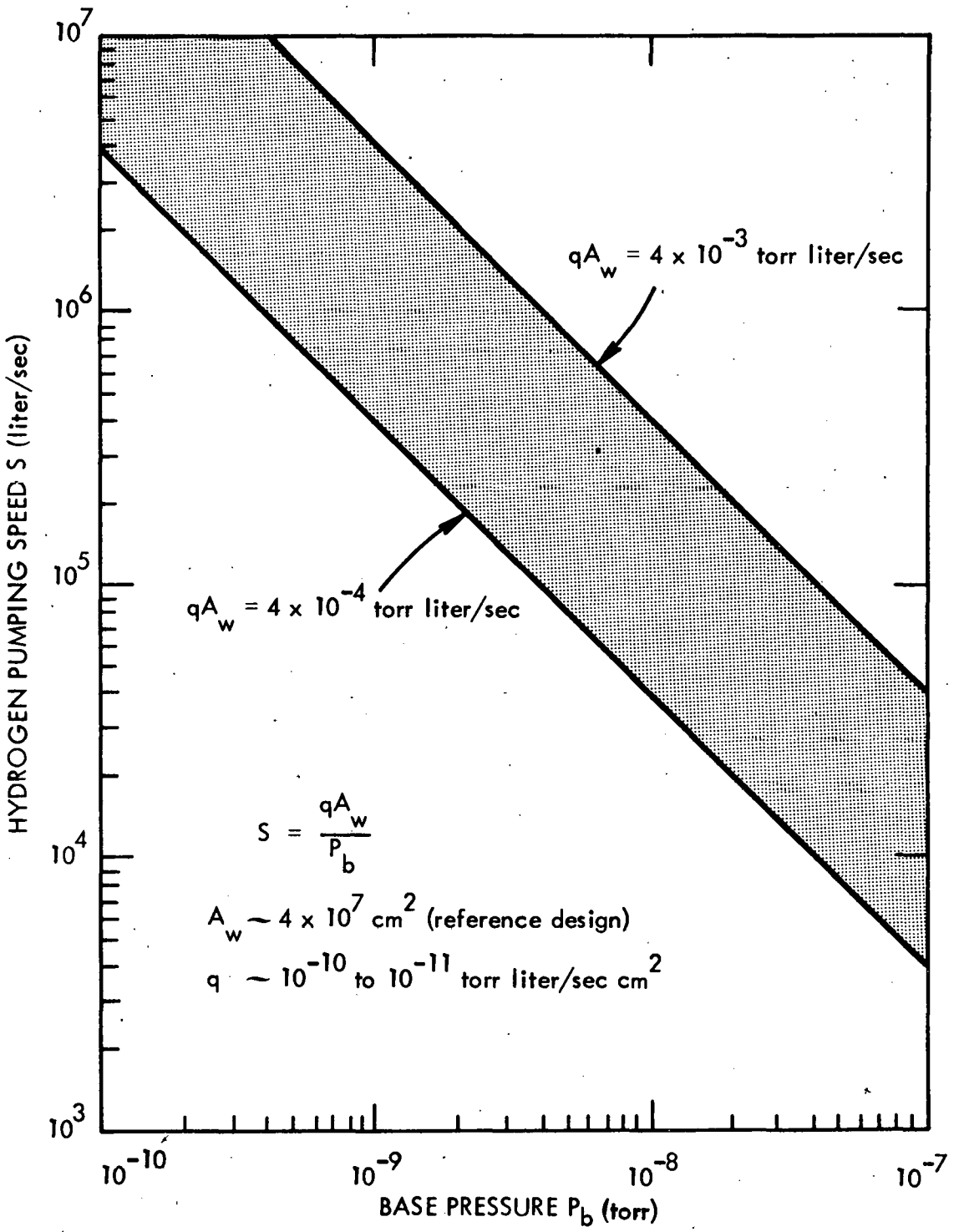

Figure 5-27. Hydrogen Pumping Speed Required to Obtain a Given Base Pressure

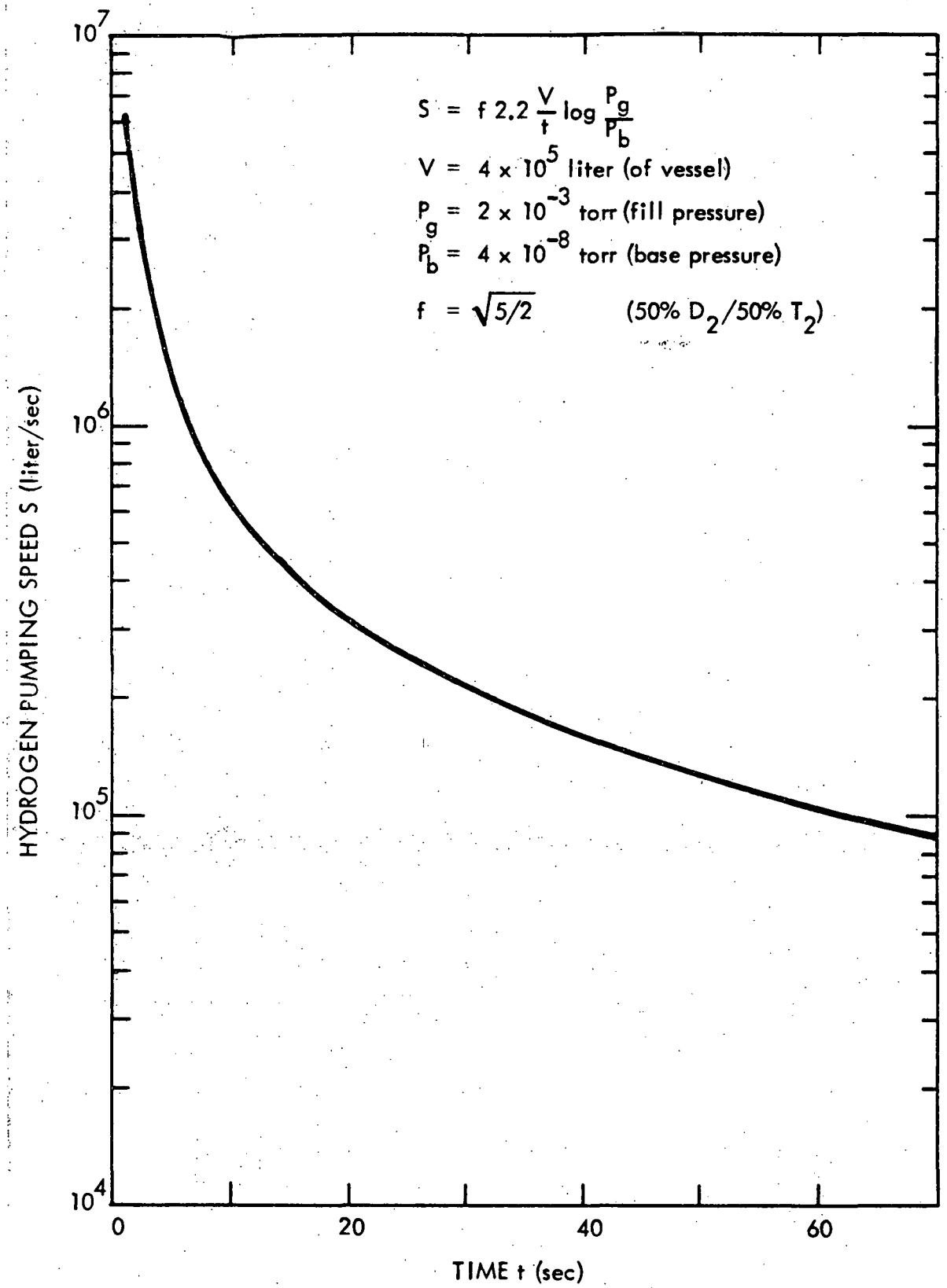

Figure 5-28. Hydrogen Pumping Speed Required to Pump Out Between Plasma Pulses on TNS

The use of Zr/Al getter units was selected as the primary system employed in pump regeneration, but other systems were examined in detail. In particular, the incorporation of an oil-free, stainless steel, diaphragm-type compressor was examined and found to be applicable. The application of compressor pumps in the backing system of the design was not fully investigated.

For purposes of sizing the TVPS in COAST, it was assumed that the basic high vacuum pumping unit of a 2-m^2 cryosorption pump was applied and that the number of pumps was proportional to the smooth surface area of the vacuum vessel. Assuming 10 pumps are required for the reference case when the vessel surface area is 370 m^2, a pump unit would be required for each 37 m^2 of vessel surface.

5.11 REMOTE SERVICING SYSTEMS

The systems that will be required to perform remote servicing operations on the machine, including maintenance and replacement of components are comprised of a variety of hardware and equipment items. Although a definitive compilation of these hardware and equipment items cannot be performed until the TNS design becomes more clearly established, a preliminary compilation has been prepared for purposes of the current studies and engineering judgements have been used in estimating the type and number of items that will likely be required along with an estimate of the cost. These estimates draw from the experience and needs identified in the fission program combined with the projected character and probable operation and maintenance expected of the TNS device. Within the context of the present trade studies on TNS, Table 5-15 provides a list of hardware and equipment needed for the remote servicing systems employed for each of the four TNS options investigated, independent of plasma size or toroidal field coil technology.

TABLE 5-15

REQUIRED REMOTE SERVICING SYSTEM EQUIPMENT AND HARDWARE

Item	Total Cost (M$)
Self-propelled, shielded maintenance modules with internal space for three people, manipulators attached outside, but controlled by individuals inside capable of performing specific operations on the device at its periphery as well as internal functions such as controlling cutting and welding operations from the inside of the vacuum vessel. (3 required)	2.0
Overhead, crane structure support, shielded-manipulator.	2.0
Wall mounted manipulators in neutral beam and hot cell. (6 required)	0.45
Manipulator - movable - post mounted at various fixed locations around the device. (6 required)	0.90
Portable shielding, casks, support equipment.	1.0
Viewing equipment, TV, borescopes, telescope, binoculars.	2.0
Remote operated transport cars, tracks, etc.	1.25
Special cutting-welding equipment.	0.60
Special handling devices (rigging fixtures, frames, support stands, etc.).	0.15
Miscellaneous special tools attached and operated by the manipulators.	0.15
Shielded windows (10 required).	4.5
Remote controllers.	2.0
Life support equipment.	0.1
Survey monitors.	0.05
Cleanup equipment.	0.04

The total estimated cost for the hardware and equipment in the Remote Servicing Systems based on this preliminary compilation is ∿ 18.0 M$. This cost has been employed as a fixed cost in the current TNS trade studies.

5.12 PLANT FACILITIES

The primary effort on plant facilities during these TNS studies was devoted to establishment of generalized space, volume and area requirements for the experimental complex including the reactor cell, power supply areas and other support structures and buildings as input to the base line for facility cost modeling. The facility cost was established on the basis that no buildings, usable for the TNS facility, would exist at the reactor site, i.e, the TNS facility would "stand alone."

To aid in determining the physical configuration of some of the major buildings and structures, functional requirements were established. Those functions associated with the Main Test Building are listed in Table 5-16.

Other major structures which are not encompassed in the Main Test Building and their functions are as follows:

FIELD COIL POWER CONVERSION BUILDING

Functional Requirements. The Field Coil Conversion Building provides space for the equipment which converts the ac power to dc where it is transmitted to the Toroidal Field (TF), Equilibrium Field (EF), and Ohmic Heating (OH) coils in the Tokamak TNS Test Cell.

NEUTRAL BEAM POWER CONVERSION BUILDING

Functional Requirements. The Neutral Beam Power Conversion Buildings house the equipment which provides electrical power to the Neutral Beam Injection System. Two basic functions are performed by this equipment: 1) transform and rectify, and 2) modulate voltage.

TABLE 5-16

FUNCTIONAL REQUIREMENTS - MAIN TEST BUILDING

FACILITY	FUNCTION(S) PERFORMED
TNS Building Complex	
Reactor Cell	Permit assembly, test, minor maintenance, and disassembly by remote means
Diagnostic Basement (Diagnostic & Equipment)	Provide shielded region for diagnostic
Tritium Storage	Provide safe storage of tritium
Hot Cell	Permit remote maintenance of activated components
Neutral Beam	Permit testing and maintenance on neutral beam injectors
Mock/Up Assembly Building	Permit checkout of special features of TNS by trial assembly. Mock-ups would be used to aid in verifying remote maintenance procedures. Final assembly of specific components such as superconducting field coils.
Shielded Bay	Provide storage area for handling fixtures and prevent activation of crane
Galleries	Provide space for viewing interior of Reactor Cell
Tritium Cleanup Equipment (Basement)	House Tritium Clean-Up System Equipment
Utility Space (Basement)	Used to stage equipment and as air lock
Shielded Storage	Temporary storage for radioactive components/materials
Storage Area (Basement)	Storage for slightly contaminated large components
Vacuum Pump Equipment (Basement)	Space for vacuum pumps for torus evacuation

TABLE 5-16
(Continued)

FACILITY	FUNCTION(S) PERFORMED
TNS Building Complex	
Utility Tunnel	Enclosed routing between source and main reactor cell for utility lines-electric bus, chilled water, helium, nitrogen, etc.
Transfer Bay	To provide for movement of equipment between reactor cell, neutral beam test cell and hot cell
Maintenance	Provide viewing and control capabilities for maintenance operations in Hot, Neutral Beam Test, and Main Reactor Cell
Control Building	House the central control for the entire complex. Provide laboratory and support space for radiation monitoring and safety personnel. Serve as primary entrance to building complex.
Mechanical	Provide space for chilling equipment, pumps, fans, filter and air handling equipment for complete TNS cooling water and heating, ventilation and air conditioning systems

MOTOR GENERATOR BUILDING

Functional Requirements. The basic function of the Motor-Generator (MG) Building will be to house the power supply for the large pulsed current required by the Toroidal Field (TF), Ohmic Heating (OH), and Equilibrium Field (EF) coils and the Neutral Beam (NB) Injection System.

Physical configuration of the reactor cell was variable in these TNS trade studies based upon the estimated size of the reactor and neutral beam arms. Figures 3-2 and 3-3 illustrate the method used in determining cell size. Estimated dimensions of the outer buildings and structures required were assigned based on the design of three separate HTGR plants, a VHTR reactor and a Mirror Hybrid Fusion-Fission Reactor. This basis is judged reasonable since a fusion plant is likely to have similar nuclear containment and design technologies as those required for fission plants.

Table 5-17 gives the required facilities and the assumed facility dimensions. The term "variable" appears in the dimension columns of the Reactor Cell, Remote Systems Operations and Basement - Service Facilities, since the sizing of these depend upon the tokamak size to be accommodated and were calculated separately for each TNS option evaluated during the trade studies.

TABLE 5-17

TNS FACILITY STRUCTURES

	Item	Dimensions (m)
1.	Reactor Cell, Cylinder with Dome - Containment	Variable
2.	Remote Systems Operations	Variable
3.	NB Test Cell - Containment Remote Maintenance Area	15 x 40 x 9 15 x 40
4.	Hot Cell - Containment Remote Maintenance Area	18 x 22 x 10 18 x 22
5.	Mock-Up Assembly Bay - Containment	30 x 37 x 14
6.	Transfer Bay - Containment Remote Maintenance Area	115 x 7 x 20 115 x 7
7.	Utility Tunnel	2 x 2 x 40
8.	Basement - Service Facilities	Variable
9.	Motor-Generator Building	38 x 55
10.	Field Coil Power Conversion Building	50 x 30 x 6
11.	Capacitor Yard	24 x 24
12.	NB Power Conversion Building	91 x 40 x 4
13.	Control & Mechanical Equipment Building	30 x 38 x 9
14.	Engineering Lab - Office Building	2800 m^2
15.	Technical Shops	980 m^2
16.	Maintenance Building	900 m^2
17.	Radwaste Processing Building	25 x 25
18.	Tritium Processing Facility	25 x 25 x 5
19.	Cryogenic Plant Building	25 x 20 x 6
20.	Cooling Water Pump House	30 x 10 x 5
21.	Switch Yard Structure	30 x 20

6.0 REFERENCES

1. D. A. Sink and E. M. Iwinski, "COAST, A Computer Code for the Costing and Sizing of TNS Tokamaks," to be published in the IEEE Proceedings of the Seventh Symposium on Engineering Problems of Fusion Research, Knoxville, Tennessee, October 1977.

2. D. L. Chapin and G. Gibson, "TNS Engineering Trade Study Analysis," WFPS-TME-069, September 30, 1977.

3. M. Roberts, et.al., "Oak Ridge Tokamak Experimental Power Reactor Study - 1976, Part 1, EPR Summary," ORNL/TM-5572, Oak Ridge National Laboratory, April 1977.

4. W. M. Stacey, Jr., et.al., "Tokamak Experimental Power Reactor Conceptual Design," ANL/CTR-76-3, Argonne National Laboratory, August 1976.

5. General Atomics Staff, "Experimental Power Reactor Conceptual Design Study," GA-A14000, July 1976.

6. H. R. Howland and T. C. Varljen, "An Approach to Decision Modeling for an Ignition Test Reactor," Proceedings of the Seventh Symposium on Engineering Problems of Fusion Research, October 1977.

7. TNS Engineering Staff, "TNS Quarterly Progress Report for the Period July/August/September 1976," WFPS-TME-049, Westinghouse Fusion Power Systems, October 1976.

8. TNS Engineering Staff, "TNS Quarterly Progress Report for the Period October/November/December 1976," WFPS-TME-050, Westinghouse Fusion Power Systems, January 1977.

9. TNS Engineering Staff, "TNS Quarterly Progress Report for the Period January/February/March 1977," WFPS-TME-051, Westinghouse Fusion Power Systems, April 1977.

10. TNS Engineering Staff, "TNS Quarterly Progress Report for the Period April/May/June 1977," WFPS-TME-052, Westinghouse Fusion Power Systems, July 1977.

11. D. R. Cohn, R. R. Parker and D. L. Jassby, Nucl. Fusion, 16, 31 (1976); also see D. L. Jassby, D. R. Cohn and R. R. Parker, Nucl. Fusion, 16, 1045 1976).

12. S. E. Attenberger, F. B. Marcus and D. G. McAlees, ORNL/TM-5509, Oak Ridge National Laboratory, 1976.

13. A. Blake, "Formulas for Canister and Pipe Design in Underground Nuclear Emplacement," Journal of Pressure Vessel Technology, Paper No. 74-PVP-2, Mar. 1974, p. 65.

14. McGraw-Hill Encyclopedia of Science and Technology: "Atmospheric High,", Vol. I, p. 640.

15. M. Holt, "A Procedure for Determining the Allowable Out-of-Roundness for Vessels Under External Pressure," Paper No. 51-A-136, Transactions of ASME, October 1952, p. 1225.

16. T-F Yang, A. Y. Lee, G. W. Ruck, "Westinghouse Compact Poloidal Divertor Reference Design," WFPS-TME-042, Westinghouse Fusion Power Systems, May 1977.

17. V. Arp, "Forced Flow Single-Phase Helium Cooling Systems," Adv. in Cryogenic Engineering, Vol. 17, p. 342, 1972.

18. M. O. Hoenig, et.al., "Cryostabilized Single-Phase Helium Cooled Cabled Conductors for Large High Field Superconducting Magnets," Proc. 6th Symposium on Engineering Problems of Fusion Research, p. 586, 1976.

INTERNAL DISTRIBUTION

R. J. Creagan (Gateway)
J. H. Fink (LLL)
C. A. Flanagan
G. Gibson
D. J. Grove (PPPL)
G. W. Hardigg (NES)
F. M. Heck
J. L. Johnson (PPPL)
A. R. Jones (ASED)
C. K. Jones (R&D)
J. Karbowski
D. Klein
W. P. Kovacik (R&D)
G. A. Krist
I. Liberman (LASL)
C. J. Mole (R&D)
R. P. Rose
Z. M. Shapiro
C. C. Sterrett (E. Pgh.)
R. Stooksbery (PPPL)
T. C. Varljen
R. W. Warren (LASL)
P. N. Wolfe (LASL)
M. K. Wright (AESD)
J. L. Young (R&D)
R. J. Gromada (AESD)
P. W. Eckels (R&D)
D. T. Hackworth (R&D)
C. J. Heyne (R&D)
P. C. Gaberson (R&D)
J. H. Murphy (R&D)
R. Gold (R&D)
R. Holland (R&D)
J. L. Kelly
J. W. H. Chi
D. L. Chapin
W. C. Brenner
H. J. Garber
H. R. Howland
E. M. Iwinski
A. Y. Lee
W. J. Lange (R&D)
G. W. Ruck
J. H. Schultz
D. A. Sink
G. S. Smeltzer
R. A. Smith
A. Ibrahim
M. Sniderman
E. W. Sucov
F. G. Tauch
T. F. Yang
R. J. Budenholzer
ARD Library - 2
Fusion Library - 15

EXTERNAL DISTRIBUTION

1. Anderson, J.L., Los Alamos Scientific Laboratory, P.O.Box 1663, Los Alamos NM 87545.
2. Anthony, D.J., General Electric Co., Schenectady NY 12345.
3. Baker, C.C., Argonne National Laboratory, 9700 S. Cass Ave., Argonne IL 60439.
4. Berry, L.A., Oak Ridge National Laboratory, P.O.Box 4, Oak Ridge TN 37830
5. Bishop, A.A., Nuclear Engineering Programs Director, Chemical Engineering Dept., University of Pittsburgh, Pittsburgh PA 15261.
6. Bogart, S.L., U.S. Dept. of Energy, Div. of Magnetic Fusion Energy, Mail Stop G-234, Washington DC 20545.
7. Buchsbaum, S.J., Bell Laboratories, Crawford Corner Road, Holmdel NJ 07733.
8. Bussard, R.W., Energy Resources Group, Inc., 1500 Wilson Blvd., Suite 505, Arlington VA 22209.
9. Chao, Yung-An, Nuclear Science and Engineering Div., Carnegie-Mellon University, Schenley Park, Pittsburgh PA 15213.
10. Cherdack, R.N., Burns & Roe, Inc., 283 Highway 17, Paramus NJ 07652.
11. Clarke, J.F., U.S. Dept. of Energy, Div. of Magnetic Fusion Energy, Washington DC 20545.
12. Coffman, F.E., U.S. Dept. of Energy, Div.of Magnetic Fusion Energy, Mail Stop G-234, Washington DC 20545.
13. Cohn, D.R., Francis Bitter Laboratory, MIT, 120 Albany St., Cambridge MA 02139.
14. Conn, R.W., Nuclear Engineering Dept., University of Wisconsin, Madison WI 53706.
15. Creutz, E.C., National Science Foundation, 1800 G Street, N.W., Washington DC 20440.
16. Cullingford, H.S., U.S. Dept. of Energy, Div. of Magnetic Fusion Energy, Mail Stop G-234, Washington DC 20545.
17. Davidson, R.C., U.S. Dept. of Energy, Div. of Magnetic Fusion Energy, Mail Stop G-234, Washington DC 20545.
18. Davies, N.A., U.S. Dept. of Energy, Div. of Magnetic Fusion Energy, Mail Stop G-234, Washington DC 20545.
19. Dean, S.O., U.S. Dept. of Energy, Div.of Magnetic Fusion Energy, Mail Stop G-234, Washington DC 20545.
20. Favale, A., Grumman Aerospace Corp., Bethpage NY 11714.
21. Fernback, S., Lawrence Livermore Laboratory, Livermore CA 94551.
22. von Fischer, E., Bechtel Corp., P.O. Box 3965, San Francisco CA 94119.
23. Forsen, H.K., Exxon Nuclear Co., 777 106th Ave. N.E., Bellevue WA 98004.
24. Fowler, T.K., University of California, Lawrence Livermore Lab, P.O. Box 808, Livermore CA 94551.
25. Furth, H.P., Princeton Plasma Physics Laboratory, Princeton University, P.O. Box 451, Princeton NJ 08540.
26. Gottlieb, M.B., Princeton Plasma Physics Laboratory, Princeton University, P.O. Box 451, Princeton NJ 08540.
27. Gough, W. C., DOE Office, Electric Power Research Institute, Palo Alto, CA 94304
28. Grace, J. Nelson, U.S. Dept. of Energy, Div. of Magnetic Fusion Energy, Mail Stop G-234, Washington DC 20545.
29. Harder, R., General Atomic Co., P.O. Box 81608, San Diego CA 92138.
30. Henning, C.D., University of California, Lawrence Livermore Laboratory, P.O.Box 808, Livermore CA 94551.
31. Hess, G.K., U.S. Dept. of Energy, Div. of Magnetic Fusion Energy, Washington DC 20545.
32. Hill, A.G., Plasma Fusion Center, Room 4-232, Massachusetts Institute of Technology, 77 Massachusetts Ave., Cambridge MA 20139.
33. Hirsch, R.L., Exxon Research & Engineering, Box 101, Florham Park NJ 07932.
34. Kammash, T., The University of Michigan, College of Engineering, Dept. of Nuclear Engineering, Ann Arbor MI 48109.
35. Kintner, E.E., U.S. Dept. of Energy, Div. of Magnetic Fusion Energy, Mail Stop G-234, Washington DC 20545.

EXTERNAL DISTRIBUTION

36. Kulcinski, G., Nuclear Engineering Dept., University of Wisconsin, Madison WI 53706.
37. Kummer, D., McDonnell Douglas, P.O. Box 516, St. Louis MO 63166.
38. Maroni, V.A., Argonne National Laboratory, 9700 S.Cass Ave., Argonne IL 60439.
39. Meade, D.M., Princeton Plasma Physics Laboratory, Princeton University, P.O. Box 451, Princeton NJ 08540.
40. Miley, G.H., Nuclear Engineering Program, 214 Nuclear Engineering Laboratory, University of Illinois, Urbana IL 61801.
41. Mills, R., Princeton Plasma Laboratory, Princeton University, P.O.Box 451, Princeton NJ 08540.
42. Morgan, O.B., Oak Ridge National Laboratory, P.O. Box 4, Oak Ridge TN 37830
43. Moses, K., U.S. Dept. of Energy, Div. of Magnetic Fusion Energy, Mail Stop G-234, Washington DC 20545.
44. Murphy, M.R., U.S. Dept. of Energy, Div. of Magnetic Fusion Energy, Mail Stop G-234, Washington DC 20545.
45. Naymark, S., Nuclear Services Corp., 1700 Dell Ave., Campbell CA 95008.
46. Neff, J.O., U.S. Dept. of Energy, Div. of Magnetic Fusion Energy, Mail Stop G-234, Washington DC 20545.
47. Ohkawa, T., General Atomic Co., P.O. Box 608, San Diego CA 92112.
48. Powell, J., Brookhaven National Laboratory, Upton, Long Island NY 11973.
49. Purcell, J.R., General Atomic Co., P.O. Box 608, San Diego CA 92112.
50. Roberts, M., Oak Ridge National Laboratory, P.O. Box 4, Oak Ridge TN 37830. (15 copies)
51. Reardon, P.J., Princeton Plasma Physics Laboratory, Princeton University, P.O. Box 451, Princeton NJ 08540.
52. Rose, D.J., Dept. of Nuclear Engineering, Massachusetts Institute of Technology, Cambridge MA 02139.
53. Sager, P., General Atomic Co., P.O. Box 608, San Diego CA 92112.
54. Sawyer, G.A., Los Alamos Scientific Laboratory, P.O. Box 1663, Los Alamos NM 87545.
55. Schmid, L.C., Pacific Northwest Laboratories, Battelle Blvd., P.O. Box 999, Richland WA 99352.
56. Schultz, M.A., Nuclear Engineering Dept., The Pennsylvania State University, 231 Sackett Building, University Park PA 16802.
57. Stacey, Weston M., Jr., Georgia Institute of Technology, Atlanta GA 30332.
58. Steiner, D., Oak Ridge National Laboratory, P.O. Box 4, Oak Ridge TN 37830.
59. Stickley, C.M., U.S.Dept.of Energy, Div.of Laser Fusion, Washington DC 20545.
60. Taylor, C.E., Lawrence Livermore Laboratory, Mail Code L-384, P.O.Box 808, Livermore CA 94550.
61. Teofilo, V., Pacific Northwest Laboratories, Battelle Blvd., P.O.Box 999, Richland WA 99352.
62. Thomassen, K., Lawrence Livermore Laboratory, P.O.Box 808, Livermore CA 94550.
63. Trivelpiece, A.W., Engineering & Research, Maxwell Laboratories, Inc., 9244 Balboa Ave., San Diego CA 92123.
64. Williams, J.M., U.S. Dept.of Energy, Div. of Magnetic Fusion Energy, Mail Stop G-234, Washington DC 20545.
65. Woodson, H.H., Department of Electrical Engineering, University of Texas, Austin TX 78712.
66. Yoshikawa, H., Westinghouse Hanford Co., P.O. Box 1970, Richland WA 99352.
67. Zwilski, K., U.S. Dept. of Energy, Div. of Magnetic Fusion Energy, Mail Stop G-234, Washington DC 20545.
68. U. S. Department of Energy, Technical Information Center, Post Office Box 62, Oak Ridge TE 37830.
69. Max-Planck-Institut für Plasmaphysiks, 8046 Garching bei München, West Germany, ATTN: Dr. L. Johannsen
70. Ribe, F., University of Washington, MS FL-10, Seattle, WA 98195
71. Amherd, N., Electric Power Research Institute, 3412 Hillview Ave., P. O. Box 10412, Palo Alto, CA 94304
72. Scott, F. R., Electric Power Research Institute, 3412 Hillview Ave., P. O. Box 10412, Palo Alto, CA 94304
73. French, J. W., Ebasco Services, Inc., TFTR Project, P. O. Box 451, Princeton, NJ 08540
74. Haubenreich, P. N., Oak Ridge National Laboratory, P. O. Box Y, Oak Ridge, TN 37830
75. Shannon, T. E., Oak Ridge National Laboratory, P. O. Box Y, Oak Ridge, TN 37830
76. Peng, Y. M., Oak Ridge National Laboratory, P. O. Box Y, Oak Ridge, TN 37830
77. Jensen, B. K., Public Service Electric and Gas Research Corp., 80 Park Place, Newark, NJ 07101